UNIVERSITY OF CHILE
FACULTY OF CHEMICAL & PHARMACEUTICAL SCIENCES

GLOBAL PERINATAL ASPHYXIA IMPAIRS MYELINATION AND OLIODENDROCYTE MATURATION IN RATS: PREVENTION BY NEONATAL MESENCHYMAL STEM CELLS TREATMENT.

Thesis presented to the University of Chile to qualify for the academic degree of Doctor of Pharmacology
by

Andrea Constanza Tapia Bustos

Thesis directors
Mario Herrera-Marschitz, MD Sci PhD
Paola Morales Retamales, MSci PhD

Thesis Co-director
Fernando Ezquer PhD

Santiago – Chile
2020

UNIVERSIDAD DE CHILE
FACULTAD DE CIENCIAS QUÍMICAS Y FARMACÉUTICAS
INFORME DE APROBACIÓN
TESIS DE DOCTORADO

Se informa a la Dirección de Postgrado de la Facultad de Ciencias Químicas y Farmacéuticas que la Tesis presentada por el candidato:

ANDREA CONSTANZA TAPIA BUSTOS

Ha sido aprobada por la Comisión Informante de Tesis como requisito para optar al Grado de Doctor en Farmacología, en el examen de defensa de Tesis público rendido el día 17 de Julio del 2020.

Director de Tesis:

Mario Herrera-Marschitz, MD Sci PhD _____

Paola Morales R, MSci PhD _____

Codirector de Tesis:

Fernando Ezquer, PhD _____

Comisión Informante de Tesis:

Pablo Caviedes F, PhD (presidente) _____

Rommy von Bernhardi M, PhD _____

Flavio Carrión, PhD _____

Juan Pablo Rodríguez V, PhD _____

AGRADECIMIENTOS

A mis tutores, profesores Mario Herrera-Marschitz, Paola Morales y Fernando Ezquer. Por su apoyo académico y personal constante. Por recibirme en sus laboratorios y guiar mi proceso de formación. Por la corrección continua en un contexto de respeto y enseñanza. Por compartir conmigo durante todos estos años. Por ser parte de muchos momentos personales importantes. Por creer en mí. Aprecio esos largos días, durante muchos años, en donde aprendí de ustedes y me llevó así lo mejor de cada uno para mis nuevos proyectos.

A mi comisión evaluadora, profesores Pablo Caviedes, Flavio Carrión, Rommy von Bernhardi y Juan Pablo Rodríguez, por guiar este proceso académico con una excelente disponibilidad y empatía frente a las dificultades que se me presentaron. Por recibirme en sus laboratorios para aclarar dudas y para realizar experimentos. Agradezco y valoro su interés por mi trabajo.

A mis compañeros de la generación 2015 del Doctorado en Farmacología. Por nuestro proceso de aprendizaje y por nuestros días compartidos.

A nuestro equipo de trabajo, especialmente a mis profesores, Mario, Paola; compañeros Valentina, Carolyne, Emmanuel y Ronald. Al Dr. Israel y la Dra. Quintanilla. Entre experimentos, exámenes y seminarios, necesarios y disfrutados fueron cada uno de los momentos que vivimos en compañía. He aprendido con y de ustedes. Un agradecimiento especial al profesor Diego Bustamante, por haber confiado en mí e invitarme a participar de este proyecto. Por toda la farmacología que me ha regalado generosamente. Gran parte de mi pensamiento farmacológico lo aprendí junto a él. Finalmente a la Sra. Carmen, por ayudarme con su buena disposición en todas mis tareas y acogerme en momentos de fatiga.

Al Centro de Medicina Regenerativa de la Universidad del Desarrollo, liderado por los profesores Fernando y Marcelo Ezquer. Agradezco a ellos y mis compañeros, por abrir las puertas de su laboratorio. Por recibirme, ayudarme, guiarme y compartir siempre desde su generosidad académica y sus experiencias.

A mi familia y a mis amigos. Especialmente a Francisco, mi compañero. Por confiar en este proyecto, comprenderlo, vivirlo y quererlo como yo. Agradezco tenerlos en mi vida para disfrutarnos. Agradezco las enseñanzas que me han regalado, es ese el sello que intento poner en mi trabajo como una forma de honrar lo importante que son para mí.

THESIS DEVELOPMENT LABORATORIES:

(1) Programme of Molecular & Clinical Pharmacology, ICBM, Medical Faculty (Mario Herrera-Marschitz laboratory)

(2) Center for Regenerative Medicine, Faculty of Medicine-Clínica Alemana, Universidad del Desarrollo, Santiago, Chile

OPERATIONAL SUPPORT AND CONTRACT GRANT SPONSORS:

- CONICYT-Chile (**ATB: # 21151232**; main sponsor)
- FONDECYT-Chile (**MHM: #1120079**; main sponsor)
- FONDECYT: N°1170291 (FE: #1170712)
- FONDECYT: N°1170291 (PM: #1190562)
- Graduate Scholarship of the Faculty of Sciences Chemicals and Pharmaceuticals of the University of Chile.

SCIENTIFIC PUBLICATIONS

Global perinatal asphyxia impairs oligodendrocyte maturation in rats: prevention by neonatal mesenchymal stem cells treatment. 2020. Scientific Reports (in review)
Tapia-Bustos A, Lespay-Rebolledo C, Vío V, Perez-Lobos R, Casanova-Ortiz E, Ezquer F, Herrera-Marschitz M, Morales P.

Modulation of Postnatal Neurogenesis by Perinatal Asphyxia: Effect of D1 and D2 Dopamine Receptor Agonists. 2016. Neurotox Res (1):109-121.
Tapia-Bustos A, Perez-Lobos R, Vío V, Lespay-Rebolledo C, Palacios E, Chiti-Morales A, Bustamante D, Herrera-Marschitz M, Morales P.

Vulnerability to a Metabolic Challenge Following Perinatal Asphyxia Evaluated by Organotypic Cultures: Neonatal Nicotinamide Treatment. 2017. Neurotox Res (3):426-443.
Perez-Lobos R, Lespay-Rebolledo C, **Tapia-Bustos A**, Palacios E, Vío V, Bustamante D, Morales P, Herrera-Marschitz M.

Gold nanorods/siRNA complex administration for knockdown of PARP-1: a potential treatment for perinatal asphyxia. 2018. Int J Nanomedicine (13):6839-6854.
Vio V, Riveros AL, **Tapia-Bustos A**, Lespay-Rebolledo C, Perez-Lobos R, Muñoz L, Pismante P, Morales P, Araya E, Hassan N, Herrera-Marschitz M, Kogan MJ.

Targeting Sentinel Proteins and Extrasynaptic Glutamate Receptors: A Therapeutic Strategy for Preventing the Effects Elicited by Perinatal Asphyxia? 2018. Neurotox Res (2):461-473.
Herrera-Marschitz M, Perez-Lobos R, Lespay-Rebolledo C, **Tapia-Bustos A,** Casanova-Ortiz E, Morales P, Valdes JL, Bustamante D, Cassels BK.

Regionally Impaired Redox Homeostasis in the Brain of Rats Subjected to Global Perinatal Asphyxia: Sustained Effect up to 14 Postnatal Days. 2018. Neurotox Res 3:660-676.
Lespay-Rebolledo C, Perez-Lobos R, **Tapia-Bustos A**, Vio V, Morales P, Herrera-Marschitz M.

The Long-Term Impairment in Redox Homeostasis Observed in the Hippocampus of Rats Subjected to Global Perinatal Asphyxia (PA) Implies Changes in Glutathione-Dependent Antioxidant Enzymes and TIGAR-Dependent Shift Towards the Pentose Phosphate Pathways: Effect of Nicotinamide. 2019. Neurotox Res (3):472-490.
Lespay-Rebolledo C, **Tapia-Bustos A,** Bustamante D, Morales P, Herrera-Marschitz M.

INDEX

FIGURE INDEX

TABLE INDEX

ABBREVIATIONS

α-MEM, Alpha-minimum essential medium

APC, Allophycocyanin

AS, Asphyxia exposed rats

a.u., Arbitrary units

BCA, Bicinchoninic acid assay

BSA, Bovine serum albumin

CNS, Central Nervous System

CO_2, Carbon dioxide

Cox-2, Cyclooxygenase-2

CS, Caesarean-delivered rat controls

DAPI, 4,6 diamino-2-phenylindol

ELISA, Enzyme-Linked ImmunoSorbent Assay

FBS, Foetal bovine serum

FITC, Fluorescein isothiocyanate

GFAP, Glial fibrillary acid protein

G22, Gestation day 22

h, Hour

HI, Hypoxia/ischemia

HIE, Hypoxic-ischemic encephalopathy

HRP, Horseradish peroxidase

H_2O_2, Hydrogen peroxide

H_2O d, Distillate water

Iba-1, Calcium binding adaptor molecule 1

IF, Immunofluorescence

IL-1β, Interleukin 1-beta

IL-6, Interleukin 6

icv, Intracerebroventricular

MBP, Myelin basic protein

min, Minute

MSCs, Mesenchymal stem cells

MMLV-RT, Moloney Murine Leukemia Virus Reverse Transcriptase

NGS, Normal goat serum

OLs, Oligodendrocytes

Olig-1, Oligodendrocyte Transcription Factor 1

Olig-2, Oligodendrocyte Transcription Factor 2

OPC, Oligodendrocyte precursor cells

P, Postnatal day

PA, Perinatal asphyxia

PBS, Phosphate-buffered saline

PE, Phycoerythrin

preOLs, Pre-oligodendrocytes

PVL, Periventricular leukomalacia

RIPA Buffer, Radio-Immune Precipitation Assay Buffer

rpm, Revolutions per minute

RT-qPCR, Reverse transcription polymerase chain reaction

SEM, Standard error of the mean

SVZ, Subventricular zone

TdT, Terminal deoxynucleotidyl transferase

TUNEL, Terminal deoxynucleotidyl transferase dUTP nick end labeling

TNF-α, Tumor necrosis factor alpha

Veh, Vehicle

I. ABSTRACT

The effect of global perinatal asphyxia (PA) on myelination, oligodendrocytes (OLs), neuroinflammation and cell viability was evaluated in telencephalon and hippocampus of rats at postnatal day (P)1, 7 and 14, covering a period characterised by a spur of neuronal networking, finding a sustained injury that may have profound adverse effects on brain development. The study evaluated the effect of neonatal treatment with mesenchymal stem cells (MSCs).

PA was induced by immersing foetus-containing uterine horns into a water bath at 37°C for 21 min. Asphyxia-exposed (AS) and sibling caesarean-delivered (CS) foetuses were resuscitated and nurtured by surrogate dams. Two hours after delivery, AS and CS neonates were injected with either 5 µl of vehicle (10% rat plasma) or $5x10^4$ rat adipose tissue-derived MSCs into the left lateral ventricle. Animals were euthanized at P1, 7 or 14, dissecting samples from telencephalon and hippocampus to be assayed for (i) myelination (myelin-basic protein, MBP) and Olig-1/Olig-2 transcriptional factors (by immunofluorescence, IF, and RT-qPCR); (ii) Glial number (OLs, MBP-DAPI/mm^3; astrocytes, GFAP-DAPI/mm^3; microglia, Iba-1-DAPI/mm^3, by IF); (iii) neuroinflammation, including proinflammatory cytokines (IL-1β, IL-6, TNF-α and Cox-2, by RT-qPCR and ELISA), and (iv) delayed cell death (by TUNEL assay).

It was found that PA produced at P7: (i) a decrease of MBP immunoreactivity in telencephalon (external capsule, corpus callosum, cingulum), but not in fimbriae of hippocampus; (ii) an increase of Olig-1 transcriptional factor mRNA levels in telencephalon; (iii) an increase of IL-6 mRNA, but not of protein levels in telencephalon; (iv) an increase of cell death, including OLs-specific cell death in telencephalon. (v) MSCs treatment prevented the effect of PA on myelination, OLs number and cell death.

The present study demonstrates that PA induces regional and developmental-dependent changes on myelination and OLs maturation, but not on astroglia and microglia. Thus, OLs are the most vulnerable glial cells to

hypoxia-reoxygenation insults at early neonatal stages, evaluated in vulnerable areas. Early neonatal MSCs treatment significantly improves survival of mature OLs and myelination in telencephalic white matter. The outcome occurred in association with decreased apoptosis. Future studies are required to elucidate the precise pharmacological mechanism.

II. INTRODUCTION

Perinatal asphyxia: clinical relevance

Perinatal asphyxia (PA), a prototype of obstetric complication, is the result of impaired gas exchange during labour or delivery, a major cause of death (20-50%), neuropsychiatric dysfunctions and learning disorders (25-60% of the survivors), in the short and long-term of the affected new-borns (Miller et al., 2005), increasing not only the costs associated with the acute treatment, but also comorbidities along the life of the individuals. In fact, the affected neonates can show multisystem dysfunctions or alterations, only to be detected along development, affecting motor and cognitive functions, progressing to neurological and/or psychiatric disorders, such as mental retardation, epilepsy, hearing loss, visual impairment, hyperactivity, memory deficits, or even schizophrenia and neurodegenerative disorders (Mercuri and Barnett, 2003; Schmidt-Kastner et al., 2006; Cannon et al., 2008; Galeano et al., 2011).

Approximately 20 per 1000 term births with biochemical and clinical evidence of PA will require significant resuscitation (see Aherne et al., 2016), but this incidence increases several times in low-income countries (see Lawn et al., 2005), probably associated to poor antenatal care, unskilled attendance during birth and lack of emergency obstetrical care for complications (see Lawn et al., 2010).

Despite progress in public health programs aimed at the care of maternal and child health, in Chile perinatal mortality increased from 8.3/1000 live births in 2002 to 12.6 /1000 live births in 2010, projecting an increase by 25% of this indicator to 2020, according to reports from the Department of Health Statistics and Information (see Donoso, 2011). In 2006, a study indicated an incidence of PA of 4-6 per 1000 term births in Chile (Latorre et al., 2006), but this could be underestimated due to limitations of infrastructure and human resources (see

Novoa et al., 2012).

Although there are advances in the intensive care and diagnosis of PA, there is no progress in neuroprotection and neuronal rescue of newborns suffering of moderate to severe encephalopathies (González et al., 2005). At present, there is no consensus on any therapeutic strategy for preventing the long-term effects resulting from severe PA. Only hypothermia has shown relevant effects but limited by a narrow therapeutic window (see Drury et al., 2014). Thus, PA is still an important paediatric issue with few therapeutic alternatives for preventing neuronal damage.

Pathophysiological features of Perinatal Asphyxia: focus on the Central Nervous System

Diminished oxygen and carbon dioxide gas exchange is the hallmark of PA. PA implies two events, hypoxia and re-oxygenation (see Fig. 1). Because oxygen and glucose are the principal driving forces for energy production in brain, during the immediate period of hypoxia, when oxygen availability is temporarily interrupted, there is a switch to anaerobic glycolysis, for neurons a poor metabolic alternative, because of a high metabolic rate and a low store of glucose in the brain (see Robertson et al., 2009). Glycolysis results in (i) un-sufficient rate of adenosine triphosphate (ATP) formation (Seidl et al., 2000); (ii) lactate accumulation (Chen et al., 1997); (iii) decreased pH (Lubec et al., 2000) and (iv) overproduction of reactive oxygen species (ROS) (Kumar et al., 2008).

The depletion in ATP reduces transcellular transport (e.g. Na^+/K^+-ATPase and Na^+/Ca^{2+} exchanger) and leads to intracellular accumulation of sodium, water and calcium (see Douglas-Escobar et al., 2015), leading to cell swelling and primary cell death by necrosis (see Davidson et al., 2015; Northington et al., 2001a, b). However, many neurons initially recover, at least partially from the first insult during a so called “latent phase", only to develop progressive dysfunction and die many

hours, or even days later (see Davidson et al., 2015). A reduction of reuptake of excitatory amino acids (EAA) by astrocyte, such as glutamate, because of failure of EAA transporters (e.g. EAAT-1 and EAAT-2), facilitates the intracellular Ca^{2+} entry via NMDA receptor-mediated channel activation, perpetuating injury by a process termed excitotoxicity (see Douglas-Escobar et al., 2015).

Re-oxygenation is a requirement for survival and restoration of functioning, but it implies a secondary energy failure, a long-term phase characterized by glutamate-dependent excitotoxicity, mitochondrial dysfunction, accumulation of free radicals and neuroinflammation (see Blomgren and Hagberg, 2006; see Liu and McCullough, 2013; see Leaw et al., 2017), triggering secondary or delayed cell death by apoptosis (Northington et al., 2001a, b). Delayed cell death is the most important end point for any therapeutic strategy (Northington et al., 2001a, b; see Herrera-Marschitz et al., 2011, 2014, 2018), providing a window of opportunities for neuroprotection (see Sävman, 2008).

After the bulk of cell death observed during the secondary phase, there is a tertiary phase of repair and reorganization. During this period, cell repairing is stimulated, implying neurogenesis, gliogenesis and sprouting of surviving neuronal circuits (see Morales et al., 2011). At the same time, there is evidence that in some regions, for example in white matter of the neocortex, physiological apoptosis may be upregulated, which impairs new cell production and survival, leading to ongoing cell loss over many months (Marin-Padilla et al., 1997, Ness et al., 2001). The precise mechanisms for this prolonged injury are not fully understood, but might reflect persistent inflammation and epigenetic changes (Fleiss and Gressens, 2012).

Perinatal Asphyxia induces neuroinflammation

Global PA activates several signalling pathways in neuronal and glial cells promoting activation of transcription factors associated with neuroinflammation,

including NF-κB (Clemens et al., 1998; Lubec et al., 2002; Herrmann et al., 2005; Neira-Peña et al., 2015), releasing a complex array of pro (i.e., TNF-α, IL-1β, IL-6) and anti-inflammatory (i.e., IL-10) cytokines (see Streit et al., 2004).

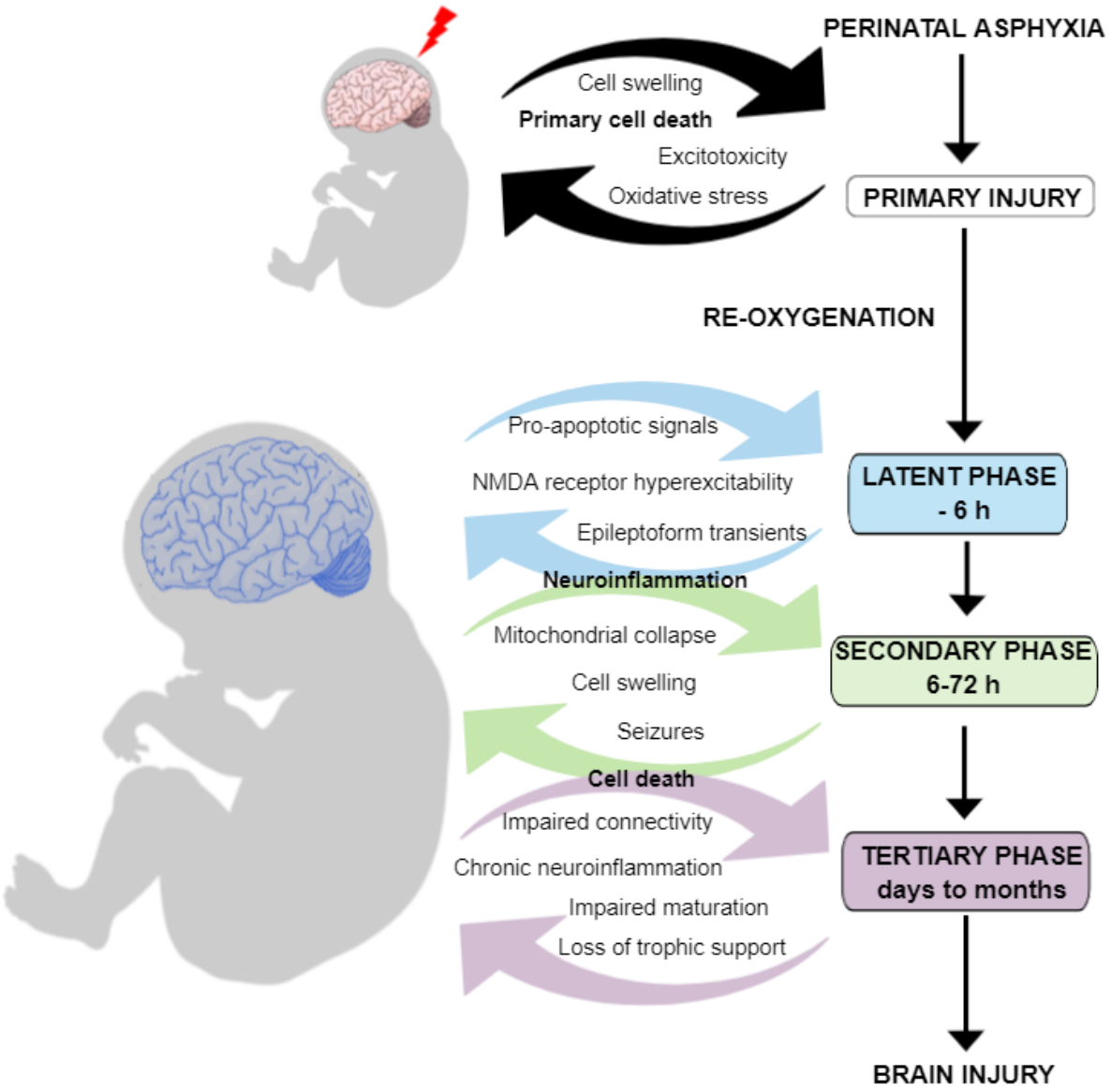

Figure 1. Pathophysiological features of PA. Mechanisms of evolving neural injury in the primary phase, latent phase, secondary phase, and tertiary phase that contribute to long-term brain damage and disability.

One major hallmark of neuroinflammation is the activation of microglia. Microglia, are resident parenchymal cells of the brain, derived from the same myeloid lineage as macrophages and dendritic cells (Greaves and Gordon, 2002), representing around 10% of the total glia cell of CNS (see Soulet and Rivest, 2008). Depending on their activation status and the pathological context, microglia can exert neurotoxic or neuroprotective functions such as sensing pathogens, phagocytic clearance of debris/dead cells, synaptic pruning, neurogenesis and migration/survival neuronal precursors (Hanisch and Kettenmann, 2007). However, over-activation of microglia can induce *de novo* synthesis and secretion of pro-inflammatory cytokines (Wang et al., 2015), contributing to a detrimental environment, causing secondary damage, and exacerbation of neuronal and glial death (Harry and Kraft, 2008).

Astrocytes, the main glial cell type found in the CNS, comprise nearly 35% of the total CNS cell population and play a critical role in homeostatic functions such as uptake of neurotransmitters, regulation of pH and ion concentrations, and metabolic support of neurons (Logica et al., 2016). Like microglia, PA activates astrocytes, which can be evidenced by specific morphological changes including increasing the thickness and length of primary processes (i.e. astrocytosis) (Sun and Jakobs, 2012). This activation promotes the release of pro-inflammatory cytokines, chemokines and ROS which in turn, promote neuronal and glial death (see Sochocka et al., 2017).

Hence, inflammatory markers can be useful for predicting the clinical outcome of PA. There are studies showing the role of proinflammatory cytokines in the adverse neurological outcomes of PA, both short (Bona et al., 1999, Kadhim et al., 2001, Foster-Baber et al., 2001) and long-term (Foster-Baber et al., 2001) after delivery. Specifically, TNF-α, IL-1β and IL-6 expression are increased 24 h after a brain insult, activating microglial and astroglial cells, producing in turn more cytokines and chemokines, amplifying the immune response, and brain damage (Bona et al., 1999; Kadhim et al., 2001; Neira-Peña et al., 2015).

Regional vulnerability

There are clinical and experimental evidences showing a regional vulnerability to the harmful effects induced by PA. The duration of the perinatal insult, a key factor for the severity of the clinical outcome (see Volpe, 1995), as well as the developmental stage of the affected regions determine the pattern of brain damage (Swarte et al., 2009; see Herrera-Marschitz et al., 2011, 2014). Brain development is a dynamic process, and the continuous progress in anatomical and physiological maturation of the CNS accounts for the differential effect of brain injury on premature or full-term neonates.

Several developing brain regions are susceptible to hypoxic damage, including the periventricular white matter, being the most vulnerable region in preterm infant (Inder et al., 1999; Craig et al., 2003). Therefore, oligodendrocytes (OLs) of the cerebral white matter are very susceptible to hypoxic damage in preterm infants (Volpe, 2001). This pattern of brain damage is the main cause of the long-term neurological sequelae known as periventricular leukomalacia (PVL), a leukodystrophy associated with PA (see Ahearne et al., 2016).

On the other hand, grey matter is a main target in the brain of on term infants (see Jensen, 2005). Thus, death or degeneration of neurons under hypoxic conditions occurs most frequently in the brain of on term infants (Ress and Inder, 2005). Several studies using global PA models in rat, showed the vulnerability of neurocircuitries of the basal ganglia (Chen et al., 1995, 1997; Bustamante et al., 2003; Klawitter et al., 2005, 2006, 2007; Perez-Lobos et al., 2017; Lespay-Rebolledo et al., 2018, 2019) and hippocampus (Morales et al., 2005, 2008, 2010 Lespay-Rebolledo et al., 2018, 2019).

The regional vulnerability to the effects of PA can be associated to metabolic imbalance shown by different regions during the re-oxygenation period, including differences in mitochondrial function, activation of intrinsic apoptotic or

antiapoptotic pathways, activation of oxidative stress and/or to recurrent postnatal insults (see Rocha-Ferreira and Hristova, 2016).

Cell vulnerability

In the CNS of mammals, neuronal and glial growth and differentiation are predominantly postnatal events (Altman et al.,1967), and therefore vulnerable to metabolic insults (see Fig. 2).

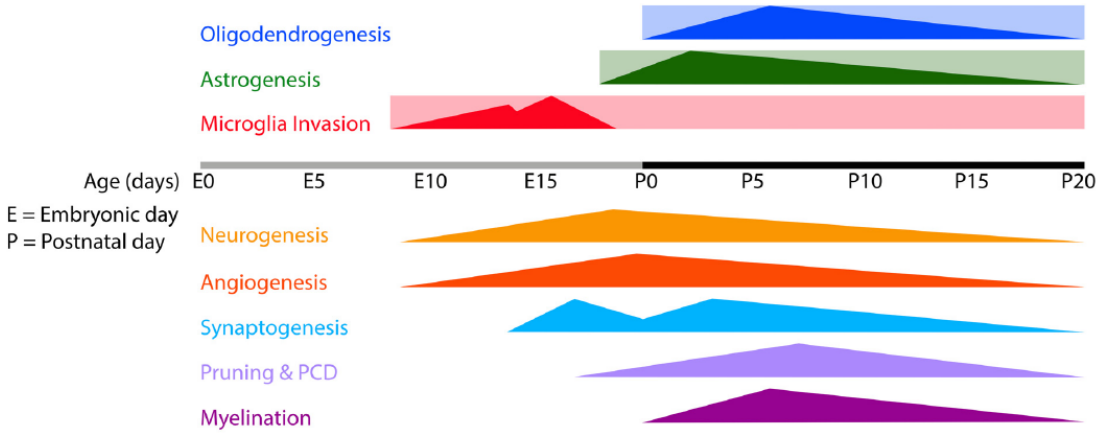

Figure 2. Timeline of microglia invasion, gliogenesis and several developmental processes in the developing rodent brain. Rectangles indicate the estimated periods during/from which microglia invasion, astrogenesis and OLs-genesis are particularly active in the brain. Triangles indicate the onset and peaks of the indicated developmental processes. Abbreviations: E, embryonic; P, postnatal; PCD, programmed cell death (Reemst et al., 2016).

Neuropathological studies indicate that many critical neuronal systems show increased vulnerability to HI injury in the immature brain (Koehler et al., 2018). The vulnerability of immature neurons relates particularly to enhanced density and function of excitatory amino acid (EEA) receptors and decreased buffering capacity to attack by ROS and reactive nitrogen (RNS) species (Volpe, 2008). For example, dopamine neurons of substantia nigra have been reported to be selectively sensitive to hypoxic conditions and oxidative stress, dying by apoptotic caspase-dependent and independent mechanisms (Morales et al., 2008; Edwards and Mehmet, 2008, Perez-Lobos et al., 2017).

Although the pathophysiology of neuronal death following PA has been extensively studied, there is less attention on glial cells, specifically on OLs.

Oligodendroglial lineage

In the CNS, mature OLs are the cells forming myelin, consisting of oligodendroglial plasma membrane loops tightly woven concentrically around the axons (see Miron et al., 2011), allowing the fast saltatory conduction of action potential. In addition to insulation, OLs play a role in growth, stability and axonal maintenance (Wilkins et al., 2003; see Simons and Nave, 2015) by secreting various trophic factors (Dai et al., 2003), participating in the establishment and consolidation of neuronal networks, suggesting that these cells play important roles during brain development, before myelination is established (Doretto et al., 2011). Thus, oligodendroglial injury and myelination deficiency disrupt CNS development, interfering with axonal function, neuronal survival and neurocircuitry consolidation, leading to motor, sensory and cognitive deficits, depending upon the affected systems (Guardia et al., 2010).

Based on the expression of stage-specific surface antigens and morphology, OLs have been classified as: (i) OLs precursor cells (OPC); (ii) pre-OLs; (iii) immature

OLs, and (iv) mature myelinating OLs (Szuchet et al., 2011; see Barateiro and Fernandes, 2014) (see Fig. 3).

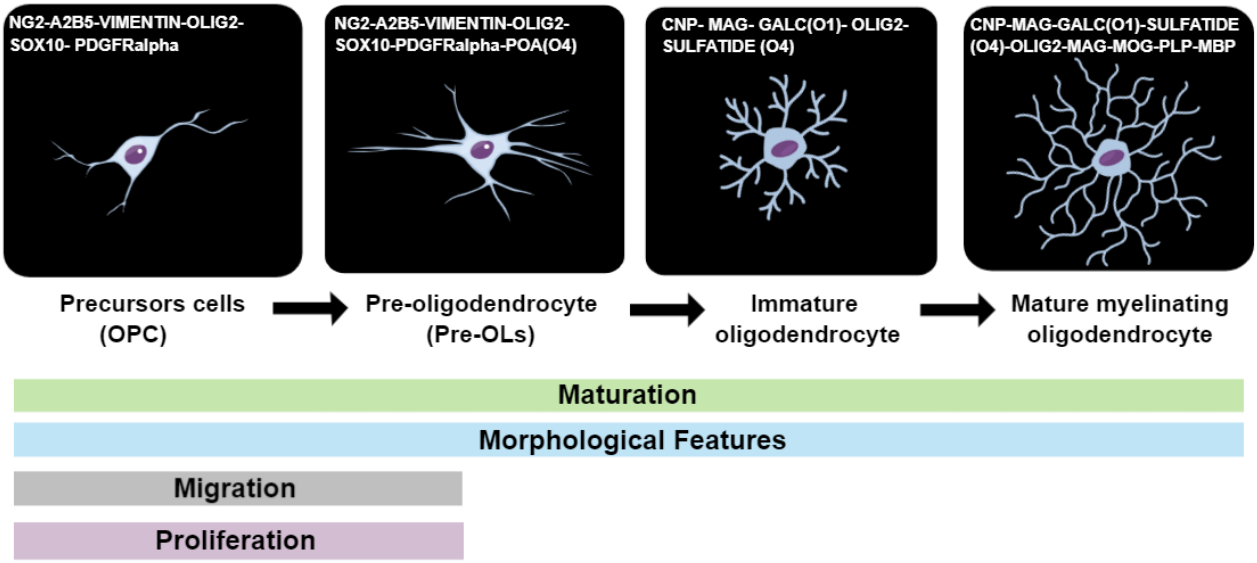

Figure 3. Progression steps of oligodendroglial lineage toward mature OLs. Four principal stages are identifiable according to their increasingly complex morphology (the figure represents *in vitro* morphology), and their ability to proliferate, migrate, differentiate and myelinate. Each stage is uniquely defined by the expression pattern of well-defined marker genes or antibodies. A2B5, O4 and O1 refer to rodent monoclonal antibodies. Olig2 and Sox10 are genes that are highly enriched in premyelinating OLs. Olig2 is also expressed at later stage in the OL lineage. NG2 indicates chondroitin sulfate proteoglycan; PDGFR-α, platelet-derived growth factor; CNPase, 2′,3′-cyclic nucleotide 3′-phosphodiesterase; MAG, myelin associated glycoprotein; GalC, galactocerebroside C; MOG, myelin oligodendrocyte glycoprotein; PLP, proteolipid protein; MBP, myelin basic protein. (Adapted from Barateiro et al., 2014).

The end point of the oligodendroglial linage is the formation of myelin, implying differentiation and maturation, starting with neural stem cells originating from subventricular zone (SVZ), leading to OPCs, which preserve their ability to migrate, proliferate and differentiate into a multipolar, mitotically active pre-OLs, progressing to their final stage, i.e. myelinating OLs (see van Tilborg et al., 2018), and once their processes contact axons they start to produce large amounts of myelin and myelin associated proteins (see Emery, 2010).

OPCs migrate to both grey and white matter areas, undergoing rapid differentiation into mature OLs. At the second postnatal day (P), rodents express pre-OLs, while proper myelination starts only at the first week (Dean et al., 2011).
During maturation, OLs lose their ability to migrate and proliferate (see Barateiro and Fernandes, 2014), changing their morphology, increasing the complexity and the number of processes that wrap around axons and form membrane sheaths of myelin, typical of mature OLs (de Castro and Bribián, 2005).

Myelination

Each step in the oligodendroglial lineage development is precisely regulated by intrinsic and extrinsic factors, ensuring a correct myelination at the right location and at the right time (Kessaris et al., 2006), implying proper formation of myelin sheaths, consisting of lipids, in particular, cholesterol and galactolipids galactosylceramide and sulfatide (see Baumann and Pham-Dinh, 2001; see Baron and Hoekstra, 2010), and of several proteins, including proteolipid protein (PLP) and myelin basic proteins (MBP; Boggs, 2006).

MBP, one of the main protein components of myelin, constitutes over 30% of the total protein content of the CNS (see Boggs, 2006). MBP is the only structural protein found, so far, to be essential for formation of myelin, presumably because of its role for myelin membrane compaction (see Ozgen et al., 2016), and for

maintaining the correct structure of myelin, interacting with the lipids of the membrane (Inouye et al., 1991).

Regulation of myelination is a multifactorial process. Intrinsic and extrinsic cues such as, secreted and contact-mediated factors, protein kinases and phosphatase signalling, extracellular matrix and cytoskeletal reorganization molecules, and transcription factors, control myelination at epigenetic, transcriptional and translational level (Bercury and Macklin, 2015).

Basic helix–loop–helix transcription factors Olig-1 and Olig-2 are co-ordinately expressed along development (see Meijer et al., 2012) and are involved in the modulation of OLs function under physiological and pathological conditions (see Ligon et al., 2006). Specifically, Olig-1 factor is involved in repair of demyelinated lesions, stimulating OLs maturation, while Olig-2 directs the process toward OLs differentiation (Labombarda et el., 2009). Any interruption of their normal biological programmes would result in aberrant myelination (see Singh et al., 2018).

Although myelination is primarily driven by different lineages of OLs, other glial cells contribute also to myelination of the developing brain under homeostatic conditions.

Role of astrocytes in myelination

Astrocytes play a pivotal role for myelination of the developing CNS, although it is relatively less explored how is that performed. Several studies suggest that astrocytes provide an adequate environment for oligodendroglial lineage differentiation (Zhang et al., 2016). Astrocytes support OLs function, since they are the main producers of platelet-derived growth factor (PDGF) and basic fibroblast growth factor (FGF2), both potent mitogens for OPCs and inhibitors of premature OLs differentiation, consequently regulating the timing of myelination (McKinnon et al., 2005). *In vivo* and *in vitro* studies suggest that other soluble factors secreted by

astrocytes, such as leukaemia inhibitory factor-like protein (LIF), brain derived neurotrophic factor (BDNF), gamma-secretase, ciliary neurotrophic factors (CNTF), insulin like growth factor-1 (IGF-1), neurotrophin-3 (NT3) and osteopontin have been implicated for enhancing axonal myelination in developing brain.

Like OLs, astrocytes also synthesize and secrete lipids that contribute to formation of myelin, by modulating cholesterol and fatty acid metabolism via sterol regulatory element binding proteins (SREBPs) and SREBP cleavage-activating protein (SCAP) (Camargo et al., 2017). These authors reported that when lipid synthesis was inactivated in either OLs or astrocytes, myelin synthesis was reduced, and when inactivated in both cell types, myelin synthesis was almost absent. Therefore, extracellular lipids provided by astrocytes contribute to myelination by OLs during normal brain development.

Physical cell-contact between astrocytes and OLs, by laminin/α6β1 integrin interaction-dependent mechanism (Corley et al., 2001), can facilitate survival and maturation of OLs (Orthmann-Murphy et al., 2007). Astrocytes and OLs also establish heterotypic gap junction coupling. Tress et al. (2012) reported that elimination of these gap junctions in mice resulted in death of OLs and delayed myelination, revealing a role for connexins and glial physical connection for myelin maintenance (Tress et al., 2012).

Astrocyte proximity to OLs, in a contact-independent manner, induces profound changes in the levels of several myelin-related genes (Iacobas and Iacobas, 2010). Nash et al. (2011) reported that activated astrocytes increased myelination, while quiescent astrocytes reduced myelinated fibres. This can be attributed to astrocyte morphological changes affecting the physical contact between astrocytes and OLs.

Role of microglia in myelination

The role of microglia on myelination of developing CNS is even less explored than that of astrocytes. Several reports show that under both non-activated and activated status, microglia may promote survival, differentiation and maturation of OPC (Miron et al., 2013). For example, non-activated microglia produce soluble factors that induce activation of the PDGF-α-receptor signalling pathway (Nicholas et al., 2001). The same authors reported that insulin-like growth factor-2 (IGF-2)-receptor signalling pathway promoted oligodendroglial survival, present in conditioned media of both non-activated and interferon gamma (IFNγ)-exposed microglia (Nicholas et al., 2001).

Also*, In vitro* studies have shown that microglia can stimulate the synthesis of sulfatide, MBP and PLP in OLs, suggesting a stimulatory role for microglia during myelinogenesis (Hamilton and Rome, 1994; Pang et al., 2013).

Perinatal asphyxia, oligodendrocyte and myelination deficits

OPCs and OLs are highly susceptible to metabolic insults (see Fig. 4), because of their neurochemical features (e.g. low antioxidant glutathione, high intracellular iron stores, high production of hydrogen peroxide (H_2O_2), expression of AMPA (α-amino-3-hydroxy-5-methyl-4-isoxazolepropionic acid) receptors lacking GluR2 subunits), complex differentiation programs, as well as high metabolic rate and ATP requirement for the synthesis of large amounts of myelin (see McTigue and Tripathi, 2008; see Benarroch, 2009; see Bradl and Lassmann, 2010). Renewal of OLs and myelin continues throughout adult life (Dimou et al, 2008; Young et al, 2013), and myelination in adult CNS maintains its plasticity to respond to brain injury (Nait Oumesmar et al., 2008).

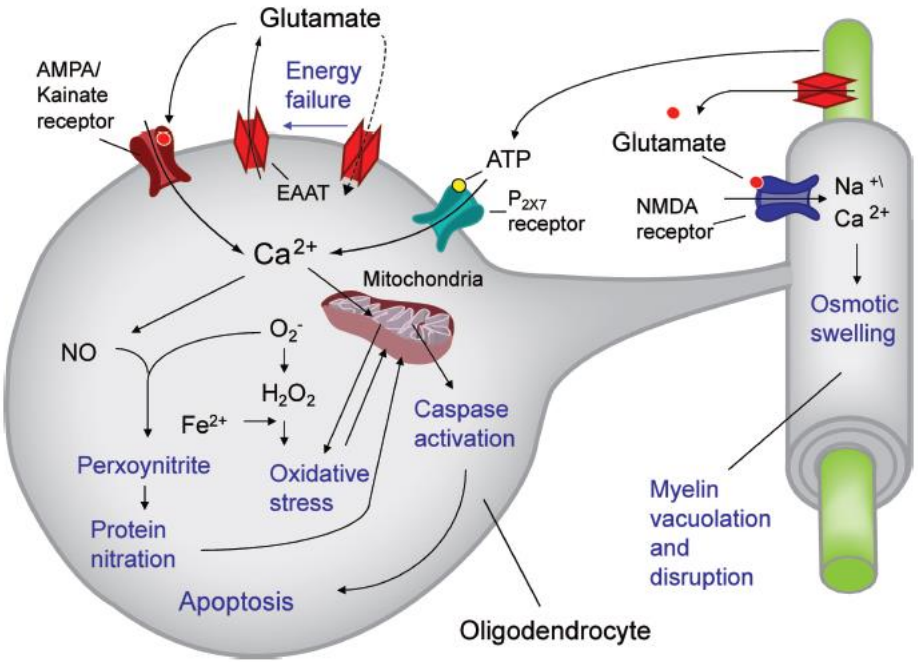

Figure 4. Proposed mechanisms of OLs vulnerability. Reversal of the excitatory amino acid transporters (EAAT) may lead to glutamate release from both OLs and axons under energy failure conditions. OLs are susceptible to injury triggered by excessive activation of calcium (Ca^{2+})-permeable AMPA, kainate, and NMDA glutamate receptors. Furthermore, the over-activation of adenosine triphosphate (ATP)–activated P_{2x7} receptors produces accumulation of cytosolic Ca^{2+}, inducing oxidative stress and apoptosis. (Adapted from Benarroch et al., 2009).

There is evidence indicating that OLs vulnerability depends upon their maturity stage. Pre-oligodendrocytes (preOLs) are particularly susceptible to metabolic insults occurring at birth (see Back and Volpe. 1997; Back et al., 2002a), affecting cerebral myelination at later ages (Ness et al., 2001). It has been reported that postnatal ischemia induces premature oligodendrogenesis and OPC migration to the site of damage, interfering, however, with OLs maturation (Bonestroo et al., 2015), decreasing myelin production (Back et al., 2002a, b; Bonestroo et al., 2015; Ziemka-Nalecz et al., 2018). Postnatal ischemia decreased the number of mature OLs, and myelination, impairing white matter integrity in the infarct area (Skoff et al. 2001; Bonestroo et al., 2015). In agreement, Kohlhauser et al. (2000) reported a long-term effect on myelination following PA, observing a patchy myelin aggregation in hippocampal fimbriae and cerebellum at adulthood. The mechanism by which PA affects white matter generation has not yet been established.

The maximal vulnerability to PVL occurs at a period before the onset of active myelination (see Back and Volpe.1997), which in humans is around postconceptional week 28–32 (Back et al., 2001), equivalent to P2-5 in rats (Craig et al., 2003), when myelination starts, reaching a peak at the second and third postnatal weeks, continuing along adulthood, albeit at a lower rate (Doretto et al., 2011). How the myelination process is performed by mature OLs is not yet fully understood (see Miron et al., 2011). A perinatal metabolic insult would result in white matter damage, implying hypomyelination, while a postnatal insult would lead to demyelination (see Vannucci et al., 1999), by failure of OPC to generate a new preOLs pool, or secondary to neuroaxonal degeneration (Dean et al., 2011). Therefore, we have attempted to elucidate here how that occurs during a developmental window equivalent to that of a preterm human baby, when preOLs phenotype predominates, the highest-risk period for white matter injury (Craig et al., 2003).

Several reports indicate that neuroinflammation can increase proliferation of OPCs, producing long-lasting defects on oligodendroglial maturation and myelination,

probably by disruption of OLs transcription factors (see Volpe et al., 2011; Favrais et al., 2011). Specifically, interferon gamma (IFN-γ) (Horiuchi et al., 2006) and IL-6 (Valerio et al., 2002) induce premature maturation of the OPC and aberrant myelination, thereby also contributing to demyelination. In addition, released proinflammatory cytokines (TNF-α, IL-1β, IL-6) from activated microglia and/or astrocytes following brain injury are also detrimental to the survival of OLs *in vivo* (Favrais et al., 2011, Bonestroo et al., 2015) and *in vitro* (Baerwald and Popko. 1998; Molina-Holgado et al., 2001; Genc et al., 2006). For example, TNF-α can initiate apoptosis in mature OLs by action on TNF-1 receptors (Cammer, 2000; Deguchi et al., 1996; Jurewicz et al., 2005; Horiuchi et al., 2006). Inflammatory mediators may also damage OLs indirectly, via stimulation of free radical production by microglia and possibly also by astrocytes (see Bradl and Lassmann. 2010).

Therapeutic strategy: Mesenchymal stem cells (MSCs)

PA is an important paediatric issue with few therapeutic alternatives. Only hypothermia has shown relevant effects but limited by a narrow therapeutic window (see Drury et al., 2014), still waiting for consensus on clinical protocols (see Ahearne et al., 2016). Recently, the use of MSCs was proposed as a promising therapeutic strategy to manage complex diseases (Ezquer et al., 2016), like hypoxic-ischemic encephalopathy (HIE), specifically PVL (see Janowska et al., 2018).

MSCs are defined as undifferentiated cells, capable of self-renewing, retaining differentiation potency into multi-lineages (see Saeedi et al., 2019). MSCs can be harvested from a wide range of tissue, including among other bone marrow, adipose tissues, deciduous teeth, synovium, periosteum, placenta and umbilical cord (de Girolamo et al., 2013). Adipose tissue stem cells are considered as a type of MSCs for stromal vascular fractions (SVF), which are isolated from fat tissue enzymatically (Chu et al., 2019). It has been demonstrated that all cells isolated

from adipose tissue, bone marrow and umbilical cord blood exhibit a similar fibroblastoid morphology, as fibroblast colony-forming (CFU-F) units, preserving multi-potential differentiation capability and expression of a typical set of surface proteins (Kern et al., 2006). However, adipose tissue is a source of a larger availability of MSCs (millions and billions of cells), allowing collection and harvesting by minimally invasive procedures, compared to those required for other sources. Therefore, adipose tissue-derived MSCs are candidates for novel cellular therapies (Chu et al., 2019).

In order to unify the definition of the basic characteristics of these cells, the International Society for Cellular Therapy (ISCT; see Dominici et al., 2006) declared that MSCs would show: (1) plastic-adherence under standard culture conditions (a minimal essential medium plus 20% fetal bovine serum); (2) specific surface antigen expression, and (3) capacity to differentiate into osteoblasts, adipocytes and/or chondroblasts *in vitro* (see Table 1). Furthermore, MSCs are hardly immunogenic due to the lack of the major histocompatibility complex (MHC) class II expression and costimulatory proteins (e.g. CD80, CD86 and CD40) (Deans et al., 2000).

Table 1. Summary of criteria to identify MSCs (Adapted from Dominici et al., 2006).

1.- Adherence to plastic in standard culture conditions		
2.- Phenotype	**Positive (≥ 95%)** CD105 CD73 CD90	**Negative (≤ 2%)** CD45 CD34 CD14 or CD11b CD79α or CD19 HLA-DR
3.- In vitro differentiation	Osteoblasts, adipocytes and chondroblasts (demonstrated by staining of in vitro cell culture)	

MSCs can selectively migrate toward the site of injury, a process known as homing. It is driven by the expression of specific membrane receptors on MSCs, while ligands are produced by the damaged tissue, facilitating trafficking, adhesion, and infiltration of MSCs to the injured site. Saeedi et al.(2019) described the homing process, pointing out the following sequentially steps: (i) MSCs chemoattraction toward inflammation sites by chemotaxis, involving chemokines and cytokines accumulated in the injured area (for example: TNF-α, IL-1, IL-6, EGF, IGF, VEGF and PDGF); (ii) MSCs adhesion to the injured cells, involving adhesion molecules, such as selectins and integrins; (iii) MSCs infiltration of inflamed tissue, helped by some enzymes, such as MMPs (matrix metalloproteinase) and TIMPs (tissue inhibitors of matrix metalloproteinase). Finally, (iv) MSCs can sense the microenvironment, changing their pattern of secretion, according to the special requirements of the damaged tissue (Ezquer et al., 2016).

Mesenchymal stem cells mechanisms of therapy

Since MSCs display both anti-inflammatory and trophic properties, they have been proposed as therapeutic tools for a number of neuropathological conditions, including those affecting white matter (see Vaes et al., 2019).

MSCs can modify their secretome *in situ,* releasing neurotrophic factors in a paracrine fashion (see Fig. 5), promoting endogenous repair and regeneration (van Velthoven et al., 2010a, b; see Drago et al., 2013), via anti-oxidant activity, proliferation of differentiated cells or activation of resident stem cells (see Saeedi et al., 2019).

MSCs can also modulate adaptive and innate immune responses, which has been therapeutically exploited by several immune disorder models (Constantin et al., 2009; Zappia et al., 2005). Immunomodulation is attributed to several cytokines and regulatory factors (see Fig.5), probably acting by inhibiting proliferation and function of immune cells (see Saeedi et al., 2019). In a pro-inflammatory microenvironment, MSCs are stimulated by cytokines, such as TNF-α and INF-γ (Sullivan et al. 2014), leading to the secretion of anti-inflammatory cytokines (Zhang et al., 2013).

MSCs can induce several anti-apoptotic mechanisms, up-regulating DNA repair, and down-regulating mitochondrial death pathways, increasing antioxidant activity and altering the expression of anti- and pro-apoptotic proteins (see Saeedi et al., 2019). Several mediators are secreted by MSCs (see Fig. 5), including stromal cell-derived factor 1 (SDF-1), insulin like growth factor 1 (IGF-1), hypoxia inducible factor (HIF), vascular endothelial growth factor (VEGF) and Nuclear factor erythroid 2-related factor 2 (Nrf2), which can down regulate pro-apoptotic proteins (Mohammadzadeh et al., 2012).

MSCs have also been associated to angiogenesis and neurogenesis by secretion of neuroprotective, angiogenic and vasculogenic factors (see Fig. 5) (Sun et al., 2015; van Velthoven et al., 2010a; Wei et al., 2015).

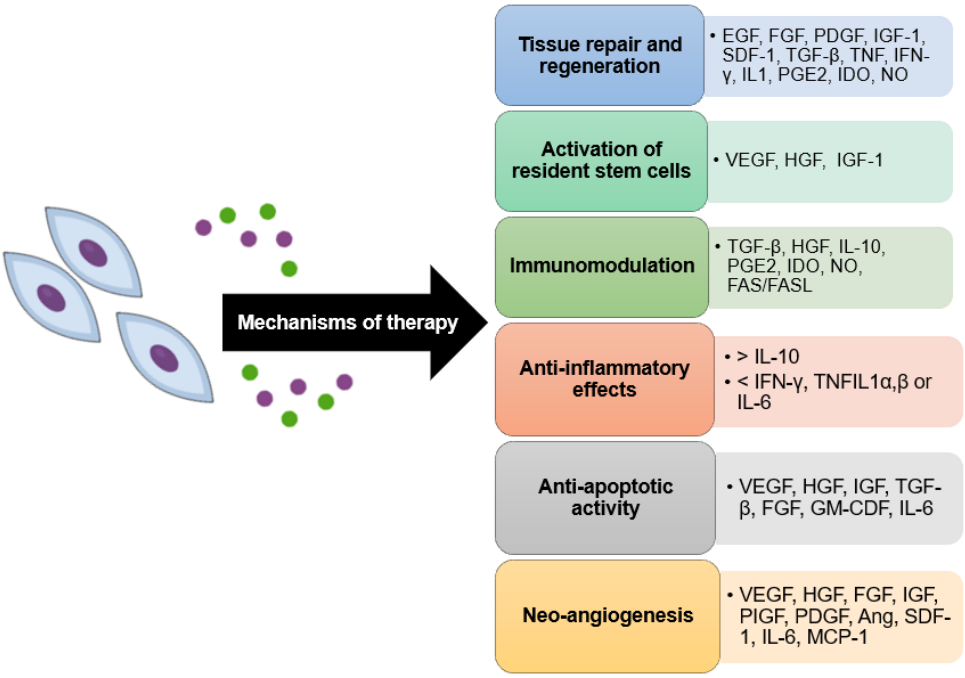

Figure 5. Summary of proposed molecules supporting the therapeutic effects attributed to MSCs. EGF, epidermal growth factor; FGF, fibroblast growth factor; PDGF, platelet-derived growth factor; IGF, insulin like growth factor; SDF-1, stromal cell-derived factor 1; TGF, transforming growth factor; TNF-α, tumour necrosis factor α; IFNγ, interferon-γ; IL, interleukins; PGE2, prostaglandin E2; IDO, indoleamine 2,3-dioxygenase; NO, nitric oxide; VEGF, vascular endothelial growth factor; HGF, hepatocyte growth factor; GM-CSF, granulocyte-macrophage colony-stimulating factor; PIGF, placental-derived growth factor; Ang, Angiopoietin; MCP, monocyte chemoattractant protein.

Mesenchymal stem cells in neonatal pathologies: focus on white matter

MSCs have been proposed as a tool for treating neonatal CNS diseases, since they can secrete neurotrophic factors or differentiate into neuronal or glial cells (see Janowska et al., 2018). van Velthoven et al. (2011), suggesting that MSCs secretome promotes multiple gene expression, involving growth factors and cytokines, pivotal for cerebral cell survival, proliferation and differentiation in response to a hypoxic milieu.

Donega et al. (2014) showed that following HI injury in mouse at P9, MSCs decreased lesion size, improved the functional outcome and reduced scar formation, by stimulating endogenous neurogenesis and lesion repair by secretion of neurotrophic factors. The administration MSCs resulted in nerve fibre remyelination and axonal regeneration, diminished loss of white and grey matter, improved sensorimotor function and improved long-term neurological recovery (Donega et al., 2013; Donega et al., 2015; Liu et al., 2010; Moran et al., 2017). van Velthoven et al. (2010a, b) and Wei et al. (2015) showed that administration of hypoxia-preconditioned MSCs promoted angiogenesis, boosted neurogenesis, oligodendrogenesis, enhancing myelination and reduced white matter loss.

Multiple studies reported reduction of postnatal ischemia-induced cerebral inflammation by MSCs treatment. In a pro-inflammatory microenvironment, MSCs are stimulated by cytokines, such as TNF-α and INF-γ (Sullivan et al., 2014), leading to secretion of anti-inflammatory cytokines (e.g. IL-10, IL-13) (Zhang et al., 2013). It has been shown that MSCs treatment decreases the expression of pro-inflammatory molecules, such as IL-1β and IL-6 (Sun et al., 2015; Wei et al., 2015; seen Orihuela et al., 2016;), and the number of activated astrocytes and microglial cells, suggesting immunomodulation (Sheikh et al., 2011; Donega et al., 2014; Wei et al., 2015). Also, MSC treatment, given within the first 10 days after injury, prevents apoptosis (Bonestroo et al., 2015; Donega et al., 2013).

In the present study, we investigated whether there is a sustained myelin deficit and OLs injury induced by PA up to P14, a critical postnatal period characterised by a spur of neuronal networking (Voorn et al., 1988; see Vitalis et al., 2005; see Herrera-Marschitz et al., 2011, 2014), evaluating the effect of neonatal MSCs treatment.

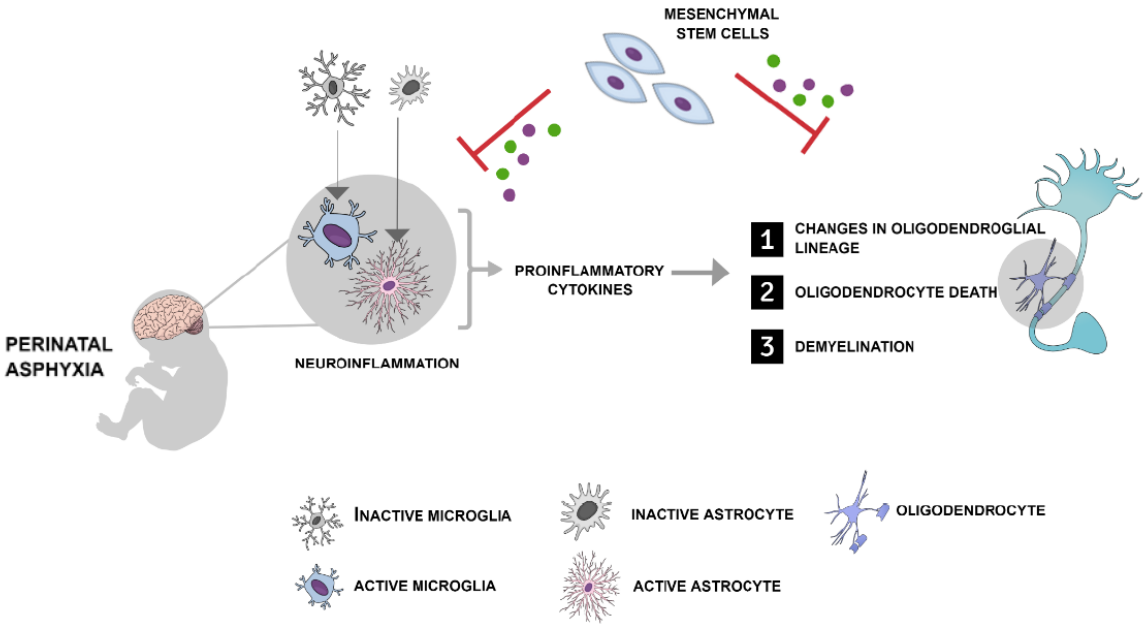

Figure 6. Research proposal. PA induces regionally differential changes on myelination, oligodendroglial lineage and viability of mature OLs. Neuroinflammation is one of the mechanisms inducing damage in the oligodendroglial linage. The study evaluated whether these effects can be prevented by intracerebral MSCs treatment.

II. HYPOTHESIS:

PA induce regionally a differential change on myelination, mature OLs, cell death and neuroinflammation that is prevented by intracerebroventricular (icv) administration of MSCs.

IV. GENERAL OBJECTIVE:

(1) To determine the short and long-term effects of PA on myelination, OLs maturity, neuroinflammation and cell death, monitored in telencephalic and hippocampal white matter of rats.

(2) To evaluate the effect of MSCs treatment on changes induced by PA.

V. SPECIFIC OBJECTIVES:

1. To determine the effect of PA on myelination, mature OLs and oligodendroglial death by immunofluorescence (IF), reverse transcription polymerase chain reaction (RT-PCR) and TUNEL in telencephalon and hippocampus of rat neonates at postnatal day (P)1, P7 and P14.

2. To determine the effect of PA on neuroinflammation, focusing on microgliosis, astrogliosis, and expression of pro-inflammatory cytokines by IF, RT-PCR and ELISA in telencephalon and hippocampus of rat neonates at P1, P7 and P14.

3. To isolate and characterise MSCs treatment according to:

   3.1 Their adipogenic, osteogenic and chondrogenic potential by Oil Red O, Alizarin Red and Safranin O staining respectively.
   3.2 Immuno-phenotypification of MSCs according to their putative murine MSCs markers and hematopoietic cell lineages markers by flow cytometry

4. To determine the short and long-term effects of MSCs treatment on functional parameters (by Apgar, open field assays), myelination, mature OLs and cell death (by IF) in telencephalon of rat neonates at P7.

VI. MATERIALS AND METHODS

1.Animals

Wistar rats from the animal station of the *Molecular & Clinical Pharmacology Programme, ICBM*, Faculty of Medicine, University of Chile, Santiago, Chile, were used along the experiments. The animals were kept at a temperature- and humidity-controlled environment with a 12/12 h light/dark cycle, with access to water and food *ad libitum* when not used in the experiments, monitoring permanently the well-being of the animals by qualified personnel.

2.Ethic Statement

All procedures were conducted in accordance with the animal care and use protocols established by a Local Ethics Committee for experimentation with laboratory animals at the Medical Faculty, University of Chile (Protocol CBA#0943 FMUCH) and by an ad-hoc commission of the Chilean Council for Science and Technology Research (CONICYT), endorsing the principles of laboratory animal care (NIH; N° 86-23; revised 1985). Animals were permanently monitored (on 24 h basis) regarding wellbeing, following the ARRIVE guidelines for reporting animal studies (www.nc3rs.org.uk/ARRIVE).

3. Global PA model

Pregnant Wistar rats within the last day of gestation (G22) were euthanized and hysterectomised. Two or three pups per dam were removed immediately and used as non-asphyxiated caesarean-delivered controls (CS). The remaining foetuses-containing uterine horns were immersed into a water bath at 37°C for 21 min (asphyxia-exposed rats, AS). Following asphyxia, the uterine horns were incised, and the pups removed, stimulated to breathe and evaluated with an Apgar scale for rats after an approximately 40 min observation period on a warming pad,

according to Dell'Anna et al. (1997), and nurtured by a surrogate dam (see Fig. 7). The physiological parameters were also monitored up to P14, comparing the same CS and AS cohorts.

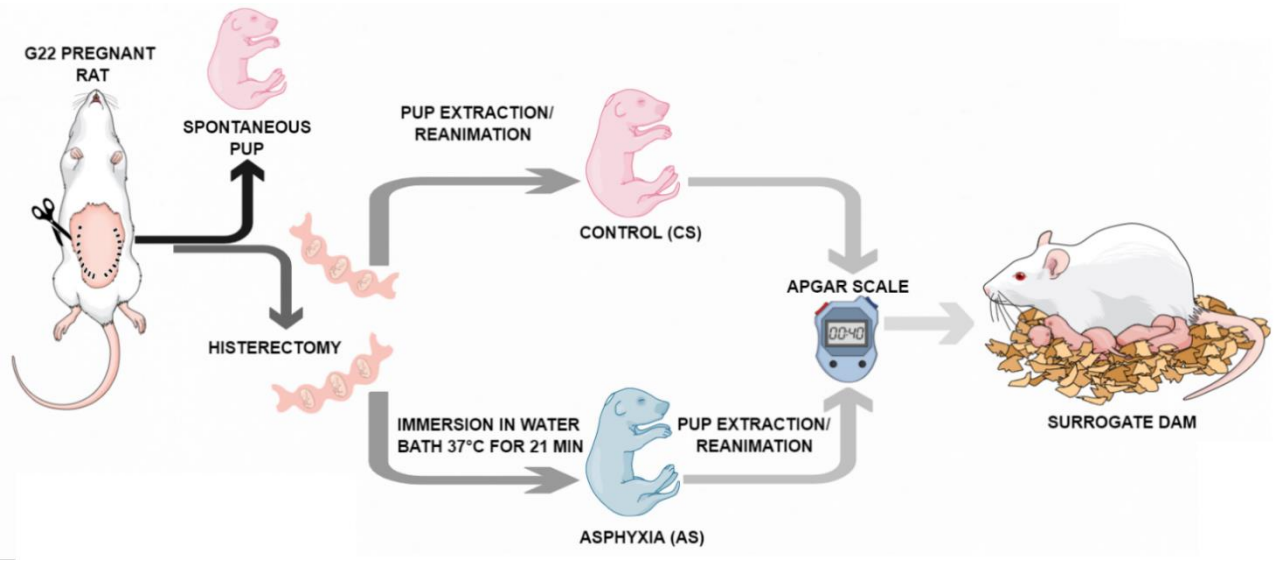

Figure 7. Model of global PA. Pregnant Wistar rats at gestation day 22 (G22) were euthanized and hysterectomised. Two or three pups were removed immediately, corresponding to caesarean-delivered controls (CS), and remaining foetuses were immersed into a water bath at 37°C for 21 min (AS) inducing severe asphyxia. Following asphyxia, pups were removed from the uterine horns, stimulated to breathe and after 40 min evaluated by an Apgar scale adapted for rats, thereafter, the neonates were given to surrogate dams, pending further experimental procedures (Bielke et al. 1991; Andersson et al. 1992; Herrera-Marschitz et al.1993).

4.Open field testing

Locomotor activity (P1 to P14) was evaluated by an open field test. Exploratory behaviour was examined in a square arena with a dimension of 21 × 29 cm, with a continuous wall of 15 cm high, lightened by one incandescent light bulb, placed in a noise-free room. The top of the arena is open to the ambient and the square arena has a white coloured background. A camera placed 10 cm over the arena and connected to a CPU was used to record the rat performance. Each animal was placed in the centre of the arena free to explore for 2 min, during which the behaviour of rats was continuously observed. The data processing algorithms were developed using an automated video-tracking Matlab routine (Mathworks, Inc, USA).

The following parameters were monitored: (i) total travelled distance (cm); (ii) total moving time (%; with respect to the total monitoring time); and (iii) total time spent in the central zone of the open-field (s).

5.Isolation and ex vivo expansion of rat adipose tissue-derived Mesenchymal stem cells

Wistar female rats (220-250 g) were anesthetised and euthanized. For isolation of MSCs, dorsal subcutaneous fat was dissected, washed with phosphate-buffered saline (PBS) and cut into small pieces. Tissue was digested with 1 mg/mL collagenase type II (Gibco, Grand Island, NY, USA) in PBS, incubated under agitation at 37°C for 90 min. At the end of digestion, 10% foetal bovine serum (FBS; Gibco, Auckland, New Zealand) was added to neutralize collagenases. The mixture was centrifuged at 400 g for 10 minutes to remove floating adipocytes. Pellets were re-suspended in alpha-minimum essential medium (α-MEM; Gibco), supplemented with 10% FBS and 0.16 mg/mL gentamicin (referred to as α-10 medium), plated at a density of 7.000 cells/cm^2. Cells were cultured at 37°C in a 5% CO2 atmosphere. When foci reached 80% confluence, cells were detached

with 0.25% trypsin (Sigma-Aldrich, St. Louis, MO, USA), centrifuged and sub-cultured at 7 x 10^3 cells/cm^2. The cells were frozen at -80 °C in a cryopreservation medium, pending further experiments.

6.Characterization of Mesenchymal stem cells

After 2 subcultures, adherent cells were characterized according to their adipogenic, osteogenic and chondrogenic potential. The cells were incubated with standard adipogenic (1 µM dexamethasone and 10 µM rosiglitazone for 14 days), osteogenic (0.1 µM dexamethasone, 50 µg/ml L-Ascorbate 2-phosphate and 10 mM b-glycerol phosphate for 21 days) and chondrogenic differentiation media (0.1 µM dexamethasone, 0.1 µg/ml L-Ascorbate 2-phosphate, 0.5 UI/mL insulin and 10 ng/ml transforming growth factor beta-3 for 10 days), as previously described (Ezquer et al., 2015, 2016). To evaluate the adipogenic potential, cultures were stained with 60% Oil Red O for 1 hour (Sigma-Aldrich).

To evaluate the osteogenic potential, cultures were fixed with 70% ethanol for 30 minutes and stained with 40 mM Alizarin Red (Sigma-Aldrich) for 10 min. To evaluate the chondrogenic potential, cultures were fixed with 70% ethanol for 10 minutes and stained with 0.1% Safranin O (Sigma-Aldrich) for 5 minutes. Once washed, cells were observed and photographed by light microscope (ECLIPSE TS100. Nikon, Japan). Immunophenotyping was performed by flow cytometric analysis after immunostaining with monoclonal antibodies against the putative murine MSCs markers CD-29 (FITC-conjugated) and CD-90 (PE-conjugated), or characterised for markers of hematopoietic cell lineages, CD-45 (APC-conjugated) and CD-11b (APC-conjugated). All antibodies were purchased from BD Biosciences (San Diego, CA, USA).

7.Administration of Mesenchymal stem cells

Two hours after PA, neonates were randomly assigned to three experimental conditions (including CS and AS animals for each condition): (i) a basal condition; (ii) a single intracerebroventricular (*icv*) administration of vehicle (5 µl of 10% rat plasma in saline); or (iii) a single *icv* administration of MSCs (5 µl of 5 x 10^4 cells) (see Fig. 8). The *icv* treatment was performed under cryoanaesthesia with a cannula implanted 1 mm lateral to Bregma, 2 mm deep under the scalp, injecting slowly with a 50-µl Hamilton syringe and a properly prepared injection cannula (0.6 mm of diameter, with a sharped tip less than 0.2 mm of diameter), connected with a dialysis tubing, kept manually in place for 2 min after the injection was performed. The neonates were continuously observed until given to a surrogate dam.

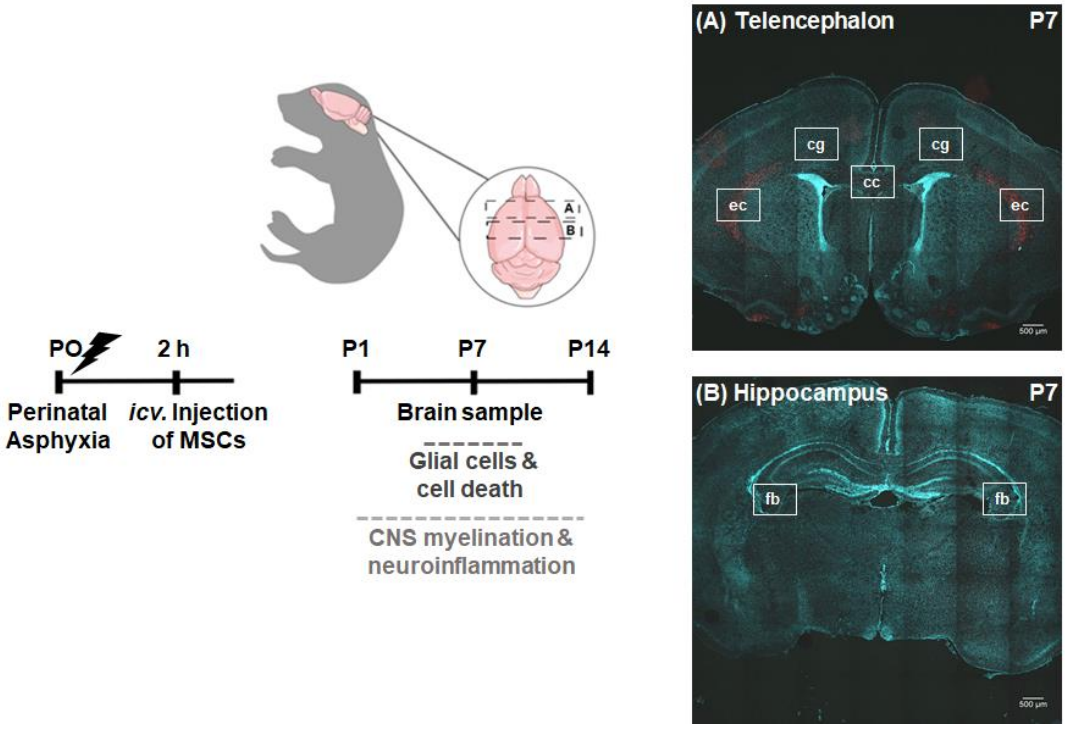

Figure 8. A schematic diagram of the experimental design. The effect of PA on CNS myelination and neuroinflammation was evaluated in vivo, focusing on (A) telencephalon (external capsule, *ec*; corpus callosum, *cc*; cingulum, *cg*), and (B)

fimbriae of hippocampus (*fb*) at P1, P7 and P14 in AS and CS rat neonates. At P7, the effect of PA on glial cells and viability was also evaluated. Rat adipose tissue-derived MSCs were intracerebroventricular (*icv*) administered 2 hours after the insult.

8.Tissue sampling for immunofluorescence (IF)

Sampling and preparation of brain tissue for IF was performed according to Morales et al. (2008). Briefly, rats at P1, P7 and P14 were anesthetised and perfused intracardially with 0.1M PBS (pH 7.4), followed by a formalin solution (4% paraformaldehyde in 0.1M PBS, pH 7.4). The brain was removed from the skull, post-fixed in the same fixative solution overnight at 4°C and immersed in 10% sucrose containing 0.1 M PBS for 2 days and subsequently in 30% sucrose at 4°C for 2 days. Coronal sections (20 µm thick) of the telencephalon (between Bregma 1.20 and 0.60 mm at P1; at 0.60 and 0.20 mm at P7; -0.40 mm and -0.20 mm at P14) and hippocampi (between Bregma -0.40 and -1.00 mm at P1; -1.40 and -2.00 mm at P7; -1.60 and -2.40 mm at P14; https://www.ial-developmental-neurobiology.com/en/publications/collection-of-atlases-of-the-rat-brain-in-stereotaxic-coordinates) were obtained using a cryostat (Thermo Scientific Microm HM 525) (see Fig. 8) and processed for IF against myelinated fibers and mature OLs (MBP), astrocytes (GFAP) and microglial (Iba-1) phenotypes.

9.Antibodies

Primary antibodies (see **Table 2**)*:* (i) anti-MBP (as marker for myelinated fibres and mature OLs phenotype, incubated in blocking solution containing 1% bovine serum albumin (BSA), 5% normal goat serum (NGS) and 0.3% Triton X 100); (ii) anti-glial fibrillary acidic protein (GFAP, as a marker for astrocyte, incubated in blocking solution containing 10% NGS and 0.3% Triton X 100); and (iii) anti-ionized calcium binding adaptor molecule 1 (Iba-1, as a microglial marker, incubated in blocking solution containing 1% BSA, 10% NGS and 0.3% Triton X

100).

Secondary antibodies (see **Table 2**)*:* (i) anti-chicken-Alexa594 (incubated in blocking solution containing 1% NGS); (ii) anti-mouse-Alexa488 (incubated in blocking solution containing 0.3% Triton X100); and (iii) anti-rabbit-Alexa488 (incubated in blocking solution containing 1% NGS).
IF: Coronal sections were rinsed with 0.1M PBS and treated with blocking solutions for 1 h, incubated with primary antibodies against glial cell phenotype (MBP, GFAP or Iba-1) in blocking solution overnight at 4°C in darkness. After repeated rinsing with 0.1M PBS, samples were incubated with the corresponding secondary antibodies and counterstained with 4,6 diamino-2-phenylindol (DAPI, Invitrogen 0.02 M; 0.0125 mg/ml; for nuclear labelling) for 2 h. After rinsed, the samples were mounted with Fluoromount and examined by confocal microscopy (Olympus-fv10i, Center Valley, PA, USA).

Table 2. Primary and secondary antibodies. The information includes manufacturers (including catalogue number), host, class (monoclonal or polyclonal), type (primary or secondary), and standardized dilution.

Antibody	**Manufac-turers**	**Host**	**Class**	**Type**	**Dilutions**
anti-MBP	Aves Labs; #MBP	Chicken	Monoclonal	Primary	1 : 750
anti-GFAP	Sigma Aldrich; #3893	Mouse	Monoclonal	Primary	1 : 500
anti-Iba-1	Wako #019-19741	Rabbit	Monoclonal	Primary	1 : 500
anti-chicken-Alexa594	Invitrogen; #A-11042	Goat	Polyclonal	Secondary	1 : 400
anti-mouse-Alexa594	Invitrogen; #A-11001	Goat	Polyclonal	Secondary	1 : 500
anti-rabbit-Alexa488	Invitrogen; #A-11034	Goat	Polyclonal	Secondary	1 : 500

10.TUNEL assay

Preparation of brain tissue for TUNEL assay was performed according to Perez-Lobos et al. (2017). Formalin-fixed coronal sections were stained with the ApoTag Peroxidase In Situ Apoptosis Detection Kit (Millipore, # 90418) according to manufacturer's instructions. Coronal sections were rinsed three time with 0.1M PBS, permeabilized with a solution containing 50% ethanol and 50% acetic acid for 5 min at 20°C and treated with 3% H_2O_2 in methanol for 10 min for endogenous peroxidase quenching. Then, the sections were washed with a commercial solution provided by the manufacturer of the TUNEL assay, to be incubated with TdT Enzyme at 37°C during 80 min. The reaction was stopped with Stop Wash Buffer and incubated with a Ready-to-Use-anti-digoxigenin HRP-conjugated antibody. After rinsing, the samples were incubated with 488 conjugated tyramide (1:100 diluted in 0.1M PBS), as substrate for HRP enzyme, at room temperature for 10 min and then rinsed with 0.1M PBS.

11.Image processing and stereological analysis

The following parameters were monitored: (i) myelination, for which a fixed intensity threshold for each area was defined, calculating the ratio of positive stained pixels for MBP, over the total pixel number, as previously described (Monin et al., 2015); (ii) number of MBP positive cells/mm^3, counterstaining for DAPI (nuclear staining) in all cases; (iii) number of GFAP-DAPI positive cells/mm^3; (iv) number of Iba-1-DAPI positive cells/mm^3; (v) TUNEL positive cell/mm^3, for quantification of apoptotic-like DNA fragmentation; and (vi) TUNEL-MBP-DAPI positive cells/mm^3.

Microphotographs were taken from highly myelinated areas of telencephalon and hippocampus, including both hemispheres, focusing on: (i) external capsule (10 fields); (ii) corpus callosum (5 fields); (iii) cingulated gyrus (2 fields); and (iv) fimbriae of hippocampus (see Fig. 8), with an Olympus confocal FV10i

microscope using 60x objective lens (NA1.30). The area inspected for each stack was 0.04 mm^2. The thickness (Z-axis) was measured for each case. The number of positive stained cells for each marker; expressed as cells/mm^3 in samples from CS and AS, was counted using ImageJ software, confirmed by proper DAPI labelling. MBP, GFAP and Iba-1 positive cells were counted manually when immunoreactivity overlapped at three levels through a section (Z-step 1 µm). An investigator blinded to the treatment made the respective quantifications for all parameters.

12.RT-qPCR and Enzyme-Linked Assay (ELISA)

Tissue sampling

The animals were euthanized at P1, P7 or P14 by decapitation. The brain was quickly removed for dissecting out telencephalon and hippocampus. Dissection was performed on ice, using a newborn rat brain slicer (Zivic Instruments Pittsburgh, PA 15237 USA). The samples were stored at -80°C pending further experiments.

Homogenization of tissue, extraction, and quantification of RNA for RT-qPCR

Telencephalon samples at P1, 7 and 14 were homogenized with a Cordless Pellet Pestle homogenizer (Kimble Chase). Total RNA was purified using TRIzol reagent (Invitrogen, USA). The concentration and purity of total RNA was determined for optical density 260/280 absorption ratios. RNA integrity was evaluated by denaturing gel electrophoresis. One microgram of total RNA was used to perform reverse transcription with MMLV reverse transcriptase (Invitrogen) and oligo dT primers. RT-qPCR reactions were performed to amplify: (i) Oligodendrocyte transcription factors Olig-1 and Olig-2; (ii) myelin basic proteins MBP, and (iii) the inflammatory cytokines IL-1β, IL-6, TNF-α and COX-2, using a Light-Cycler 1.5 thermocycler (Roche, Indianapolis, IN). RT-qPCR was performed using 2X Brilliant III SYBR® Green QPCR Master Mix (Agilent Technologies, USA) in a MX3000 system (Stratagene, La Jolla, CA, USA). Primer sequences used for amplification

are indicated in table 3. β-Actin was chosen as housekeeping gene based on the similarity of mRNA expression across all sample templates. Relative quantification was performed by the ΔΔCT method.

Table 3. Specific primers for RT-qPCR amplification.

Genes	Primer Forwards	Primer Reverse	Amplicon size
MBP	AGTCGCAGAGGACCCAAGAT	GACAGGCCTCTCCCCTTTC	103 bp
Olig-1	GCCCAGGCCACGAGTACAAA	TCCACTCCGAAACCCAACGA	121 bp
Olig-2	GAAATGGAATAATCCCGAACTACT	CCCCTCCCAAATAACTCAAAC	232 bp
Cox-2	GTTTGGAACAGTCGCTCGTCATC	TGTATGCTACCATCTGGCTTCGG	94 bp
TNF-α	AAATGGGCTCCCTCTCATCAGTTC	TCTGCTTGGTGGTTTGCTACGAC	111 bp
IL-1β	CACCTCTCAAGCAGAGCACAG	GGGTTCCATGGTGAAGTCAAC	79 bp
IL-6	TCCTACCCCAACTTCCAATGCTC	TTGGATGGTCTTGGTCCTTAGCC	79 bp
β-actin	AAGTCCCTCACCCTCCCAAAAG	AAGCAATGCTGTCACCTTCCC	97 bp

Homogenization of tissue and protein quantification for ELISA

Telencephalon obtained at P7 was lysed and homogenized with a Cordless Pellet Pestle homogenizer (Kimble Chase) in RIPA lysis buffer (Thermo, Waltham, MA), supplemented with protease inhibitors (Thermo, Waltham, MA). The lysates were incubated under agitation at 4°C for 20 min, centrifuged at 8,000 g, 4°C, for 5 min. The supernatant was transferred to fresh Eppendorf tubes, and stored at -80°C, pending further experiments.

Total protein concentration was determined by a commercially available Microplate Bicinchoninic acid (BCA) protein assay kit-reducing agent compatible from Pierce (Thermo Fisher Scientific). Absorbance was measured at 562 nm in a Multi-Mode Microplate Reader (Synergy HT Biotek Instruments, Inc., Winooski, VT, USA). Quantification of IL-6 protein levels was performed by a Rat IL-6 ELISA kit (BMS625; Invitrogen) following manufacturer's instructions. Briefly, 50 µL of standard, control or sample was added into microplates coated with a monoclonal antibody against IL-6 and incubated with a biotin-conjugated anti-rat IL-6 antibody for 2 h at room temperature in shaker at 400 rpm. Plates were washed and incubated with 100 µL of Streptavidin conjugated with horseradish peroxidase (HRP) for 1 h at room temperature in shaker at 400 rpm. The plates were rinsed and incubated with 100 µL of the substrate solution, containing hydrogen peroxide (H_2O_2) and tetramethylbenzidine as chromogen for 30 min at room temperature. The reaction was stopped and optical density was determined using a Multi-Mode Microplate Reader (Biotek® Instruments, Inc) set at 450 nm. The concentration of protein levels was calculated by interpolation from a standard curve for IL-6 (from 8 standard dilutions: 31.3–4,000 pg/mL), using a five-parameter curve fit model (MyAssay software).

13.Statistics

Data analysis was performed with a XLSTAT software, version 2019. 16.0.11601 (ADDINSOFT SARL, Paris, France). Parametric comparisons were performed by t-test or two-way ANOVA followed by Benjamini-Hochberg correction as a post hoc test for multiple comparisons. All results are expressed as means ± standard error of the means (SEM). For statistically significant differences, the probability of error was set up to less than 5%.

VII. RESULTS

Perinatal Asphyxia: Apgar Scale and postnatal evaluation

Apgar scale. Table 4 shows the outcome of the insult. The physiological status was evaluated by an Apgar scale applied 40 min after delivery (the time of the uterine excision), comparing AS versus CS rat pups. The following parameters were also monitored at P1, P7 and P14 after delivery: (i) survival (yes/no, in % for the corresponding litter); (ii) body weight (g); (iii) presence of gasping (yes/no; in % for the corresponding litter); (iv) respiratory frequency (events/min); (v) skin colour (pink, P to blue, B); (vi) spontaneous movements (0–4; 0 = no movements; 4 = coordinated movements of forward and hind legs, as well as head and neck), and (vii) vocalisation (yes/no; in % for the corresponding litter). The rate of survival shown by AS neonates was ~60%, while it was 100% for CS neonates. Surviving pups showed decreased respiratory frequency (by ~50%, supported by forced gasping), decreased vocalization (by ~50%), blue (cyanotic) skin, rigidity and akinesia, indicating a severe insult.

Postnatal evaluation (see **Table 4**). The animals were observed up to P14, monitoring reception by the surrogate dam. When received by surrogate dams, no significant differences were observed on survival rate among AS and CS neonates. However, there were some signs of a sustained physiological deficit, mainly affecting respiratory parameters. AS neonates showed a decreased respiratory frequency along P1 (by~20%), P7 (by ~20%) and P14 (by ~14%).

Table 4. Apgar Scale and postnatal evaluation. Data is expressed as means ± SEM, whenever the parameters were monitored by continuous scales, or by % of the corresponding litter in cases of qualitative no continuous scales (n, number of pups; m, number of dams). The effect perinatal asphyxia (PA) (b) was evaluated on (i) survival ($F(1, 45)= 7.701$, $P < 0.0001$); (ii) body weight ($F(6,322)= 119.283$, $P < 0.0001$); (iii) gasping (yes/no; in % for the corresponding litter) ($F(4, 60) =4.746$, $P< 0.002$); (iv) respiratory frequency (events/min) ($F(4,178) = 107.689$, $P < 0.0001$); (v) colour of skin (% pink-blue P-B, blue-pink B-P, or blue B, colour skin ($F(4, 45) =23.828$, $P < 0.0001$); (vi) spontaneous movements (0–4; 0 = no movements; 4 = coordinated movements of forward and hind legs, as well as head and neck) ($F(4, 138)= 98.523$, $P < 0.0001$); (vii) vocalisation % (yes/no; in % for the corresponding litter) ($F(4,70)= 10.440$, $P < 0.0001$). (Benjamini-Hochberg as a post hoc test). *P < 0.05, **P < 0.01, ***P < 0.001 and ****P < 0.0001 (Bold).

Table 4. Apgar Scale and postnatal evaluation.

A. CS (n=75; m = 20)	**40 min**	**P1**	**P7**	**P14**
Survival (%)	100	100	100	100
Body weight (g)	6.07±0.08	6.60±0.09	14.86±0.93	23.05±3.36
Gasping (%)	1.053±1.05	0	0	0
Respiratory frequency (events/min)	74.29±1.36	81.33±3.77	94.67±4.92	100±5.59
Skin colour (P%)	98±1	100	100	100
Spontaneous Movements (4–0)	3.74±0.07	4	4	4
Vocalisations (%)	98±1	100	100	100
B. AS (n= 72; m= 20)				
Survival (%)	63±6 **(by ~40%)b******	100	100	100
Body weight (g)	7.38 ± 0.64	7.73±0.91	13.90 ± 0.63	16.54 ± 2.49
Gasping (%)	**36.76±10.51 (> 35x)b****	0	0	0
Respiratory frequency (events/min)	**32.53±2.00 (by ~55%)b******	**59.00±1.92 (by ~20%)b******	**75.20±6.47 (by ~20%)b******	**86.00±2.00 (by ~14%)b******
Skin colour (P%)	0	100	100	100
Spontaneous Movements (4–0)	**0.50±0.10 (by ~90%)b******	4	4	4
Vocalisations (%)	**44.72±10.55 (by ~55%)b******	100	100	100

Motor impairment observed in AS-exposed versus CS rats

The following parameters were monitored: (i) total travelled distance (cm); (ii) total moving time (%; with respect to the total monitoring time), both at P1-P14; and (iii) total time spent in the central zone of the open-field (s) at P14, for each experimental condition.

Figure 9 shows the exploratory behaviour examined in a square arena (open field) at P1 to P14. At P1 and P7, the trunks of all rats remained in contact with the floor of the field during resting, as shown in Geisler et al. (1993). At P7 the pups remained in a prone position along the observation period, except after an accidental turn on the back. At P14, the neonates walked with a slow and tremulous pattern. At P7 and P14, *total travelled distance* (cm) was increased in both CS and AS conditions in all experimental group, compared to that corresponding to observed at P1, without any differences between CS and AS animals. There was a decrease in *total travelled distance* (cm) and in *moving time* in AS at only P1, compared to that observed in CS group (see Fig. 9A-9B). Figure 9C shows that there were no significant differences between CS and AS groups at P14 respect to the *time spent in the centre of the arena.*

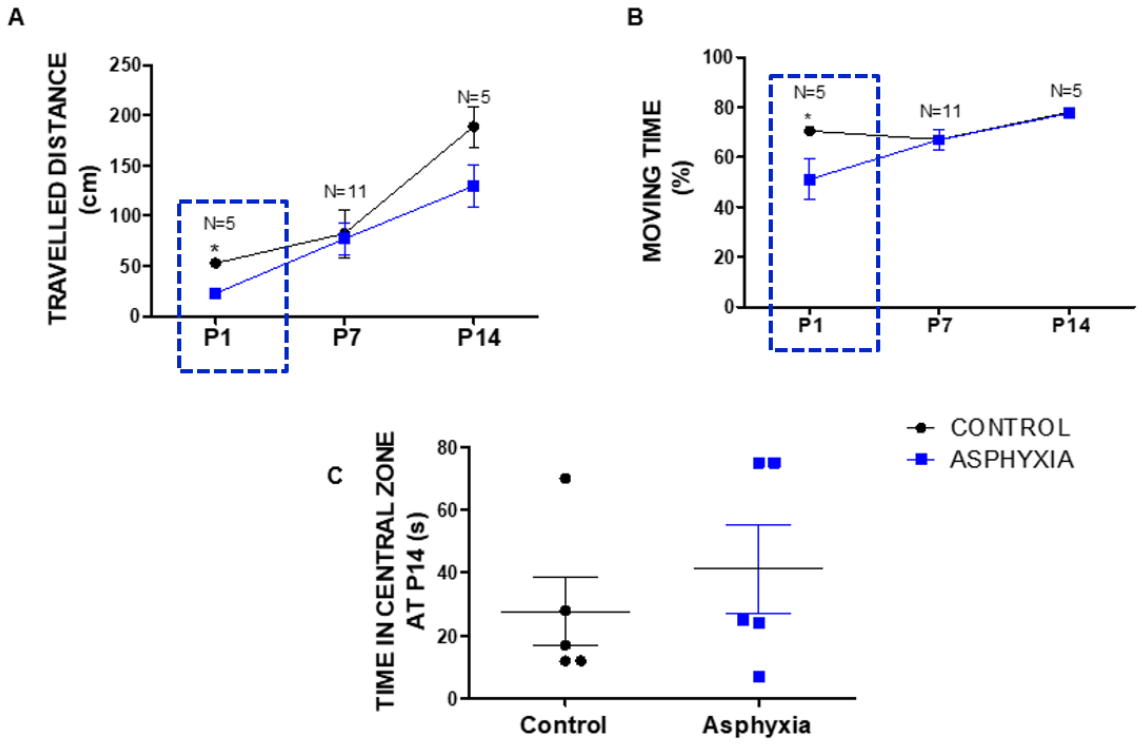

Figure 9. Motor behaviour monitored at P1 to P14: Effect of PA. The following parameters were monitored after delivery: (A) total travelled distance (cm); (B) total moving time (%; with respect to the total monitored time), both at P1 to P14; and (C) total time spend in the centrum of the arena, obtained from neonates after their eyes opened at P14. Data are as means ± S.E.M (from N=5 independent experiments). Unbalanced two-way ANOVA was used for testing the effect of PA and P on total travelled distance ($F_{(3,38)}$ = 9.377, P < 0.0001); and total moving time ($F_{(4,37)}$ = 4.395, P= 0.005). Benjamini-Hochberg was used as a post hoc test. Student's t –test was used for comparing the effect of PA on total time spent in the centrum of the arena at P14 (t= -0.749 df= 8, p= 0.476). *P < 0.05, **P < 0.01, ***P < 0.001 and ****P < 0.0001 (italics) vs. CS group.

Effect of neonatal development and PA on myelination in telencephalon (external capsule, corpus callosum, cingulum) and fimbriae of hippocampus at P1, P7 and P14.

Figure 10 shows representative microphotographs obtained by confocal microscopy showing DAPI (nuclei, blue) and MBP fluorescence (labelling OLs and myelination, red) in *external capsule* (A), *corpus callosum* (B), *cingulum* (C) and *fimbriae of hippocampus* (D) of control (CS) and asphyxia-exposed (AS) neonates at P1, P7 and P14. A similar amount of DAPI positive nuclei was observed under all experimental conditions. No MBP was seen at P1, but MBP labelling was significantly increased at P7 (as OLs or myelin fibres), and at P14 (mainly as compact packages of myelin), both in CS and AS neonates. The myelination progression was, however, different in the analysed regions.

At P7, both OLs and myelin fibres were evident in *external capsule*, while at P14, OLs could not be seen any longer as independent structures, because of the dense amount of MBP positive fibres, both in CS and AS animals. In *corpus callos*um, OLs with long and branched processes were evident at P7, while at P14, as for external capsule, MBP positive fibres dominated over individual OLs. In *cingulum*, some OLs and myelin fibres could be seen, but MBP fibres also dominated at P14. In *fimbriae of hippocampus* few OLs could be seen at P7, but again MBP fibres dominated at P14.

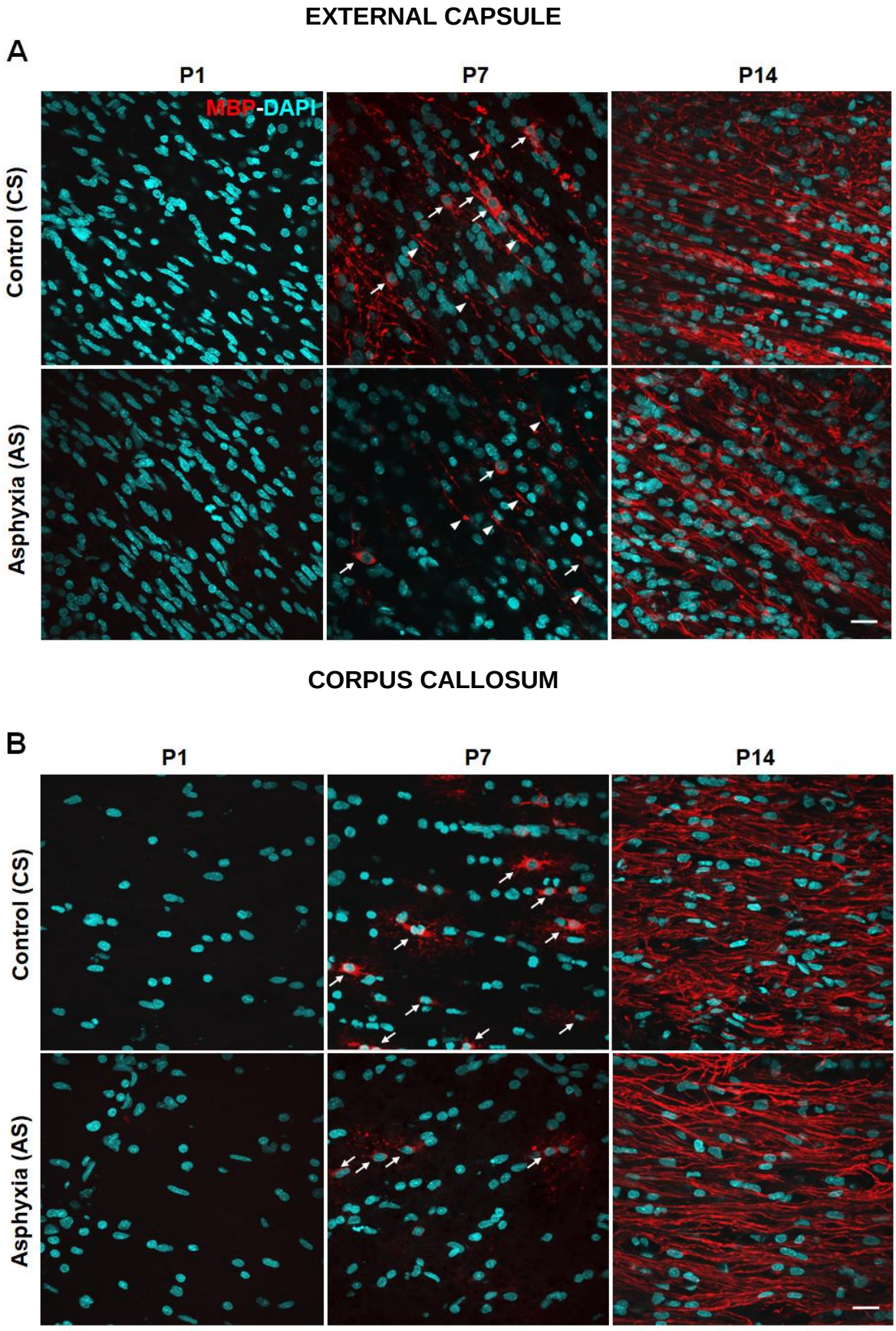
EXTERNAL CAPSULE
A
P1
P7
P14
MBP-DAPI
Control (CS)
Asphyxia (AS)
CORPUS CALLOSUM
B
P1
P7
P14
Control (CS)
Asphyxia (AS)

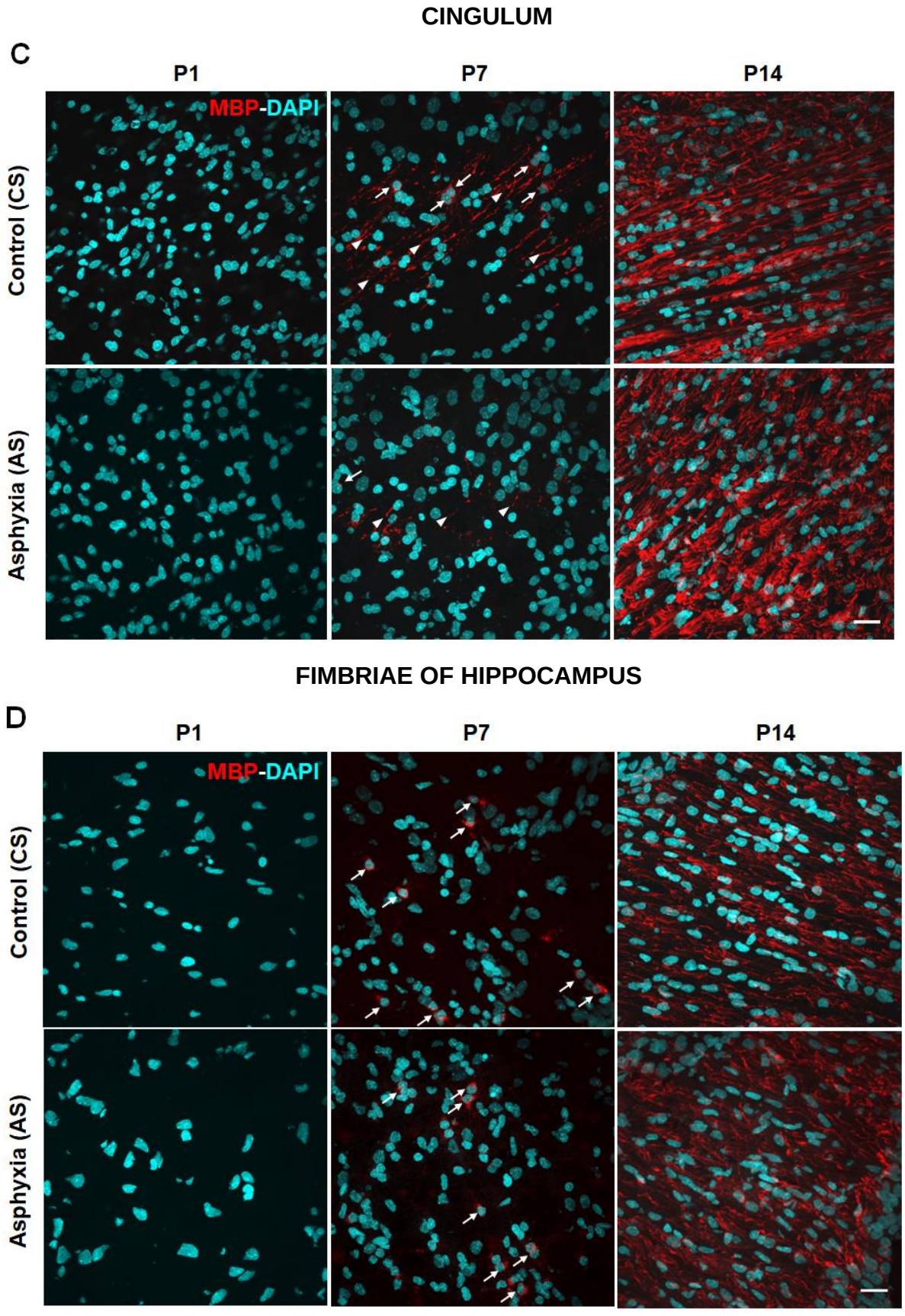
CINGULUM
C
P1
P7
P14
MBP-DAPI
Control (CS)
Asphyxia (AS)
FIMBRIAE OF HIPPOCAMPUS
D
P1
P7
P14
MBP-DAPI
Control (CS)
Asphyxia (AS)

Figure 10. Effect of neonatal development and perinatal asphyxia (PA) on myelination at P1, P7 and P14, measured in external capsule (A); corpus callosum (B); cingulum (C) and fimbriae of hippocampus (D) of rat neonates. Representative microphotographs obtained by confocal microscopy showing myelin basic protein (MBP; red) and DAPI (blue; nuclei)-positive cells in external capsule (A); corpus callosum (B); cingulum (C); and fimbriae of hippocampus (D) from control (CS) and asphyxia-exposed (AS) rat neonates. Microphotographs show MBP, indicating both myelinated fibres and mature oligodendrocytes. Scale bar: 20 μm. At P1, no MBP immunoreactivity was observed in any of the analysed regions and the experimental conditions. The density of MBP increased significantly along development. At P7, the density of MBP fibres (white head arrows) was low, letting visualize individual mature oligodendrocyte (OLs) (white arrows). In corpus callosum and fimbriae of hippocampus some individual OLs can also be seen, showing long and branched processes. In AS, there was a decrease in the density of MBP in external capsule, corpus callosum and cingulum compared to that in CS. No differences could be seen in fimbriae of hippocampus at P7. At P14 a dense network of MBP fibres can be seen in all regions, but no independent OLs soma can be distinguished.

Figure 11 shows the simultaneous quantification of the effect of PA on the number of DAPI (cells/mm^3) and MBP positive pixels/total pixels in white matter of telencephalon (external capsule, corpus callosum, cingulum), and fimbriae of hippocampus from CS and AS rat neonates at P1, P7 and P14. No significant differences in DAPI positive cells/mm^3 were observed among the different experimental conditions (Fig. 11A), quantifying around 30-40 x 10^4 cells/mm^3 for each condition along development.

No MBP immunostaining could be quantified in any of the studied regions at P1, sampled from CS and AS-exposed rats, but yes at P7. MBP positive pixels were, however, decreased in *external capsule* (by ~50%), *corpus callosum* (by ~60%) and *cingulum* (by ~70%) of AS, compared to that of CS animals. No differences were observed in *fimbriae of hippocampus*. At P14, the MBP immunostaining was remarkable increased, compared to that observed at P7, in CS animals by >2 X (external capsule >2 X; corpus callosum >10 X; cingulum >6 X, and fimbriae of hippocampus >25 X), reflecting a spur of myelination. In AS, that spur was even more remarkable, increased by >5 X (external capsule >5 X; corpus callosum >30 X; cingulum >20 X, and fimbriae of hippocampus >30X; Fig. 11B, *see supplementary table 1*).

A.

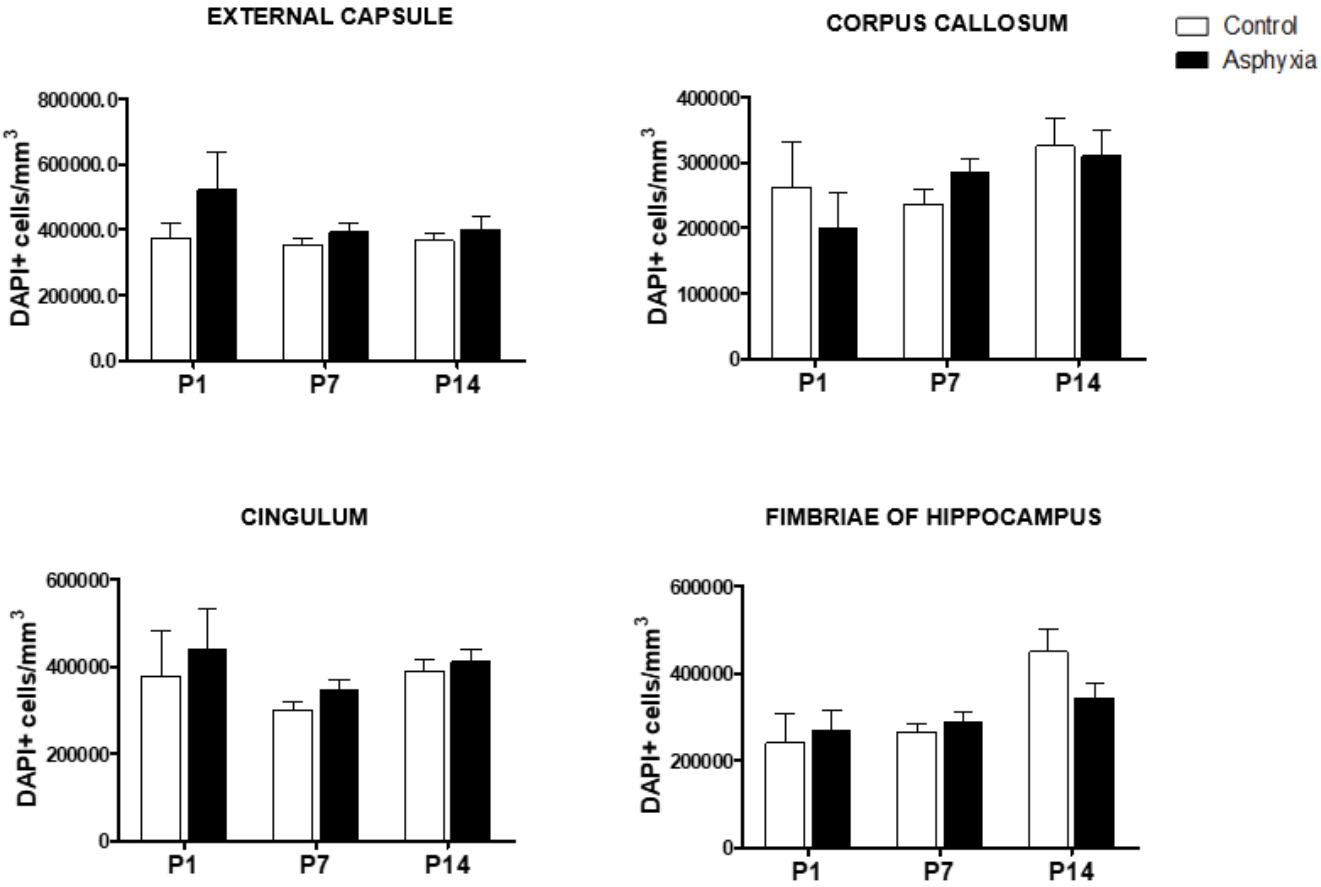
EXTERNAL CAPSULE
CORPUS CALLOSUM
CINGULUM
FIMBRIAE OF HIPPOCAMPUS
Control
Asphyxia
DAPI+ cells/mm3
800000.0
600000.0
400000.0
200000.0
0.0
400000
300000
200000
100000
0
600000
P1
P7
P14

B.

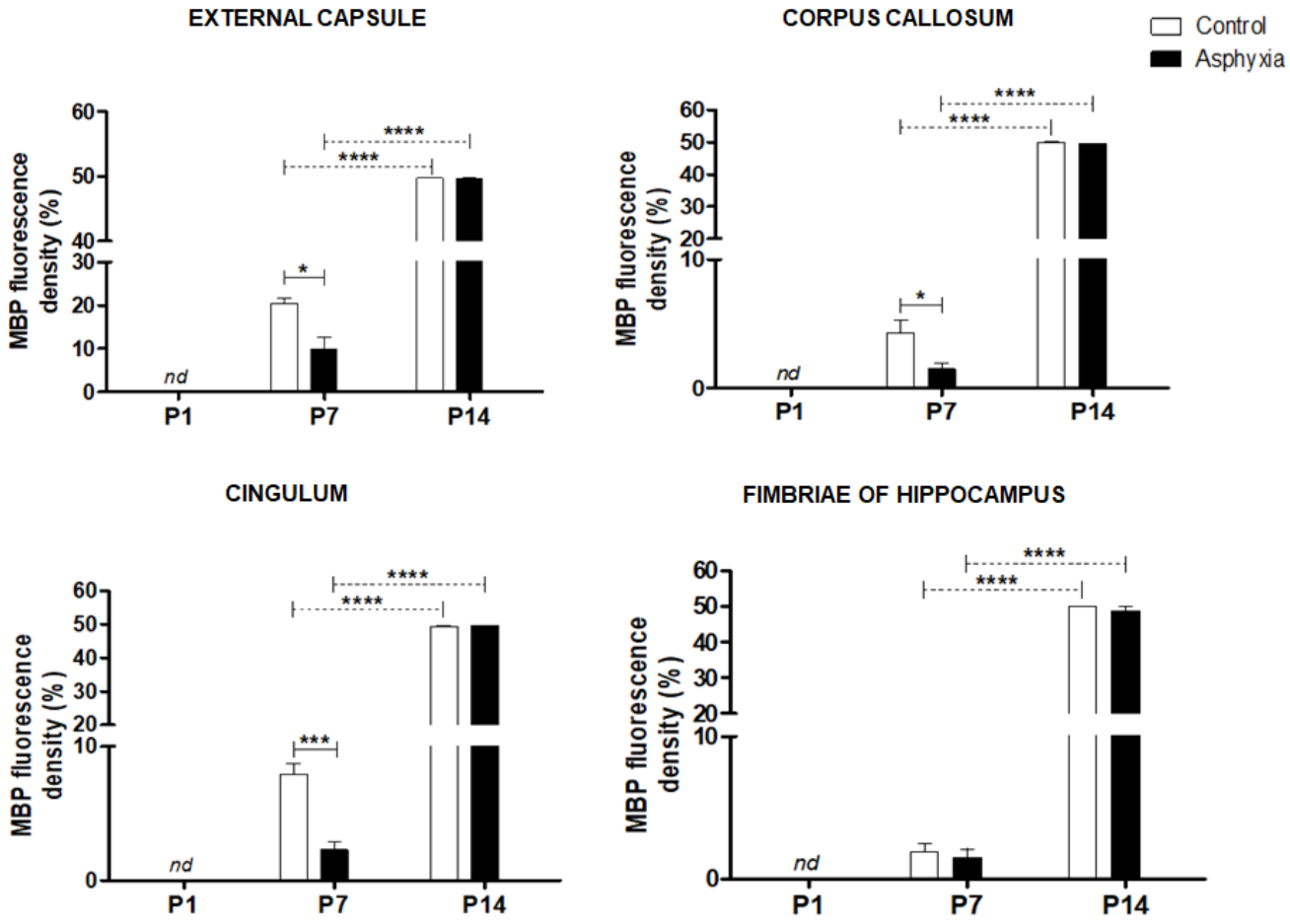
EXTERNAL CAPSULE
CORPUS CALLOSUM
Control
Asphyxia
CINGULUM
FIMBRIAE OF HIPPOCAMPUS
MBP fluorescence density (%)
nd
P1
P7
P14
*
***
****

Figure 11. Effect of neonatal development and perinatal asphyxia (PA) on myelination (MBP; pixels/total pixels) in telencephalon (external capsule, corpus callosum, cingulum and fimbriae of hippocampus) at P1, P7 and P14. Coronal sections of telencephalon were treated for immunohistochemistry against myelin basic protein (MBP), counterstained with DAPI. Microphotographs (two-five samples per brain region) were taken from external capsule, corpus callosum, cingulum and fimbriae of hippocampus, in the field of a confocal-inverted Olympus-fv10i microscope at 60x. The mean percentage of MBP immunopositive pixels over the total pixel number was estimated using ImageJ software. Data are shown as means ± S.E.M from at least N=5 independent experiments. Unbalanced two-way ANOVA indicated a significant effect of postnatal days (neonatal development) on MBP (pixels/total pixels), increased in both CS (>2 X, external capsule; >10 X, corpus callosum; >6 X, cingulum, and >25 X in fimbriae of hippocampus) and AS (>5 X, external capsule; >30 X, corpus callosum; >20 X, cingulum, and >30 X in fimbriae of hippocampus) animals. At P7, MBP levels were decreased in external capsule, corpus callosum and cingulum of AS versus CS animals in external capsule ($F_{(4, 25)}$= 230.066, P < 0.0001); corpus callosum ($F_{(4, 25)}$= 3669.906, P < 0.0001); cingulum ($F_{(4, 25)}$= 2037.145, P < 0.0001), but not in fimbriae of hippocampus ($F_{(4, 25)}$= 0.045, P = 0.833). Benjamini-Hochberg was used as a post hoc test. *P < 0.05, **P < 0.01, ***P < 0.001, ****P < 0.0001 (Bold). No statistically significant differences were observed in DAPI per mm^3 in any of the evaluated regions.

Effect of neonatal development and Perinatal Asphyxia on MBP and Oligodendrocyte transcription factors (Olig-1 and Olig-2) mRNA levels evaluated in telencephalon by RT-qPCR at P1, P7 and P14 (Fig. 12).

Gene transcripts were amplified by RT-qPCR, quantified by the ΔΔCT method, using β-actin as housekeeping gene, normalizing mRNA levels of each target genes to that observed in CS neonates at P1. Figure 12 shows fold/changes in mRNA levels, monitored in telencephalon of CS (A) and AS (B) rat neonates at P1, P7, and P14.

MBP, Olig-1 and Olig-2 mRNA levels (see supplementary *table 2A).*

As already shown by immunocytochemistry, the MBP mRNA levels increased along development in CS neonates, by 20 X at P7, and by >1000 X at P14. A similar increase was observed in AS neonates. Olig-1 and Olig-2 mRNA levels increased in telencephalon at P14 in CS, but only Olig-1 mRNA levels increased in AS neonates along development. Olig-1 mRNA levels were already increased at P7 in AS, compared to that in CS (>1.4 X; Fig. 12B-C).

MBP

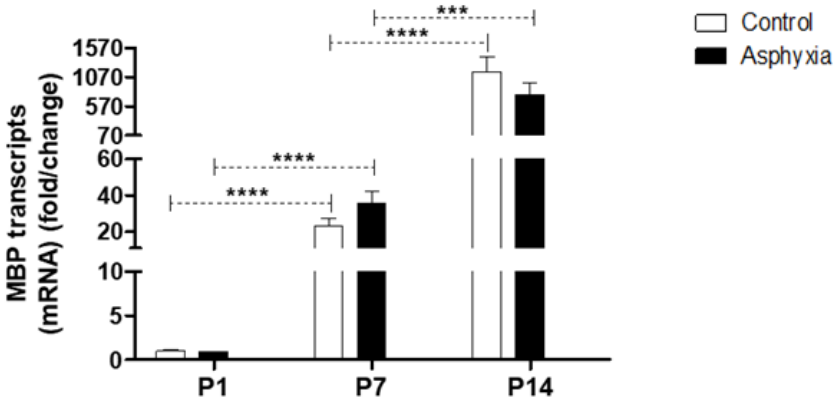

Olig-1

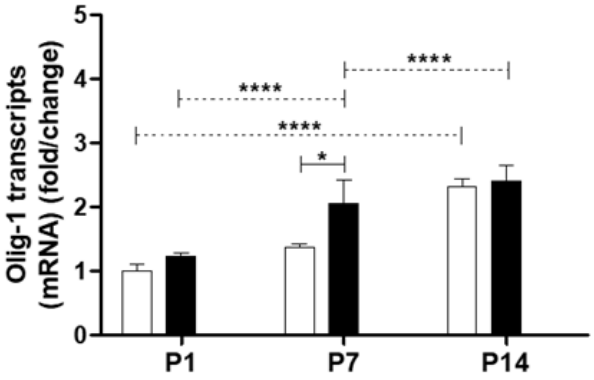

Olig-2

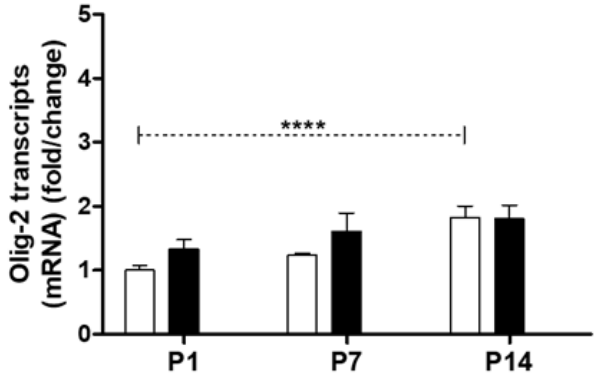

Figure 12. Effect of neonatal development and PA on MBP and Oligodendrocyte Transcription Factor (Olig-1, Olig-2) mRNA expression in telencephalon at P1, P7 and P14, from control (CS) and asphyxia-exposed (AS) rats. Effect of PA on MBP, Olig-1 and Olig-2 mRNA (a.u.) expression was determined by quantitative RT-PCR analysis. Target genes were normalized by the housekeeping (β-actin) and expressed as fold/change for each experimental group, compared to that evaluated at CS-P1. Data are shown as means ± S.E.M., for independent experiments (N=5). Unbalanced two-way ANOVA indicated a significant effect of PA and postnatal day on MBP ($F_{(4, 23)}$= 16.626, P < 0.0001); Olig-1 ($F_{(4, 25)}$= 11.992, P <0.0001); and Olig-2 ($F_{(4, 26)}$= 5.573, P < 0.01) mRNA expression. Benjamini-Hochberg was used as a post hoc test. *P < 0.05, **P < 0.01, ***P < 0.001, ****P < 0.0001 (italics).

Effect of neonatal development and PA on pro-inflammatory cytokines (Cox-2, TNF-α, IL-β, IL-6) mRNA levels evaluated in telencephalon and hippocampus by RT-qPCR at P1, P7 and P14 (Fig. 13).

Gene transcripts were amplified by RT-qPCR, quantified by the ΔΔCT method, using β-actin as housekeeping gene, normalizing the mRNA levels of each target genes to that observed in CS neonates at P1. Figure 13 shows fold/changes in mRNA levels, monitored in telencephalon and hippocampus of CS (A) and AS (B) rat neonates at P1, P7, and P14.

Pro-inflammatory cytokines (Cox-2, TNF-α, IL-β, IL-6) mRNA levels (*see supplementary Table 2).*

Telencephalon:
In CS animals, IL-1 β (>2 X) and IL-6 (>1.8 X) mRNA levels increased at P14, while no significant differences were observed in TNF-α mRNA levels. Cox-2 levels increased along development, both in CS and AS animals, at P7 (>5 X) and P14 (20 X). In AS neonates, IL-6 and TNF-α mRNA levels increased along development, with a maximum observed at P14 (>1.8 X and >18 X, respectively), but not significant differences were observed in IL-1 β mRNA levels (see Fig. 13A). No differences were observed among CS and AS animals in IL-6 protein levels ($F(2, 23)= 0.194$, $P= 0.825$; see supplementary Fig. 1).

Hippocampus:
Only Cox-2 mRNA levels increased along development, both in CS and AS neonates, a maximum observed at P14. Furthermore, IL-1β mRNA levels increased at P14 in AS, compared to CS (>2 X; see supplementary table 2B). No differences were observed in Cox-2, TNF-α and IL-6 mRNA levels among AS compared to CS animals in any of the experimental conditions (see Fig. 13B).

A. TELENCEPHALON

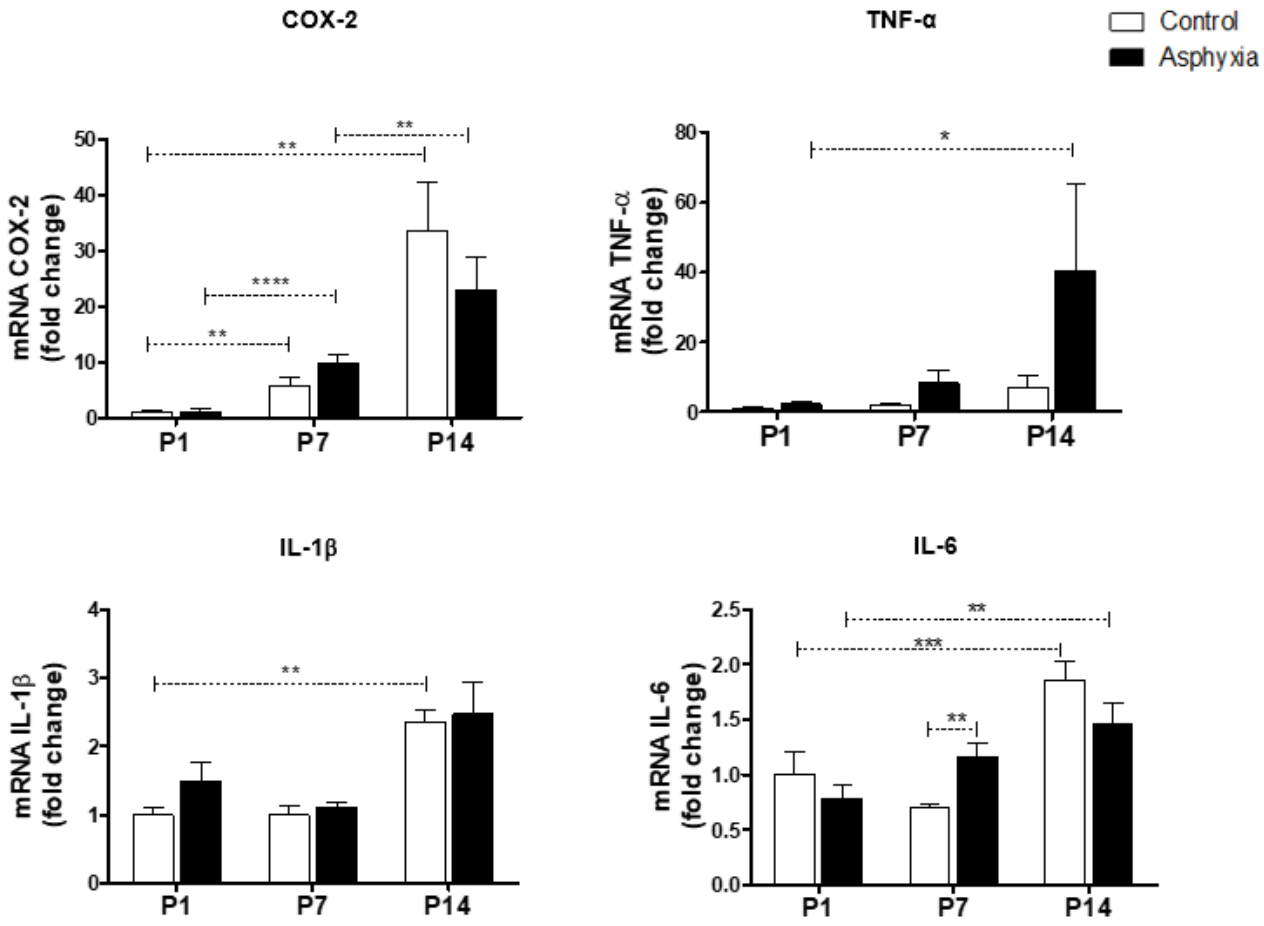

B. HIPPOCAMPUS

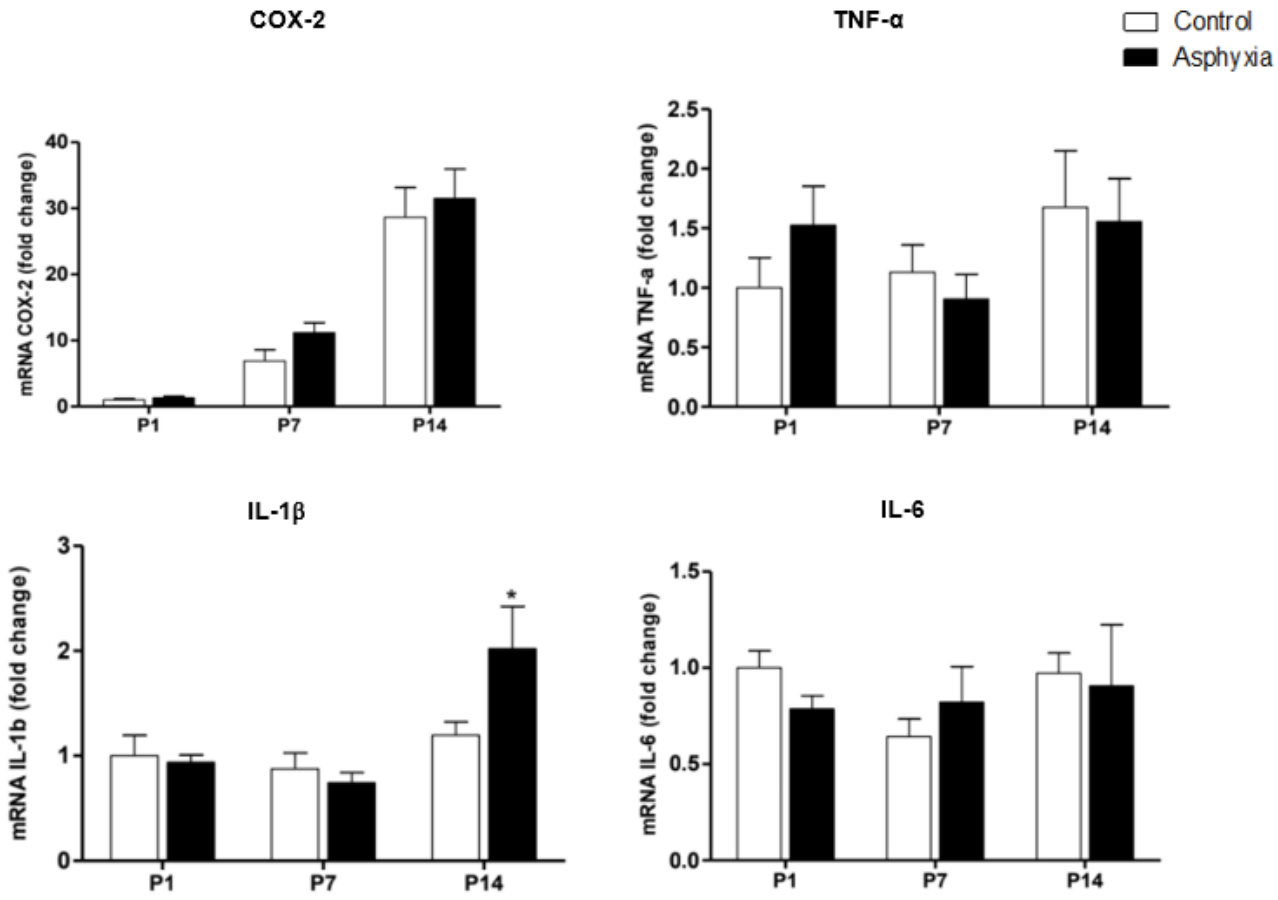

Figure 13. Effect of neonatal development and PA on pro-inflammatory cytokines (Cox-2 TNF-α, IL-1β, IL-6) mRNA expression in (A) telencephalon and (B) hippocampus at P1, P7 and P14, from control (CS) and asphyxia-exposed (AS) rats. Effect of PA on pro-inflammatory cytokines mRNA expression (a.u.) was determined by quantitative RT-qPCR analysis. Target genes were normalized by the housekeeping (β-actin) and expressed as fold/change for each experimental group, compared to that evaluated at CS-P1. Data are shown as means ± S.E.M., for independent experiments (N=5). In telencephalon, unbalanced two-way ANOVA indicated a significant effect of PA and postnatal day on COX-2 ($F_{(4, 24)}$= 11.118, P <0.0001); TNF-α ($F_{(4, 22)}$= 2.335, P= 0.087); IL-1β ($F_{(4, 24)}$= 11.539, P < 0.0001); and IL-6 ($F_{(4, 23)}$= 8.459, P < 0.0001) mRNA expression. In hippocampus, unbalanced two-way ANOVA was used for testing the effect of PA and postnatal days on COX-2 ($F_{(3, 28)}$= 41.832, P <0.0001); TNF-α ($F_{(3, 27)}$= 1.211, P= 0.327); IL-1β ($F_{(4, 24)}$= 6.408, P= 0.001); and IL-6 ($F_{(3, 28)}$= 0.894, P= 0.458) mRNA expression. Benjamini-Hochberg was used as a post hoc test. *P < 0.05, **P < 0.01, ***P < 0.001, ****P < 0.0001 (italics).

Effect of Perinatal Asphyxia on glial cells measured in telencephalon and hippocampus at P7, focusing on mature oligodendrocyte (MBP), astrocytes (GFAP) and microglia (Iba-1) (Fig. 14 and Fig. 15).

The issue of mature OLs, astrocytes and microglia, was further investigated in an independent cohort of experiments analysed at P7, the time when individual OLs could be observed, both in CS and AS neonates, but significantly decreased in AS animals.

Figure 14 shows microphotographs of OLs (MBP-positive), astroglia (GFAP-positive), and microglia (Iba-1-positive) in external capsule (Fig. 14A), corpus callosum (Fig. 14B), cingulum (Fig. 14C) and fimbriae of hippocampus (Fig. 14D) of CS and AS rat neonates at P7. In adjacent microphotographs, OLs (red), astroglia (red) and microglia (green) intermingled with DAPI (blue) signalling.

A. EXTERNAL CAPSULE

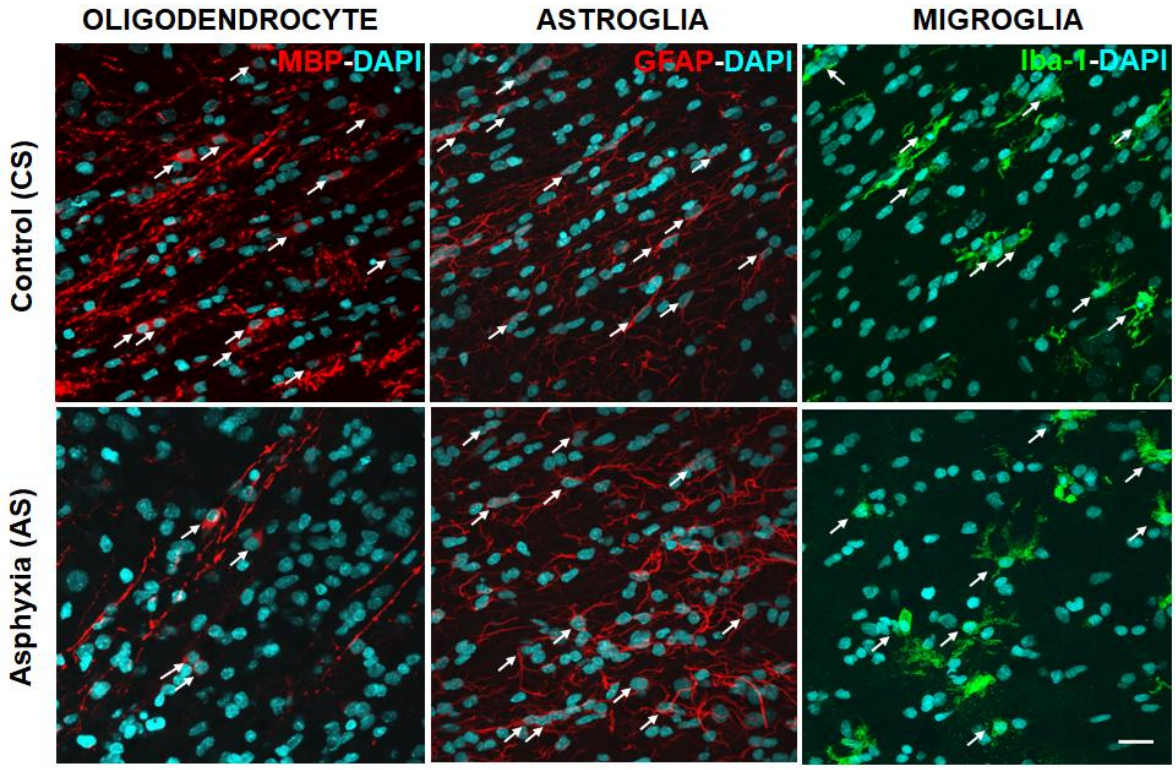

B. CORPUS CALLOSUM

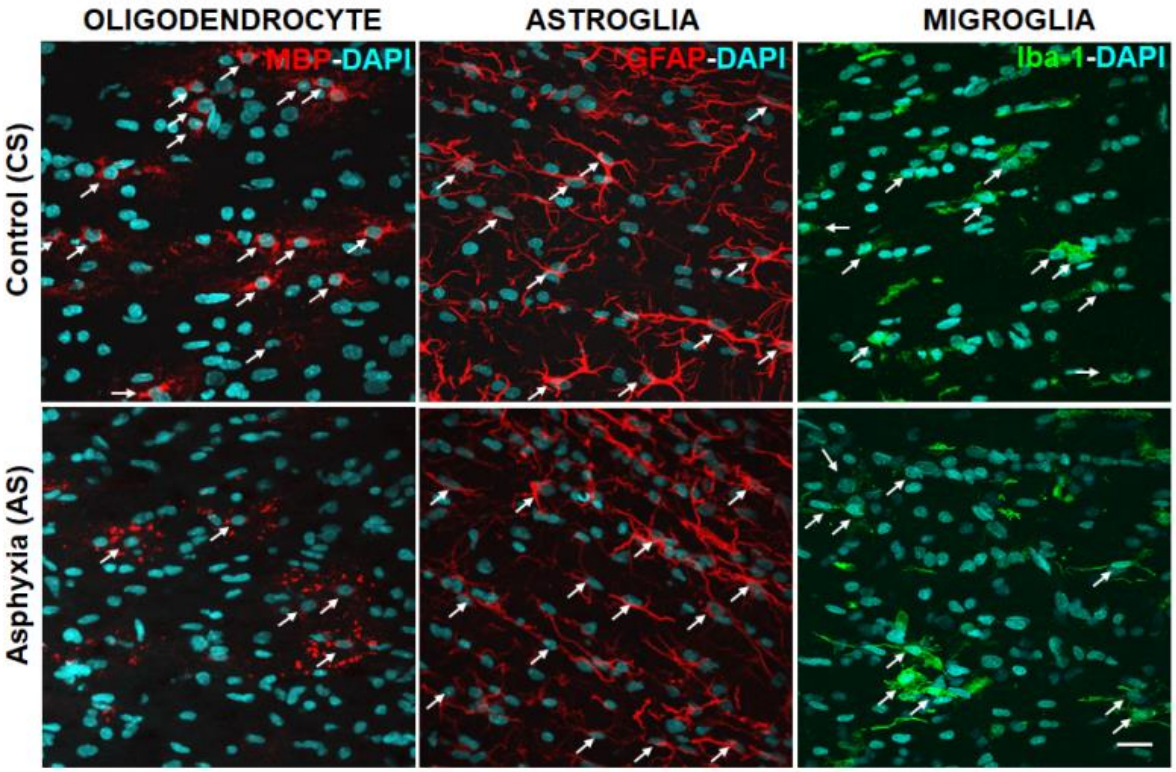

C. CINGULUM

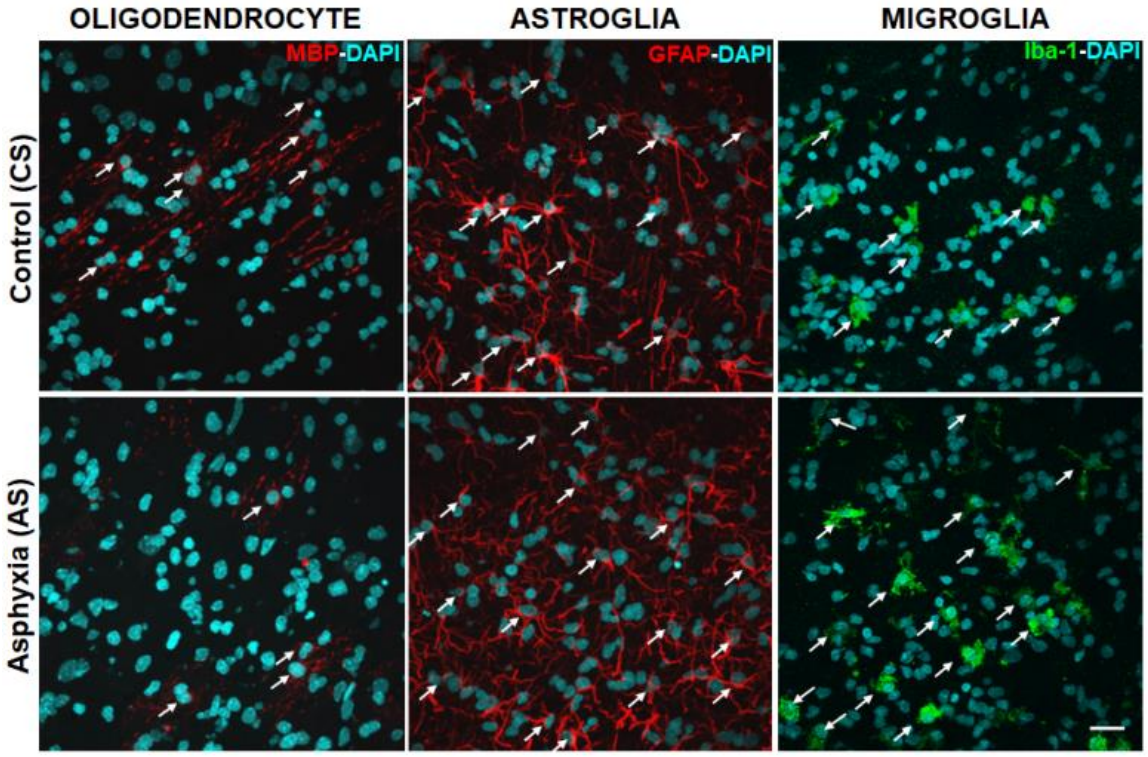

D. FIMBRIAE OF HIPPOCAMPUS

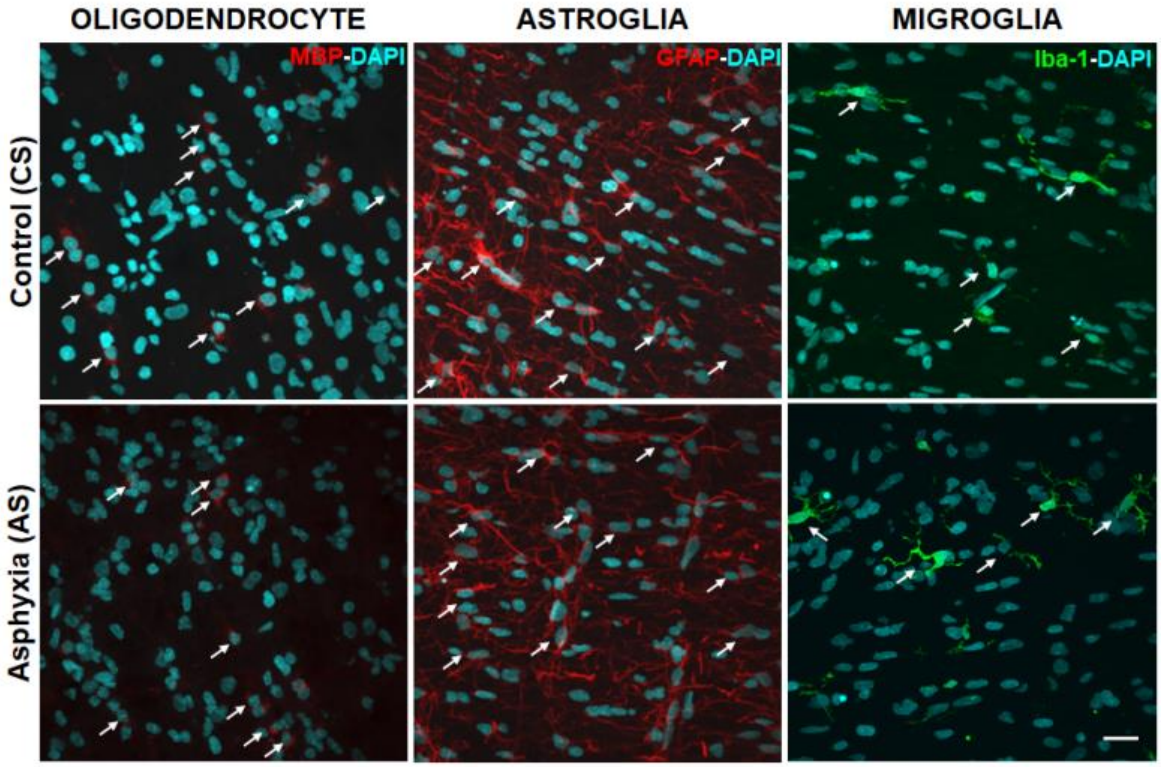

Figure 14. Effect of PA on glial cells at P7, measured in external capsule (A); corpus callosum (B); cingulum (C) and fimbriae of hippocampus (D) of rat neonates. Representative microphotographs obtained by confocal microscopy showing myelin basic protein (MBP; red), glial fibrillary acidic protein (GFAP; red), ionized calcium binding adaptor molecule 1 (Iba-1; green) and DAPI (blue; nuclei)-positive cells in external capsule (A); corpus callosum (B); cingulum (C); and fimbriae of hippocampus (D), from CS and PA-exposed (AS) rat neonates. White arrows show mature oligodendrocyte (OLs), astrocyte and microglia phenotype. Scale bar: 20 μm. The number of MBP-DAPI+ cells/mm3 decreased after PA in external capsule, corpus callosum and cingulum, but not in fimbriae of hippocampus.

Figure 15 shows the quantification of DAPI, MBP-DAPI, GFAP-DAPI and Iba-1-DAPI cells/mm^3. The number of DAPI positive nuclei (cells/mm^3) found at P7 was similar to that shown above at different cohorts of CS and AS neonates (c.f. supplementary Table 1 versus supplementary Table 3). OLs, astrocytes and microglia represent approximately 15% of the total number of DAPI cells in CS and AS group. The number of MBP-DAPI cells/mm^3 observed in AS at P7 was, however, decreased by approximately 50% compared to that observed in CS neonates. No significant differences were observed in GFAP-DAPI cells/mm^3 or Iba-1-DAPI cells/mm^3 between CS and AS neonates, apart of that in cingulum, where the number of Iba-1-DAPI cells/mm^3 increased >1.5 X in AS, compared to that observed in CS animals (see supplementary table 3).

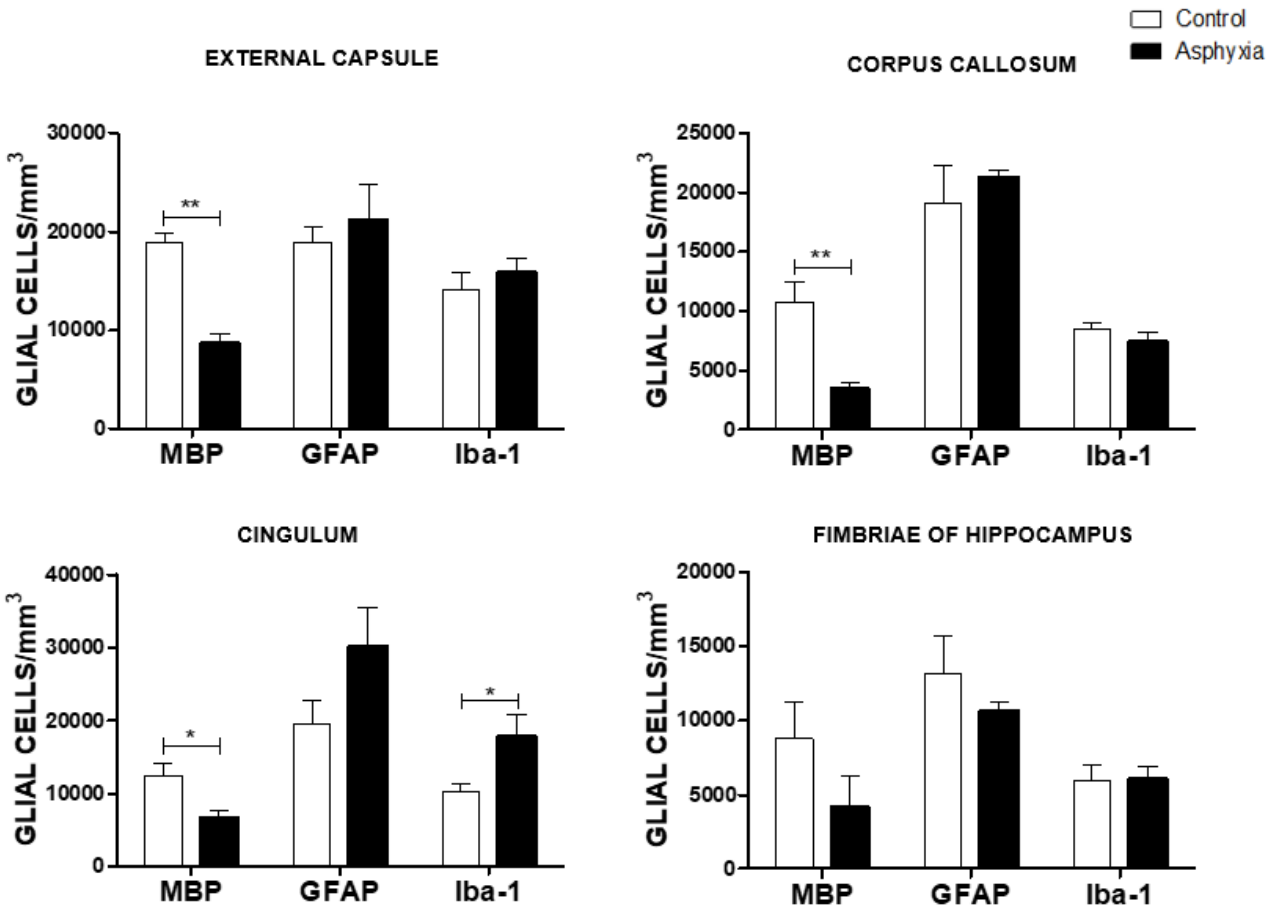
Control
Asphyxia
EXTERNAL CAPSULE
CORPUS CALLOSUM
CINGULUM
FIMBRIAE OF HIPPOCAMPUS
GLIAL CELLS/mm3
MBP
GFAP
Iba-1
**
*

Figure 15. Effect of PA on glial cells at P7, from control (CS) and asphyxia-exposed (AS) rats. Coronal sections of telencephalon and fimbriae of hippocampus were treated for IF against myelin basic protein (MBP), glial fibrillary acidic protein (GFAP), ionized calcium binding adaptor molecule 1 (Iba-1) and counterstained with DAPI. Microphotographs (two-five samples per brain region) were taken from external capsule, corpus callosum, cingulum and fimbriae of hippocampus, in the field of a confocal-inverted Olympus-fv10i microscope with a 60x. Mean number of glial cells per mm^3 was estimated using ImageJ software. Data are shown as means ± S.E.M from N=5 independent experiments. Student's t-test indicated a significant effect of PA on MBP-DAPI cells/mm^3 in external capsule (t= 3.472 df= 8, p= 0.008), corpus callosum (t= 4.143 df= 8, p= 0.003), cingulum (t= 2.947 df= 8, p= 0.019), but not in fimbriae of hippocampus (t= 1.462 df= 8, p= 0.174). No significant differences were observed in the AS group, compared to that in CS on GFAP-DAPI cells/mm^3 in the external capsule (t= 0.564 df= 8, p= 0.588), corpus callosum (t= 0.669 df=8, p= 0.523), cingulum (t= 1.696 df= 8, p= 0.128), and fimbriae of hippocampus t= 1.003 df= 8, p= 0.345). Significant differences were observed in the AS group compared to the CS on Iba-1-DAPI cells/mm^3 in the in the cingulum (t= 2.329 df= 8, p= 0.048), but not in external capsule (t= 0.793 df= 8, p=0.451), corpus callosum (t= 1.118 df= 8, p= 0.296), and fimbriae of hippocampus (t= 0.042 df= 8, p= 0.968).*p < 0.05, **p < 0.01, ***p< 0.001, ****p < 0.0001.

Characterization of MSCs according to their adipogenic, osteogenic and chondrogenic potential by Oil Red O, Alizarin Red and Safranin O staining respectively (see Fig. 16).

MSCs were isolated and expanded under standard culture conditions. After passage 3, plastic-adherent cells showed fibroblast like (elongated spindle) morphology with large cytoplasm and nuclei (Fig. 16A). MSCs were characterized according to their adipogenic, osteogenic and chondrogenic potential. Fatty vacuole deposits were visualized by Oil Red O staining after 14 days of differentiation (Fig. 16B). Calcium deposits were visualized by Alizarin Red staining after 21 days of differentiation (Fig. 16C). Proteoglycans were visualized by Safranin-O staining in the extracellular matrix, surrounding the chondrocytes after 10 days of differentiation (Fig. 16D).

Immuno-phenotypification of MSCs according to their putative murine MSCs markers and hematopoietic cell lineages markers by flow cytometry (see Fig. 16).

Flow cytometry analysis showed that MSCs expanded in α-10 medium, exhibited high levels (≥ 95%) of cell adhesion molecules (putative murine MSCs markers, CD-29 and CD-90), but no expression (≤ 2%), or markers of hematopoietic cell lineages (CD-45 and CD-11b) (Figure Fig. 16E).

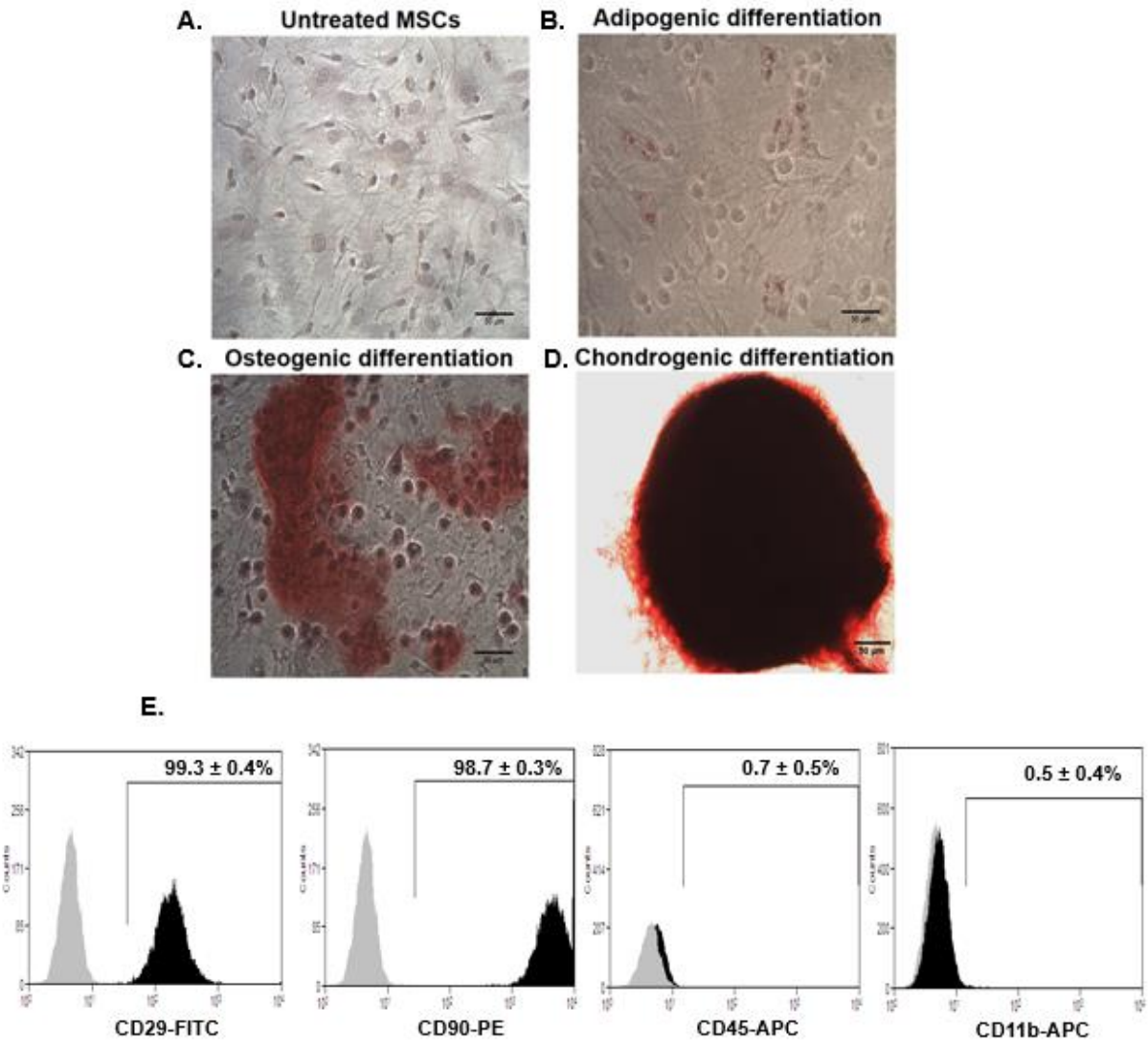

Figure 16. Rat adipose-derived MSCs display mesenchymal stem cell characteristics. (A) Representative microphotographs of plastic-adherent cells isolated from rat adipose tissue differentiated into (B) adipogenic, (C) osteogenic and (D) chondrogenic lineages. (E) Immuno-phenotypification of adherent cells according to the expression of putative murine MSCs markers (CD29 and CD90), and the non-expression of markers characteristics of other cell types (CD45 and CD11b). Black histograms represent cells labelled with specific antibodies; grey histograms represent cells stained with isotype control antibodies. FITC: fluorescein isothiocyanate, PE: phycoerythrin, APC: allophycocyanin.

Effect of Perinatal Asphyxia on apoptotic-like DAPI (TUNEL-DAPI/mm^3) and oligodendrocyte-specific cell death (TUNEL-DAPI-MBP/mm^3) at P7 (Fig. 17 and Table 5A-C).

Superior panels of figure 17 show microphotographs for the co-localization of TUNEL and DAPI in external capsule, corpus callosum and cingulum of CS and AS neonates at P7. DAPI and TUNEL co-localization increased in AS, as compared to CS in all analysed regions, which was particularly notable in *external capsule*.

A. EXTERNAL CAPSULE

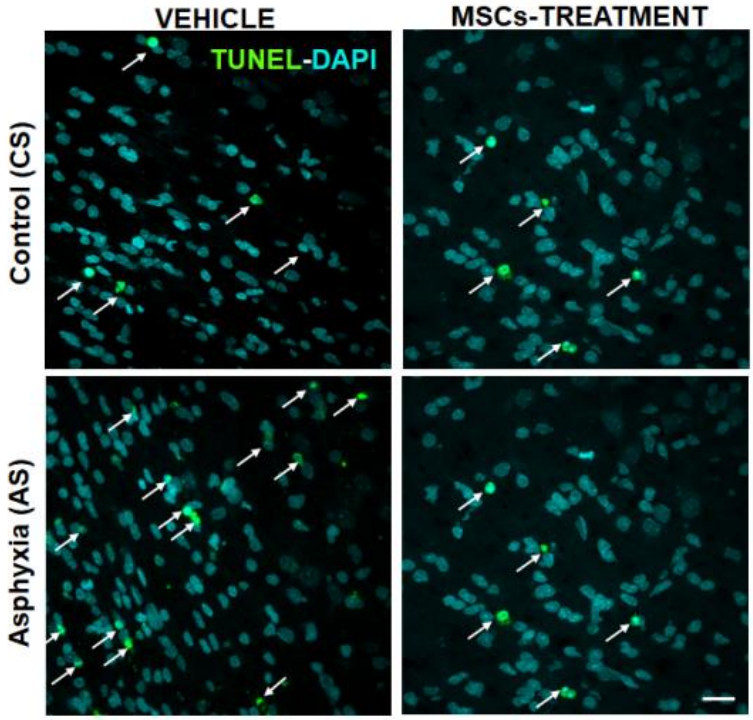

B. CORPUS CALLOSUM

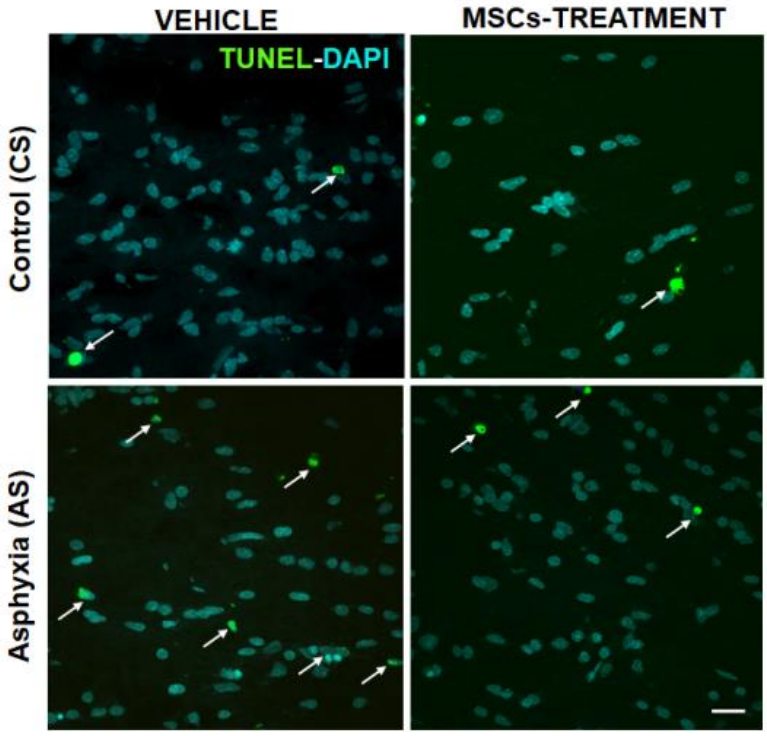

C. CINGULUM

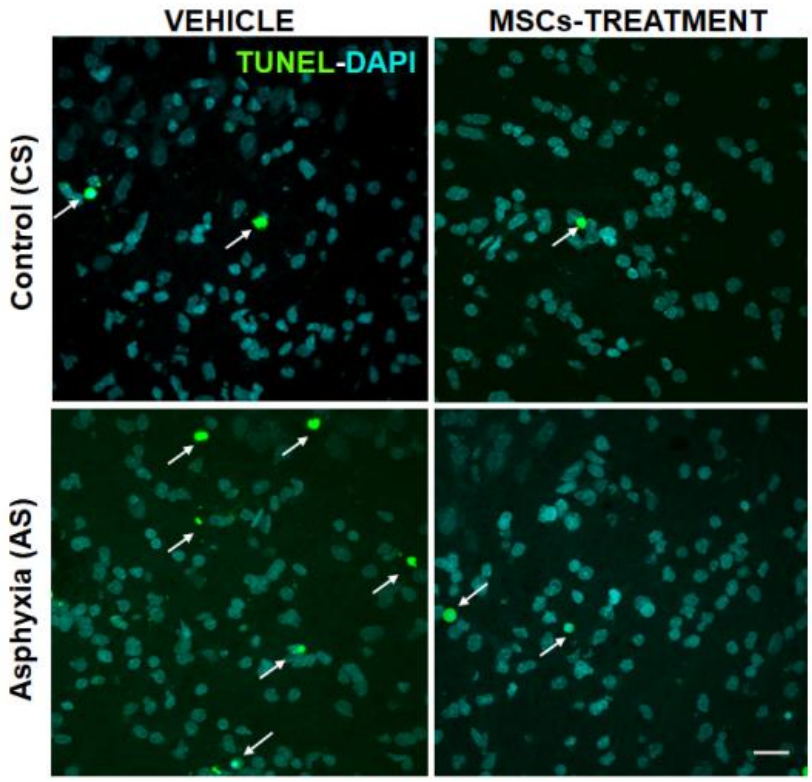

Figure 17. Effect of MSCs treatment on cell death induced by perinatal asphyxia (PA), measured at P7 in external capsule (A); corpus callosum (B), and cingulum (C) of CS (a) and AS (b) rat neonates. Representative microphotographs obtained by confocal microscopy showing TUNEL (green), and DAPI+ (nuclei, blue) merge of positive cells in (A) external capsule; (B) corpus callosum, and (C) cingulum from vehicle- and MSCs-treated CS and AS neonates. Scale bar: 20 μm. (A-C). The number of TUNEL-DAPI cell/mm^3 is increased when comparing vehicle-treated AS versus CS neonates, but the number of TUNEL-DAPI cell/mm^3 is decreased in MSCs- versus vehicle-treated AS rat neonates in all evaluated regions.

As shown in Table 5A, TUNEL-DAPI/mm^3 co-localization could be estimated to approximately 2% of DAPI/mm^3 in vehicle-treated CS neonates, and that proportion was duplicated in vehicle-treated AS neonates (Table 5C), indicating an increased apoptotic-like cell death following PA.

The TUNEL- MBP-DAPI /mm^3 suggests OLs-specific cell death**,** which at P7 was 15%, 6%, and 20% of the total MBP-DAPI /mm^3 in external capsule, corpus callosum and cingulum of vehicle-treated AS rat neonates, respectively. In vehicle-treated CS neonates, TUNEL- MBP-DAPI /mm^3 OLs-specific cell death was 1.1% in external capsule, and 12% in cingulum. No OLs-specific cell death could be estimated in corpus callosum of CS animals (c.f. Table 5 and 6). The rate of OLs-specific cell death increased in external capsule and corpus callosum of AS compared to that in CS animals evaluated at P7. In cingulum, the rate of OLs-specific cell death was similar in vehicle-treated CS and AS neonates.

Table 5. Effect of PA on apoptotic-like (TUNEL-DAPI/mm^3) and OLs-specific (TUNEL-MBP-DAPI/mm^3) cell death at P7, from control (CS) and asphyxia-exposed (AS) rats: Prevention by MSCs treatment. Coronal sections of telencephalon were treated for immunohistochemistry against TUNEL, myelin basic protein (MBP), counterstained with DAPI. Microphotographs (two-five samples per brain region) were taken from external capsule, corpus callosum and cingulum, in the field of a confocal-inverted Olympus-fv10i microscope at 60x. Means of DAPI positive cells per mm^3, alone and colocalizing with TUNEL/mm^3, and MBP-TUNEL/mm^3 were estimated using ImageJ software. Data are shown as means ± S.E.M from N=5 independent experiments. Unbalanced two-way ANOVA indicated a significant effect of PA on TUNEL-DAPI/mm^3, decreasing significantly in external capsule ($F_{(2, 17)}$= 10.430, P=0.001); corpus callosum ($F_{(2, 17)}$= 6.690, P=0.007); and cingulum ($F_{(2, 16)}$= 6.495, P= 0.009) of MSCs- compared to vehicle-treated AS rat neonates. No statistically significant difference were observed in DAPI per mm^3 in any of the evaluated regions (external capsule $F_{(2, 17)}$= 2.477, P=0.114); corpus callosum ($F_{(2, 17)}$= 3.279, P=0.662); and cingulum ($F_{(2, 17)}$= 1.257, P=0.310). Benjamini-Hochberg was used as a post hoc test. *P < 0.05, **P < 0.01, ***P < 0.001, ****P < 0.0001 (italics).

Experimental groups	**P7**		
A. CS vehicle (n= 5)	**DAPI+/mm^3**	**TUNEL-DAPI+/mm^3**	**TUNEL-MBP-DAPI/mm^3**
External capsule	382789±29017	8145±3543	152±92.74
Corpus callosum	196023±12124	5239±1007	Nd
Cingulum	346834±7511	7310±2231	1138±915.80
B. CS MSCs (n= 5)			
External capsule	378613±16522	9198±2064	277 ±191.20
Corpus callosum	203899±7019	3975±476	Nd
Cingulum	379610±4365	4402±1541	Nd
C. AS vehicle (n= 5)			
External capsule	341872±12628	**22837±3732 (> 2.5x)a*** **	**1034±132.20 (>6.5x)a**** **
Corpus callosum	241023±21694	**9276±1942 (>1.7x)a*** **	261±124.30
Cingulum	332495±28634	**14333±2035 (>1.9x)a*** **	786±423.90
D. AS MSCs (n= 5)			
External capsule	404578±21398	**8145±3543 (by ~60%)b**** **	**143±89.23 (by 85%)b**** **
Corpus callosum	220892±8903	**4523±642 (by ~50%)b*** **	Nd
Cingulum	324002±44070	**7147±1790 (by ~50%)b**** **	Nd

*nd: *not detectable*

Effect of MSCs treatment on total cell death, number of OLs and myelination at P7 (Fig. 18; Table 5B,D; Table 6B,D).

MSCs treatment or the corresponding vehicle was administered two hours after delivery (*icv*). Brain samples were taken and analysed at P7, focusing on *external capsule*, *corpus callosum* and *cingulum*. The fimbriae of hippocampus were not evaluated, since no differences in myelination and mature OLs number between AS and CS were observed (c.f. Fig. 10 and 14).

Number of total (TUNEL-DAPI/mm^3) and OLs-specific (TUNEL- MBP-DAPI/mm^3) cell death.

The number of DAPI positive nuclei (cells/mm^3) found at P7 was similar to that shown above for different cohorts of CS and AS neonates under all experimental conditions, despite the *icv* administration of vehicle or MSCs treatment. No differences were observed in the total number of DAPI (TUNEL-DAPI) or OLs-specific (TUNEL-MBP-DAPI) cell death, between vehicle- and MSCs-treated CS neonates, except in cingulum where no oligodendroglial death was detected in the MSCs-treated CS group (c.f. Table 5A versus Table 5C). MSCs treatment prevented the observed increase in total DAPI (TUNEL-DAPI/mm^3) and OLs-specific (TUNEL-MBP-DAPI /mm^3) cell death observed in AS neonates at P7 (c.f. Table 5C versus Table 5D).

Number of mature oligodendrocytes (MBP-DAPI/mm^3) and myelination (MBP positive pixels/total pixels)

No differences were observed in the number of OLs and myelination between vehicle and MSCs-treated CS neonates (c.f. Table 6A versus Table 6B). MBP-DAPI/mm^3 were decreased in external capsule (by ~50%) and cingulum (by >50%), while MBP positive pixels were decreased in external capsule (by ~30%) and cingulum (by ~40%), but these changes were not seen in corpus callosum from vehicle-treated AS, compared to that from vehicles-treated CS animals at P7 (c.f. Table 6A versus Table 6C).

MSCs treatment prevented the decrease observed in OLs number (MBP-DAPI/mm^3) in AS rat neonates (c.f. Table 6C versus Table 6D). MSCs treatment also prevented the decrease in myelination (*MBP positive pixels/total pixels*) observed in AS neonates (c.f. Table 6C versus Table 6D).

A. EXTERNAL CAPSULE

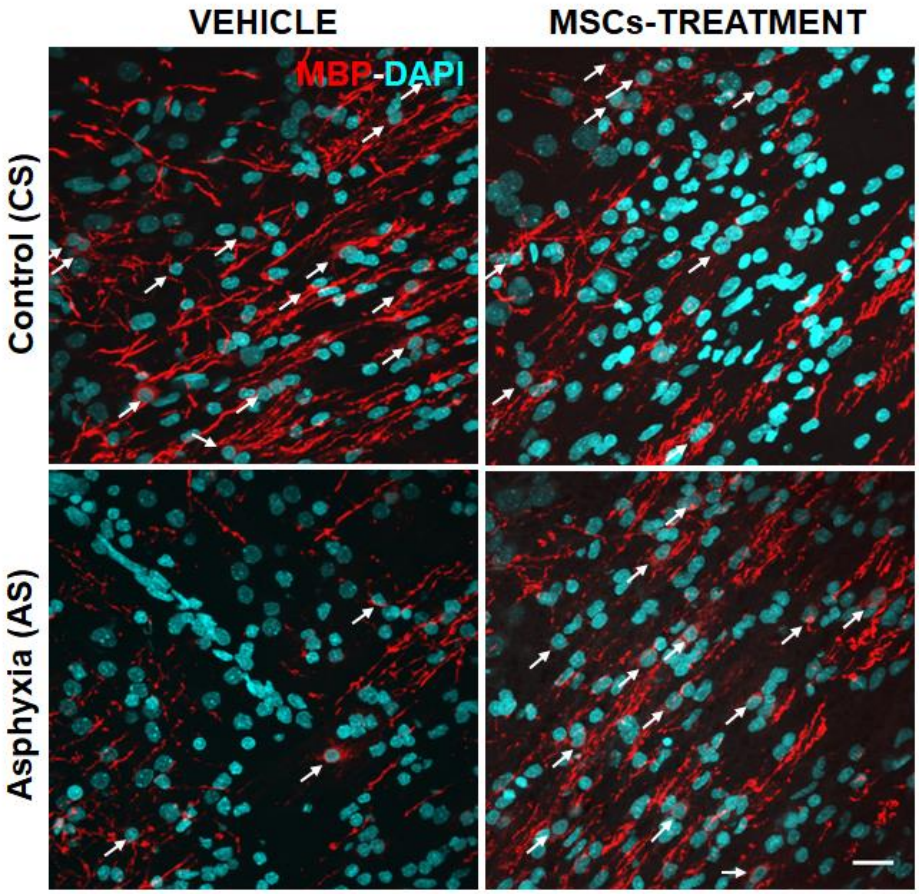

B. CINGULUM

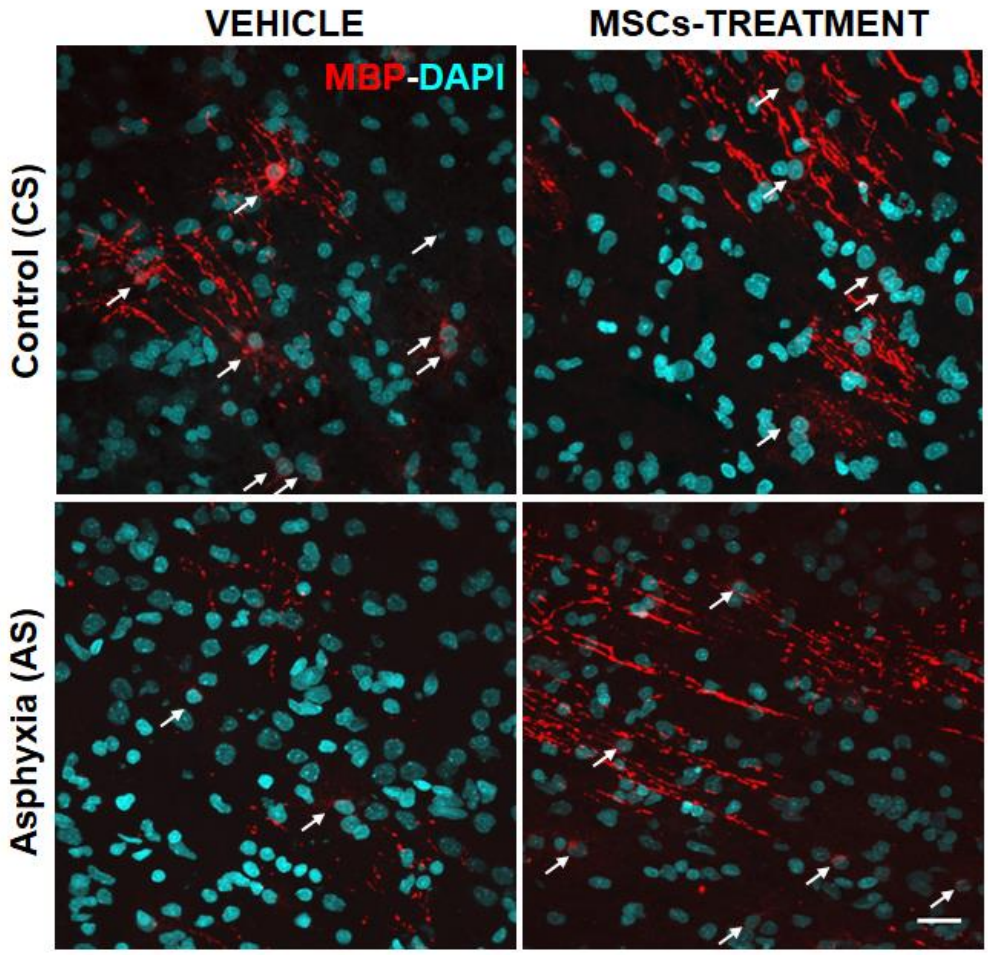

Figure 17. Effect of MSCs treatment on myelination and mature oligodendrocyte (OLs) injury induced by perinatal asphyxia (PA), measured at P7 in external capsule (A), and cingulum (B) of CS (a) and AS (b) rat neonates. Representative microphotographs obtained by confocal microscopy showing myelin basic protein (MBP; red) and DAPI (blue; nuclei)-positive cells in (A) external capsule; and (B) cingulum from control (CS) and asphyxia-exposed (AS) rat neonates, including vehicle and MSCs treatment groups. Microphotographs show MBP, indicating myelinated fibres (white head arrows) and mature oligodendrocytes (OLs) (white arrows). Scale bar: 20 μm. The density of MBP and number of MBP-DAPI cell/mm3 is increased in MSCs- versus vehicle-treated AS neonates in all evaluated regions.

Table 6. Effect of perinatal asphyxia (PA) on oligodendrocytes (MBP-DAPI/mm^3) and myelination (MBP positive pixels/total pixels) at P7, from control (CS) and asphyxia-exposed (AS) rats: Effect on neonatal MSCs treatment. Coronal sections of telencephalon were treated for immunohistochemistry against myelin basic protein (MBP), counterstained with DAPI. Microphotographs (two-five samples per brain region) were taken from external capsule, corpus callosum and cingulum, in the field of a confocal-inverted Olympus-fv10i microscope at 60x. Mean number of the glial cells per mm^3 and percentage of MBP immunopositive pixels over the total pixel number was estimated using ImageJ software. Data are shown as means ± S.E.M from N=5 independent experiments. Unbalanced two-way ANOVA indicated a significant effect of PA on MBP-DAPI/mm^3 and myelination, increasing significantly in external capsule ($F(2, 15)= 4.412$, $P=0.031$; $F(2, 16)= 2.813$, $P=0.034$, respectively); and cingulum ($F(2, 13)= 2.632$, $P= 0.039$; $F(2, 13)= 3.177$, $P=0.032$, respectively) of MSCs- compared to vehicle-treated AS rat neonates, but not in corpus callosum ($F(2, 15)= 0.738$, $P=0.450$; $F(2, 14)= 1.484$, $P=0.151$, respectively); and. Benjamini-Hochberg was used as a post hoc test. *P < 0.05, **P < 0.01, ***P < 0.001, ****P < 0.0001 (italics).

Experimental groups	**P7**	
A. CS vehicle (n= 5)	**MBP-DAPI/mm^3**	**MBP (pixels/ total pixels)**
External capsule	13833±1801	19.60±1.32
Corpus callosum	6126±1345	2.66±0.44
Cingulum	9172±2078	9.27±1.61
B. CS MSCs (n= 5)		
External capsule	13632±1783	16.36±3.05
Corpus callosum	5972±2775	2.24±0.46
Cingulum	6572±1585	8.91±1.49
C. AS vehicle (n= 5)		
External capsule	**6690±2173 (by ~50%)a***	**13.08±0.81 (by ~30%)**a**
Corpus callosum	3942± 1255	1.54±0.42
Cingulum	**3840±509.30 (by ~55%)a***	**4.52±0.10 (by 40%)**a*
D. AS MSCs (n= 5)		
External capsule	**13628±2237 (>2)b***	**17.53±1.70 (>1.3)**b*
Corpus callosum	7835±2339	2.73±0.62
Cingulum	**6194±2145 (>1.6)b***	**7.07±1.47 (>1.5)**b*

VII. DISCUSSION

PA implies interruption of oxygen availability, leading to death if oxygenation is not promptly re-established, and to short- and long-lasting sequelae affecting the surviving infants when re-oxygenation is re-established. Periventricular leukomalacia (PVL) is a typical damage pattern associated to PA, and a major contributor to cerebral palsy, characterized by injury of white matter (see Back and Volpe.1997; Miller et al*.,* 2005). The pathophysiology underlying PVL is not fully understood, hampering the ability to develop preventing treatments.

The issue has been investigated with a rat model of global PA (Bjelke et al.,1991; Andersson et al.,1992; Herrera-Marschitz et al.,1993). The effect of the insult was characterised by an Apgar scale, measuring critical parameters for this experimental model, monitoring survival, respiratory function, periphery blood perfusion and behavioural parameters, including spontaneous movements and vocalization at 40 min up to P14 after birth. The percentage of survival (~60%) and recovery directly determine the severity of the insult. The recovery period can also prolong a hypoxic condition, as the surviving pups may show changing in cardiovascular function, as shown by Herrera-Marschitz et al. (2011), reporting a decreased of ATP levels and CDK activity, implying a metabolic distress and interruption of replication and differentiation of cells in heart; and low peripheral and/or central blood perfusion as shown by Lespay et al. (2018).

In this report, the surviving pups showed a sustained decrease in respiratory rate frequency. In rat pups, lung development occurs postnatally during the first 2 weeks, hence vulnerable to metabolic insult by hypoxia/reoxygenation. Studies in neonate rats have shown that hypoxia may compromise alveolar, airway, and pulmonary vascular development, predisposing to less efficient gas exchange, contributing to the pathogenesis of multiple pulmonary diseases (Truog et al., 2008 and Vogel el al., 2015). The issue is clinically relevant, because the impairment of gas exchange may lead to both cardiovascular and

respiratory defects. After asphyxia, the newborns undergo a period of apnoea or bradypnea, which is also associated with bradycardia (Polglase et al., 2016). Thus, the downstream consequences of asphyxia are detrimental to multiple organ systems (Lubec et al.,1997a,b; Herrera-Marschitz et al., 2011), and therefore, the contribution of cardiovascular and respiratory system deficits to the long-term consequences of PA needs to be further investigated.

Postnatal development is reflected among others by the maturation of neurological reflexes and motor coordination, representing thus a hallmark for CNS development (Lubics et al., 2005). It has been reported that PA led to a marked delay in neurobehavioral development (Simola et al., 2008, Kiss et al., 2009, Allende et al., 2012). Recent studies in our laboratory showed that PA induced remarkable developmental delay in the performance of righting and cliff aversion reflexes (Carril J. et al., SOFARCHI congress 2019).

In the present report, animals were monitored for evaluating motor coordination (coordinated movements of forward and hind legs), as well as head and neck, motor and exploratory behaviour at P1 up to P14. At P1, a decrease in total travelled distance and in the moving time was observed after PA. At P7 and P14 no locomotor differences were observed, probably reflecting a high degree of plasticity shown by the neonatal rat brain (Jansen et al., 1997; Lubics et al., 2005). Interestingly, the outcome of sensorimotor parameters 24 h after HI is correlated with long-term deficits in motor coordination (Ten et al., 2003). In agreement, previous studies of our laboratory showed that adult rats exposed to asphyxia at delivery displayed motor coordination deficits, possible related to a partial and/or mild reduction in dopaminergic tone induced by PA (Chen et al., 1995, 1997; Kirik et al., 1998; Barneoud et al., 2000; Deumens et al., 2002; Bustamante et al. 2002). Nevertheless, no changes in gross motor activity, defined as locomotor activity and/or total motor activity, have been reported (Simola et al., 2008). However, there is no consensus respect to the effect of PA on locomotor behaviour evaluated in open field. It has been found that PA can

induce hypo- or hiper-motor activity, depending upon the time after the type of insult used for the observation (Antier et al., 1988, Balduini et al., 2001, Lubics et al., 2005).

The effect of global PA on myelination and OLs maturation has been scarcely explored, although it is a highly clinically relevant issue. Thus, the present study reports on the effect of PA, focused on myelination, expression of oligodendrocyte transcription factors, neuroinflammation, glial cells and cell death in telencephalon and hippocampus of rats at P1, P7 and P14, prevented by neonatal MSCs treatment. While the aim of the study was to monitor the effects of PA occurring at P1 to P14, a critical postnatal period characterised by a spur of neuronal networking, we found that the most relevant changes occurred at P7.

It was found that PA produced: (i) a decrease of MBP immunoreactivity at P7 in telencephalon (external capsule, corpus callosum, cingulum), but not in fimbriae of hippocampus; (ii) an increase of Olig-1 transcriptional factor mRNA levels at P7; (iii) an increase of IL-6 mRNA, but not of protein levels at P7; (iv) an increase of cell death, including OLs-specific cell death at P7. (v) MSCs treatment prevented the effect of PA on myelination, OLs number and cell death.

In the present report, no MBP immunostaining was observed in any of the analysed regions at P1, under any of the experimental conditions. OLs and/or myelin fibres were only evident at P7, while at P14, the soma of OLs could not be seen as independent structures, because of the dense amount of MBP positive fibres, both in CS and AS animals. At P7 and P14, MBP immunoreactivity increased, both in CS and AS neonates, mainly in the external capsule, cingulum and corpus callosum, regions myelinated at earlier stages than the fimbriae of hippocampus, also investigated in the present report. This agrees with the idea that myelination progresses in an age and region-

dependent manner (Ziemka-Nalecz et al., 2018). Indeed, myelination occurs in response to functional demands, such as suckling reflex, and other motor and sensory requirements related to early nursing and behavioural skills (Downes et al., 2014). It was found here that PA induced a decrease in myelination and OLs number, probably related to the long-term white matter dysfunction reported at adulthood by Kohlhauser et al. (2000). During development OLs play also an important role for the formation and sculpturing of neurocircuitries, exerting regulatory functions, guiding and stabilizing neuronal connections, regardless of the onset of myelination, preventing aberrant connections at adulthood (Mathis et al., 2003; Collin et al., 2007). It was previously reported the neonatal genetic ablation of OLs during the first postnatal week induced a severe structural and functional impairment of the cerebellar cortex, even after recovery of OLs and myelination (Doretto et al., 2011). Thus, long term changes in white matter observed following PA could imply interruption of an early OLs regulatory function, required for neurocircuitry and synapse formation.

The end point of the oligodendroglial linage is the formation of myelin, implying differentiation and maturation, starting with neural stem cells originating from subventricular zone (SVZ), leading to OPCs, which preserve their ability to migrate, proliferate and differentiate to preOLs, progressing to their final stage, i.e. myelinating OLs (see van Tilborg et al., 2018). The maximal vulnerability to PVL occurs at a period before the onset of active myelination (see Back and Volpe.1997), which in humans is around postconceptional week 28–32 (Back et al., 2001), equivalent to P2-5 in rats (Craig et al., 2003), when myelination starts, reaching a peak at the second and third postnatal weeks, continuing along adulthood, albeit at a lower rate (Doretto et al., 2011). The process of myelination is performed by mature OLs (see Miron et al., 2011), therefore a perinatal metabolic insult would result in white matter damage, implying hypomyelination, while a postnatal insult would lead to demyelination (see Vannucci et al., 1999), by failure of OPCs to generate a new preOLs pool, or secondary to neuroaxonal degeneration (Dean et al., 2011). Thus, we have focused here on a developmental

window equivalent to a preterm human baby, when preOLs phenotype predominates, the highest-risk period for white matter injury (Craig et al., 2003).

Prematurity is a relevant issue. There are studies reporting that vulnerability to HI depends on the maturity of the oligodendroglial lineage. preOLs are a selectively vulnerable phenotype, due to low antioxidant defences, increased expression of calcium permeable glutamate receptors, impaired glutamate transport, and susceptibility to proinflammatory cytokines-induced cell death (see Back and Volpe. 1999; Back et al., 2002a, b; see Jensen et al., 2005; see Volpe et al., 2008). In rat at P7, immature OLs predominate (Dean et al., 2011), showing a phenotype with greater resistance to cell death induced by hypoxia than preOLs (Back et al., 2002a), but similar to that shown by mature OLs. However, a metabolic insult at a delayed developing phase can still interrupt myelination, by acting on areas showing persistence of the preOLs phenotype, as that occurring in cerebral cortex (Dean et al., 2011).

Clinical and experimental studies (Buser et al., 2012) have shown that the long-term consequences of PA depend on the severity and duration of the insult, as well as on the developmental stage of the affected region, implying differences in antioxidant defences, local metabolic imbalance during the re-oxygenation period and rescue mechanisms (see Rocha-Ferreira and Hristova, 2016). Thus, the ability of OPC proliferation and differentiation to overcome metabolic deficits might explain the regional differences observed in myelination. We previously showed *in vivo* (Morales et al., 2008) and *in vitro* (Morales et al., 2007; Tapia-Bustos et al., 2017) studies showing that PA increased BrDU positive cell proliferation in hippocampus and subventricular zone, but only approximately a 40% of BrDU positive cells were double-labelled with MAP-2, suggesting a predominance of gliogenesis, implying a newly generated population of OLs, able to complete the process of axonal myelination. A newly generated population of OLs may explain why no differences in myelination were observed between CS and AS animals in any of the analysed regions at P14. The possibility also exists, however, that an

excess of OPC are generated during ontogenesis, remaining in an undifferentiated stage, forming part of the CNS parenchyma along the lifespan, mobilised in response to pathological signals, contributing to restoration of axon myelination (Ziemka-Nalecz et al., 2018).

Regulation of the oligodendroglial lineage is a multifactorial process. Basic helix–loop–helix transcription factors Olig-1 and Olig-2 play an essential role in oligodendroglia development (see Ligon et al., 2006). These transcription factors are co-ordinately expressed along development (see Meijer et al., 2012), playing a pivotal role in biological processes, including OLs proliferation, differentiation, maturation and myelination/remyelination (see Mei et al., 2013; Arnett et al., 2004). Persistent expression of Olig-2 throughout oligodendroglial development has been reported, suggesting that this factor is involved in OPCs specification and differentiation, repressing OLs maturation and myelination (Mei et al., 2013). Nevertheless, it was found here that Olig-1, but not Olig-2 mRNA increased in telencephalon at P7 in AS neonates. Olig-1 factor is an important marker of OPCs (Lu et al., 2002; see Ross et al., 2003), and it can stimulate differentiation and maturation to OLs (see Meijer et al., 2012), but also reparation (Arnett et al., 2004). However, controversial results have also been reported. French et al., (2009) showed that oxidative stress following postnatal HI reduces the expression of Olig-1, while Cheng et al., (2015) reported a decrease in Olig-1 protein levels 1-3 days after postnatal HI, but an increase when measured 7-21 days after HI, although failing to reach the levels observed following normoxia conditions.

Neuroinflammation can increase proliferation of OPCs, producing long-lasting defects in oligodendroglial development and myelination, probably by disruption of Olig-1 and Olig-2 transcription factors (see Volpe et al., 2011; Favrais et al., 2011). Pro-inflammatory cytokines (IL-1β, IL-6, TNF-α, Cox-2) have been reported to produce cytotoxic effects on OLs, *in vitro* (Baerwald and Popko, 1998; Molina-Holgado et al., 2001; Genc et al., 2006) and *in vivo* (Favrais et al., 2011; Bonestroo et al., 2015), inducing premature maturation of the existing precursors and aberrant

myelination, thereby contributing to hypomyelination. In this study, it was found that there was an increase of IL-6 mRNA levels, but not of protein levels in telencephalon at P7. Previous studies in our laboratory showed that IL-1β and TNF-α mRNA and protein levels were increased 24 h after the insult, but only in mesencephalon (Neira-Peña et al., 2015). These differences could be explained by temporally and regionally selective changes.

Activation of microglia and astrocytes is one of the signatures of neuroinflammation (see Tjalkens et al., 2017). Hence astrocytes and microglial cells were also monitored, since there is a glia-glia crosstalk playing an important role in the modulation of OLs homeostasis, along with myelination, demyelination, and re-myelination (see Domingues et al., 2016). Astrocyte activation is an early indicator of neuropathology, measured as increased GFAP expression and morphological alterations (see O'Callaghan and Sriram, 2005; see Parpura et al., 2012). No changes were observed, however, in the number of GFAP-DAPI/mm^3 in telencephalon and fimbriae of hippocampus, in agreement with previous reports (Perez-Lobos et al., 2017). Nevertheless, astrocyte morphology was not monitored, although a preliminary study showed no differences among CS and AS animals (data not shown). Microglial cells are the primary effectors of the innate immune response within the CNS, whose activation occur at early stages of diseases, often preceding overt neuropathology (see Gehrmann et al., 1995; see Hirsch and Hunot, 2009). No changes were observed in Iba-1-DAPI/mm^3 in external capsule, corpus callosum and fimbriae of hippocampus, but an increase was observed in cingulum. These results emphasize the idea that in the evaluated areas, OLs are the most vulnerable glial cells to hypoxia-reoxygenation insult.

TUNEL/DAPI co-labelling indicated an apoptotic mechanism for dying cells, mainly at the DNA fragmentation stage, considered to be an early event of apoptosis (Labat-Moleur et al., 1998). In this report, it was found that there was a decrease in the number of OLs and an increase of total and OLs-specific cell death in telencephalic regions, suggesting a developmental disruption in differentiation

processes, but also a direct damage to the mature OLs phenotype. Mature OLs are subject to a precisely regulated multistep process of differentiation from their precursors. This multistep process is highly energy dependent, regulated by the expression of numerous genes susceptible to hypoxia (see Janowska et al., 2018). Indeed, OLs are vulnerable to metabolic insults, oxidative stress, inflammation and/or excitotoxicity (see Mc Tigue and Tripathi. 2008; Bradl and Lassmann. 2010), being pre-OLs the most vulnerable linage (see Back and Volpe.1997; Back et al., 2002a). This vulnerability is enhanced by local low oxidative stress defences, diminished ATP-dependent ion transport and extracellular glutamate accumulation, increasing NMDA-dependent calcium conductance and intracellular neurotoxic proinflammatory-cascades, overpassing the antioxidant defences (see Back and Volpe, 1999).

Several lines of evidence indicate that pre- and immature OLs undergo a reactive response to neonatal HI, characterized by morphological changes in cell soma and processes, with a distribution that overlaps that of reactive astrocytes and reactive microglia (Back et al., 2002a). It has been shown that there is an accelerated maturation of reactive pre-OLs to immature OLs (Back et al., 2002b; Casaccia-Bonnefil et al., 1997; Durand et al.,1997; Tikoo et al.,1998), which may be maladaptive, delaying or even arresting differentiation and maturation (Buser et al., 2012; Bonestroo et al., 2015, Back et al., 2002b), causing hypomyelination.

There is an extent list of preclinical evidences indicating that MSCs administration can be an effective option to prevent neurodegenerative cascades, altering OLs differentiation and/or preventing cell death (see Janowska et al., 2018). It was found here, that MSCs treatment increased significantly MBP levels in the external capsule and cingulum. It is suggested that MSCs treatment decreases brain damage by either (i) inhibiting injuring signals; (ii) replacing lost tissue, and/or (iii) enhancing endogenous repair processes (Li et al., 2002, 2005; Chen et al., 2003; Deng et al., 2006; Ohtaki et al., 2008; see van Velthoven et al., 2009; see Zhang and Chopp. 2009). Thus, several plastic mechanisms can take place in a region

and time dependent manner, expecting therefore differential effects by MSCs treatment.

The present results agree with that reported by van Velthoven et al., (2010a,b), who demonstrated that a single acute administration of MSCs increases the number of OLGs, decreased by neonatal HI, increasing myelination. MSCs treatment might enhance endogenous cell proliferation/survival and/or differentiation of OLGs progenitors. In addition, inhibition of deleterious processes may also contribute to the beneficial effects of MSC treatment, restoring myelination (Chen et al., 2003; Li et al., 2005; Ohtaki et al., 2008).

VIII. GENERAL CONCLUSIONS

In conclusion, the present findings provide evidence that PA induces regional and developmental-dependent changes on myelination and OLs maturation, but not on astroglia and microglia. Thus, OLs are the most vulnerable glial cells to hypoxia-reoxygenation insults at early neonatal stages, evaluated in vulnerable areas.

Early neonatal MSCs treatment significantly improves survival of mature OLs and myelination in telencephalic white matter. The outcome occurred in association with decreased apoptosis.

IX. REFERENCES

1. **Ahearne, C.E.,** Boylan, G.B., Murray, D.M., 2016. Short and long term prognosis in perinatal asphyxia: An update. World J. Clin. Pediatr. 5(1),67–74.

2. **Allende-Castro, C.,** Espina-Marchant, P., Bustamante, D., Rojas-Mancilla, E., Neira, T., Gutierrez-Hernandez, M.A., Esmar, D., Valdes, J.L., Morales, P., Gebicke-Haerter, P.J., Herrera-Marschitz, M., 2012. Further studies on the hypothesis of PARP-1 inhibition as a strategy for lessening the long-term effects produced by perinatal asphyxia: effects of nicotinamide and theophylline on PARP-1 activity in brain and peripheral tissue: nicotinamide and theophylline on PARP-1 activity. Neurotox. Res. 22(1), 79-90.

3. **Andersson, K**., Blum, M., Chen, Y., Eneroth, P., Gross, J., Herrera-Marschitz, M., Bjelke, B., Bolme, P., Diaz, R., Jamison, L., Loidl, F., 1995. Ungethüm, U. Åström, G. Ögren, SÖ. Perinatal asphyxia increases bFGF mRNA levels and DA cell body number in mesencephalon of rats. Neuroreport 6:375–378.

4. **Antier, D.,** Zhang, B.L., Mailliet, F., Akoka, S., Pourcelot, L., Sannajust, F., 1998. Effects of neonatal focal cerebral hypoxia–ischemia on sleep-waking pattern, EcoG power spectra and locomotor activity in the adult rat. Brain Res. 807, 29–37.

5. **Arnett, H.A.,** Fancy, S.P., Alberta, J.A., Zhao, C., Plant, S.R., Kaing, S., Raine, C.S., Rowitch, D.H., Franklin, R.J., Stiles, C.D., 2004. bHLH transcription factor Olig1 is required to repair demyelinated lesions in the CNS. Science. 306, 2111–2115.

6. **Back, S.A.,** Volpe, J.J., 1997. Cellular and molecular pathogenesis of periventricular white matter injury. Ment. Retard. Dev. Disabil. Res. 3, 96-107.

7. **Back, S.A.,** Volpe, J.J., 1999. Approaches to the study of diseases involving oligodendroglial death. Cell Death and Diseases of the Nervous System. 19, 401-427.

8. **Back, S.A.** Luo N,L. Borenstein N.S., Levine, J.M., Volpe, J.J., Kinney, H.C., 2001. Late oligodendrocyte progenitors coincide with the developmental window of vulnerability for human perinatal white matter injury. J. Neurosci. 21(4), 1302–1312.

9. **Back, S.A.,** Han, B.H., Luo, N.L., Chricton, C.A., Xanthoudakis, S., Tam, J., Arvin, K.L., Holtzman, D.M., 2002a. Selective vulnerability of late oligodendrocyte progenitors to hypoxia-ischemia. J. Neurosci. 22(2), 455-463.

   Back, S.A., Luo, N.L., Borenstein, N.S., Volpe, J.J., Kinney, H.C., 2002b. Arrested oligodendrocyte lineage progression during human cerebral white

matter development: dissociation between the timing of progenitor differentiation and myelinogenesis. J. Neuropathol. Exp. Neurol. 61(2), 197-211.

10. **Balduini, W.,** De Angelis, V., Mazzoni, E., Cimino, M., 2001. Simvastatin protects against long-lasting behavioral and morphological consequences of neonatal hypoxic/ischemic brain injury. Stroke 32, 2185–2191.

11. **Baerwald, K.D.,** Popko, B., 1998. Developing and mature oligodendrocytes respond differently to the immune cytokine interferon-gamma. J. Neurosci. Res. 52, 230–239.

12. **Barateiro, A.,** Fernandes, A., 2014. Temporal oligodendrocytes lineage progression: in vitro models of proliferation, differentiation and myelination. Biochim. Biophys. Acta. 1843, 1917-1926.

13. **Baron, W.,** Hoekstra, D., 2010. On the biogenesis of myelin membranes: sorting, trafficking and cell polarity. FEBS Lett. 584(9),1760-1770.

14. **Baumann, N.,** Pham-Dinh, D., 2001. Biology of oligodendrocyte and myelin in the mammalian central nervous system. Physiol. Rev. 81(2), 871-927.

15. **Barneoud, P.,** Descombris, E., Aubin, N., Abrous, D.N., 2000. Evaluation of simple and complex sensorimotor behaviours in rats with a partial lesion of the dopaminergic nigrostriatal system. Eur. J. Neurosci. 12, 322–336.

16. **Benarroch, E.E.,** 2009. Oligodendrocytes: Susceptibility to injury and involvement in neurologic disease. Neurology. 72(20), 1779-1785.

17. **Bercury, K.K.,** Macklin, W.B., 2015. Dynamics and mechanisms of CNS myelination. Dev Cell. 32(4), 447-458.

18. **Bjelke, B.,** Andersson, K., Ögren, S., Bolme, P., 1991. Asphyctic lesion: proliferation of tyrosine hydroxylase immunoreactivity nerve cell bodies in the rat substantia nigra and functional changes in dopamine neurotransmission. Brain Res. 543,1–9.

19. **Blomgren, K.,** Hagberg, H., 2006. Free radicals, mitochondria, and hypoxia-ischemia in the developing brain. Free Radic. Biol. Med. 40(3), 388–397.

20. **Boggs, J.M.,** 2006. Myelin basic protein: a multifunctional protein. Cell Mol. Life Sci. 63(17), 1945-1961.

21. **Bona, E.,** Andersson, A.L., Blomgren, K., Gilland, E., Puka-Sundvall, M., Gustafson, K., Hagberg, H., 1999. Chemokine and inflammatory cell response to hypoxia ischemia in immature rats. Pediatr. Res. 45, 500–509.

22. **Bonestroo, H.J.,** Heijnen, C.J., Groenendaal, F., van Bel, F., Nijboer, C.H., 2015. Development of cerebral gray and white matter injury and cerebral inflammation over time after inflammatory perinatal asphyxia. Dev. Neurosci. 37(1), 78-94.

23. **Bradl, M.,** Lassmann, H., 2010. Oligodendrocytes: biology and pathology. Acta Neuropathol. 119(1), 37-53.

24. **Buser, J.R.,** Maire, J., Riddle, A., Gong, X., Nguyen, T., Nelson, K., Luo, N.L., Ren, J., Struve, J., Sherman, L.S., Miller S.P., Chau, V., Hendson, G., Ballabh, P., Grafe, M.R., Back, S.A., 2012. Arrested preoligodendrocyte maturation contributes to myelination failure in premature infants. Ann. Neurol. 71(1), 93-109.

25. **Bustamante, D.,** Goiny, M., Åström, G., Gross, J., Andersson, K., Herrera-Marschitz, M., 2003. Nicotinamide prevents the long-term effects of perinatal asphyxia on basal ganglia monoamine systems in the rat. Exp. Brain Res. 148, 227–232.

26. **Camargo, N.,** Goudriaan, A., van Deijk, A.L.F., Otte, W.M., Brouwers, J.F., Lodder, H., Gutmann, D.H., Nave, K.A., Dijkhuizen, R.M., Mansvelder, H.D., 2017. Oligodendroglial myelination requires astrocyte-derived lipids. PLoS Biol. 15, e1002605.

27. **Cammer, W.,** 2000. Effects of TNF[alpha] on immature and mature oligodendrocytes and their progenitors in vitro. Brain Research. 864, 213–219.

28. **Cannon, T.D.,** Yolken, R., Buka, S., Torrey, E.F., Collaborative Study Group on the Perinatal Origins of Severe Psychiatric Disorders., 2008. Decreased neurotrophic response to birth hypoxia in the etiology of schizophrenia. Biol. Psychiatry. 64(9), 797-802.

29. **Casaccia-Bonnefil, P**., Tikoo, R., Kiyokawa, H., Friedrich, V., Chao, M.V., Koff, A., 1997. Oligodendrocyte precursor differentiation is perturbed in the absence of the cyclin-dependent kinase inhibitor p27kip1. Genes Dev. 11(18), 2335-2346.

30. **Chen, Y.,** Ögren, S.O., Bjelke, B., Bolme, P., Eneroth, P., Gross, J., Loidl, F., Herrera-Marschitz, M., Andersson, K., 1995. Nicotine treatment counteracts perinatal asphyxia-induced changes in the mesostriatal/ limbic dopamine systems and in motor behaviour in the four-week old male rat. Neuroscience. 68, 531–538.

31. **Chen, Y.,** Engidawork, E., Loidl, F., Dell'Anna, E., Goiny, M., Lubec, G., Andersson, K., Herrera-Marschitz, M., 1997. Short- and long-term effects of perinatal asphyxia on monoamine, amino acid and glycolysis product levels measured in the basal ganglia of the rat. Brain Res. Dev. Brain Res. 104(1-2), 19-30.

32. **Chen, J.,** Li, Y., Katakowski, M., Chen, X., Wang, L., Lu, D., Lu, M., Gautam, S.C., Chopp, M., 2003. Intravenous bone marrow stromal cell therapy reduces apoptosis and promotes endogenous cell proliferation after stroke in female rat. J. Neurosci. Res. 73(6), 778–786.

33. **Cheng, T.,** Xue, X., Fu, J., 2015. Effect of OLIG1 on the development of oligodendrocytes and myelination in a neonatal rat PVL model induced by hypoxia-ischemia.

34. **Chu, D.T.,** Nguyen Thi Phuong, T., Tien, N.L., Tran, D.K., Minh, L.B., Thanh, V.V., Gia Anh, P., Pham, V.H., Thi Nga, V., 2019. Adipose Tissue Stem Cells for Therapy: An Update on the Progress of Isolation, Culture, Storage, and Clinical Application. J. Clin. Med. 8(7), 917-936.

35. **Clemens, J.A.,** Stephenson, D.T., Yin, T., Smalstig, E.B., Panetta, J.A., Little, S.P., 1998. Drug-induced neuroprotection from global ischemia is associated with prevention of persistent but not transient activation of nuclear factor-kappa B in rats. Stroke 29(3), 677-682.

36. **Collin, L.** Doretto, S. Malerba, M. Ruat, M. Borrelli, E., 2007. Oligodendrocyte ablation affects the coordinated interaction between granule and Purkinje neurons during cerebellum development. Exp. Cell Res. 313(13), 2946–2957.

37. **Corley, S.M.,** Ladiwala, U., Besson, A., Yong, V.W., 2001. Astrocytes attenuate oligodendrocyte death in vitro through an alpha(6) integrin-laminin-dependent mechanism. Glia. 36, 281–294.

38. **Constantin. G.,** Marconi, S., Rossi, B., Angiari, S., Calderan, L., Anghileri, E., Gini, B., Bach, S.D., Martinello, M., Bifari, F., Galie, M., Turano, E., Budui, S., Sbarbati, A., Krampera, M., Bonetti, B., 2009. Adipose-derived mesenchymal stem cells ameliorate chronic experimental autoimmune encephalomyelitis. Stem Cells. 27(10), 2624–2635.

39. **Craig, A.,** Ling Luo, N., Beardsley, D.J., Wingate-Pearse, N., Walker, D.W., Hohimer, A.R., Back, S.A., 2003. Quantitative analysis of perinatal rodent

oligodendrocyte lineage progression and its correlation with human. Exp. Neurol.181(2), 231-240.

40. **Dai, X.,** Lercher, L.D., Clinton, P.M., Du, Y., Livingston, D.L., Vieira, C., Yang, L., Shen, M.M., Dreyfus, C.F., 2003. Trophic role of oligodendrocytes in the basal forebrain. J. Neurosci. 23, 5846-5853.

41. **Davidson, J.O.,** Wassink, G., van den Heuij, L.G., Bennet, L., Gunn, A.J., 2015. Therapeutic Hypothermia for Neonatal Hypoxic–Ischemic Encephalopathy – Where to from Here? Front. Neurol. 6,198.

42. **de Girolamo, L.,** Lucarelli, E., Alessandri, G., Avanzini, M.A., Bernardo, M.E., Biagi, E., Brini, A.T., D'Amico, G., Fagioli, F., Ferrero, I., Locatelli, R.M., Marazzi, M., Parolini, O., Pessina, A., Torre, M.L. Mesenchymal Stem/Stromal Cells: A New "Cells as Drugs" Paradigm. Efficacy and Critical Aspects in Cell Therapy. Curr. Pharm. Des.19, 2459–2473.

43. **de Castro, F.,** Bribián, A., 2005. The molecular orchestra of the migration of oligodendrocyte Precursors during development. Brain Res. Rev. 49, 227-241.

44. **Dean, J.M.,** Moravec, M.D., Grafe, M., Abend, N., Ren, J., Gong, X., Volpe, J.J., Jensen, F.E., Hohimer, A.R., Back, S.A., 2011. Strain-specific differences in perinatal rodent oligodendrocyte lineage progression and its correlation with human. Dev. Neurosci. 33(3-4), 251-260.

45. **Deans, R.J.,** Moseley, A.B., 2000. Mesenchymal stem cells: biology and potential clinical uses. Exp. Hematol. 28(8), 875-884.

46. **Deguchi, K.,** Mizuguchi, M., Takashima, S., 1996. Immunohistochemical expression of tumor necrosis factor alpha in neonatal leukomalacia. Pediatr Neurol. 14, 13–16.

47. **Dell'Anna, E.,** Chen, Y., Engidawork, E., Andersson, K., Lubec, G., Luthman, J., Herrera-Marschitz, M., 1997. Delayed neuronal death following perinatal asphyxia rat. Exp. Brain Res. 115(1), 105-115.

48. **Deng, J.,** Petersen, B.E., Steindler, D.A., Jorgensen, M.L., Laywell, E.D., 2006. Mesenchymal stem cells spontaneously express neural proteins in culture and are neurogenic after transplantation. Stem Cells. 24(4),1054–1064.

49. **Deumens, R.,** Blokland, A., Prickaerts, J., 2002. Modeling Parkinson's disease in rats: an evaluation of 6-OHDA lesions of the nigrostriatal pathway. Exp. Neurol. 175, 303–317.

50. **Dimou, L.,** Simon, C., Kirchhoff, F., Takebayashi, H., Götz, M., 2008. Progeny of Olig2-expressing progenitors in the gray and white matter of the adult mouse cerebral cortex. J. Neurosci. 28(41), 10434-10442.

51. **Dominici, M.,** Le Blanc, K., Mueller, I., Slaper-Cortenbach, I., Marini, F., Krause, D., Deans, R., Keating, A., Prockop, Dj., Horwitz, E., Minimal criteria for defining multipotent mesenchymal stromal cells. 2006. The International Society for Cellular Therapy position statement. Cytotherapy. 8(4),315-317.

52. **Domingues, H.S.,** Portugal, C.C., Socodato, R., Relvas, J.B., 2016. Oligodendrocyte, Astrocyte, and Microglia Crosstalk in Myelin Development, Damage, and Repair. Front. Cell Dev. Biol. 4, 71.

53. **Donega, V.,** Nijboer, C.H., Braccioli, L., Slaper-Cortenbach, I., Kavelaars, A., van Bel, F., Heijnen, C.J., 2014. Intranasal administration of human MSC for ischemic brain injury in the mouse: in vitro and in vivo neurodegenerative functions. PLoS One. 9(11):e112339.

54. **Donoso, E.,** 2011. ¿Está aumentando la mortalidad perinatal en Chile? Rev Chil Obstet Ginecol 76(6), 377-379.

55. **Doretto, S.,** Malerba, M., Ramos, M., Ikrar, T., Kinoshita, C., De Mei, C., Tirotta, E., Xu, X., Borrelli, E., 2011. Oligodendrocytes as regulators of neuronal networks during early postnatal development. PLoS One 6(5), e19849.

56. **Douglas-Escobar, M.,** Weiss, M.D., 2015. Hypoxic-ischemic encephalopathy: a review for the clinician. JAMA Pediatr. 169(4), 397-403.

57. **Downes, N.,** Mullins, P., 2014. The development of myelin in the brain of the juvenile rat. Toxicologic Pathology. 42, 913-922.

58. **Drago, D.,** Cossetti, C., Iraci, N., Gaude, E., Musco, G., Bachi, A., Pluchino, S., 2013. The stem cell secretome and its role in brain repair. Biochimie. 95(12), 2271-2285.

59. **Drury, P.P.,** Gunn E.R., Bennet, L., Gunn, A.J., 2010. Mechanism of hypothermic neuroprotection. Clin. Perinatol. 41(1), 161-175.

60. **Durand, B.,** Gao, F.B., Raff, M., 1997. Accumulation of the cyclin-dependent kinase inhibitor p27/kip1 and the timing of oligodendrocyte differentiation. EMBO. J. 16(2), 306-317.

61. **Edwards, A.,** Mehmet, H., 2008. Apoptosis in perinatal hypoxic-ischaemic cerebral damage. Neuropathology and Applied Neurobiology. 22, 494-498.

62. **Emery, B.,** 2010. Regulation of oligodendrocyte differentiation and myelination. Science. 330(6005), 779-782.

63. **Ezquer, F.,** Giraud-Billoud, M., Carpio, D., Cabezas, F., Conget, P., Ezquer, M., 2015. Pro-regenerative microenvironment triggered by donor mesenchymal stem cells preserves renal function and structure in mice with severe diabetes mellitus. Biomed. Res. Int. 2015,164703.

64. **Ezquer, M.,** Urzua, C.A., Montecino, S., Leal, K., Conget, P., Ezquer, F., 2016. Intravitreal administration of multipotent mesenchymal stromal cells triggers a cytoprotective microenvironment in the retina of diabetic mice. Stem Cell Res. Ther. 7, 42-59.

65. **Favrais, G.,** van de Looij, Y., Fleiss, B., Ramanantsoa, N., Bonnin, P., Stoltenburg-Didinger, G., Lacaud, A., Saliba, E., Dammann, O., Gallego, J., Sizonenko, S., Hagberg, H., Lelievre, V., Gressens, P., 2011. Systemic inflammation disrupts the developmental program of white matter. Ann. Neurol. 2011. 70(4), 550-65.

66. **Fleiss, B.,** Gressens, P., 2012. Tertiary mechanisms of brain damage: a new hope for treatment of cerebral palsy? Lancet Neurol.11(6), 556-66.

67. **Foster-Barber, A.,** Dickens, B., Ferriero, D.M., 2001. Human perinatal asphyxia: correlation of neonatal cytokines with MRI and outcome. Dev. Neurosci. 23, 213–218.

68. **French, H.M.,** Reid, M., Mamontov, P., Simmons, R.A., Grinspan, J.B., 2009. Oxidative Stress Disrupts Oligodendrocyte Maturation.

69. **Galeano, P.,** Blanco Calvo, E., Madureira de Oliveira, D., Cuenya, L., Kamenetzky, G.V., Mustaca, A.E., Barreto, GE., Giraldez-Alvarez, L.D., Milei, J. Capani, F., 2011. Long-lasting effects of perinatal asphyxia on exploration, memory and incentive downshift. Int. J. Dev. Neurosci. 29(6), 609-619.

70. **Gehrmann, J.,** Matsumoto, Y., Kreutzberg, G.W., 1995. Microglia: intrinsic immuneffector cell of the brain. Brain Res. Rev. 20(3), 269-287.

71. **Geisler, H.** Westerga, J. Gramsbergen, A., 1993. Development of posture in the rat. Acta Neurobiol. Exp. 53, 517-523.

72. **Genc, K.,** Genc, S., Baskin, H., Semin, I., 2006. Erythropoietin decreases cytotoxicity and nitric oxide formation induced by inflammatory stimuli in rat oligodendrocytes. Physiol. Res. 55, 33-38.

73. **González, H.,** Toso, P., Kattan, J., Mesa, T., Pérez, E., 2005. Treatment of perinatal asphyxia with total body hypothermia: a clinical case. Rev. Chil. Pediatr. 76(3), 275-280.

74. **Greaves, D.R.,** Gordon, S., 2002. Macrophage-specific gene expression: current paradigms and future challenges. Int. J. Hematol. 76, 6–15.

75. **Guardia, C.M.,** Pasquini, L.A., Soto, E.F., Pasquini, J.M., 2010. Apotransferrin-induced recovery after hypoxic/ischaemic injury on myelination. ASN Neuro. 2(5), e00048.

76. **Hanisch, U.,** Kettenmann, H., 2007. Microglia: active sensor and versatile effector cells in the normal and pathologic brain. Nat. Neurosci. 10, 1387–1394.

77. **Hamilton, S.P.,** Rome, L.H., 1994. Stimulation of in vitro myelin synthesis by microglia. Glia. 11, 326-335.

78. **Harry, G.J.,** Kraft, A.D., 2008. Neuroinflammation and microglia: considerations and approaches for neurotoxicity assessment. Expert Opin Drug Metab. Toxicol. 4, 1265-1277.

79. **Herrera-Marschitz, M**., Loidl, C.F., Andersson, K., Ungerstedt, U., 1993. Prevention of mortality induced by perinatal asphyxia: hypothermia or glutamate antagonism? Amino Acids. 5, 413–419.

80. **Herrera-Marschitz,** M., Morales, P., Leyton, L., Bustamante, D., Klawitter, V., Espina-Marchant., Allende, C., Lisboa, F., Cunich, G., Jara-Cavieres, A., Neira, T., Gutierrez-Hernandez, M.A., Gonzalez-Lira, V., Simola, N., Schmitt, A., Morelli, M., Tasker, R.A., Gebicke-Haerter, P.J., 2011. Perinatal asphyxia: current status and approaches towards neuroprotective strategies, with focus on sentinel proteins. Neurotox. Res. 19(4), 603-627.

81. **Herrera-Marschitz, M.,** Neira-Peña, T., Rojas-Mancilla, E., Espina-Marchant, P., Esmar, D., Pérez, R., Muñoz, V., Gutierrez-Hernandez, M., Rivera, B., Simola, N., Bustamante, D., Morales, P., Gebicke-Haerter, P., 2014. Perinatal asphyxia: CNS development and deficits with delayed onset. Frontiers in Neuroscience. 8,47.

82. **Herrera-Marschitz, M.,** Perez-Lobos, R., Lespay-Rebolledo, C., Tapia-Bustos, A., Casanova-Ortiz, E., Morales, P., Valdes, J.L., Bustamante, D., Cassels, B.K., 2018. Targeting sentinel proteins and extrasynaptic glutamate receptors: a therapeutic strategy for preventing the effects elicited by perinatal asphyxia? Neurotox. Res. 33(2),461–473.

83. **Herrmann, O.,** Baumann, B., Lorenzi, R., Muhammad, S., Zhang, W., Kleesiek, J., Malfertheiner, M., Köhrmann, M., Köhrmann, M., Potrovita, I., Maegele, I., Beyer, C., Burke, K.R., Hasan, M.T., Buiard, H., Wirth, T., Pasparakis, M., Schwaninger, M., 2005. IKK mediates ischemia-induced neuronal death. Nat. Med. 11(12):1322-1329.

84. **Hirsch, E.C.,** Hunot, S., 2009. Neuroinflammation in Parkinson's disease: a target for neuroprotection? Lancet Neurol. 8(4), 382-397.

85. **Horiuchi, M.,** Itoh, A., Pleasure, D., Itoh, T., 2006. MEK-ERK signaling is involved in interferon-gamma -induced death of oligodendroglial progenitor cells. J. Biol. Chem. 281, 20095–20106.

86. **Inder, T.E.,** Huppi, P.S., Warfield, S., Kikinis, R., Zientara, G.P., Barnes, P.D., Jolesz, F., Volpe, J,J., 1999. Periventricular white matter injury in the premature infant is followed by reduced cerebral cortical gray matter volume at term. Ann Neurol. 46, 755-760.

87. **Inouye, H.** Kirschner D.A., 1991. Folding and function of the myelin proteins from primary sequence data. J. Neurosci. Res. 28(1),1-17.

88. **Iacobas, S.,** Iacobas, D.A., 2010. Astrocyte proximity modulates the myelination gene fabric of oligodendrocytes. Neuron Glia Biol. 6(3), 157-69.

89. **Janowska, J**., Sypecka, J., 2018. Therapeutic strategies for leukodysthrophic disorders resulting from perinatal asphyxia: focus on myelinating oligodendrocytes. Mol. Neurobiol. 55(5), 4388–4402.

90. **Jansen, E.M.,** Solberg, L., Underhill, S., Wilson, S., Cozzari, C., Hartman, B.K., Faris, P.L., Low, W.C., 1997. Transplantation of fetal neocortex ameliorates sensorimotor and locomotor deficits following neonatal ischemic-hypoxic brain injury in rats. Exp. Neurol. 147, 487–97.

91. **Jensen, F.E.,** 2005. Role of glutamate receptors in periventricular leukomalacia. J. Child Neurol. 20(12), 950-9.

92. **Jurewicz, A.,** Matysiak, M., Tybor, K., Kilianek, L., Raine, C.S., Selmaj, K., 2005. Tumour necrosis factor-induced death of adult human oligodendrocytes is mediated by apoptosis inducing factor. Brain. 128, 2675–2688.

93. **Kadhim, H.,** Tabarki, B., Verellen, G., De Prez, C., Rona, A.M., Sébire, G., 2001. Inflammatory cytokines in the pathogenesis of periventricular leukomalacia. Neurology. 56, 1278–1284.

94. **Kern, S.,** Eichler, H., Stoeve, J., Klüter, H., Bieback, K., 2006. Comparative analysis of mesenchymal stem cells from bone marrow, umbilical cord blood, or adipose tissue. Stem Cells. 24(5),1294-301.

95. **Kesssaris, N.,** Fogarty, M., Iannarelli, P., Grist, M., Wegner, M., Richardson, W.D., 2006. Competing waves of oligodendrocytes in the forebrain and postnatal elimination of an embryonic lineage. Nat. Neurosci. 9(2), 173-179.

96. **Kiss, K.,** Szogyi, D., Reglodi, D., Horvath, G., Farkas, J., Lubics, A., Tamas, A., Atlasz, T., Szabadfi, K., Babai, N., Gabriel, R., Koppan, M., 2009. Effects of perinatal asphyxia on the neurobehavioral and retinal development of newborn rats.

97. **Kirik, D.,** Rosenblad, C., Bjorklund, A., 1998. Characterization of behavioral and neurodegenerative changes following partial lesions of the nigrostriatal dopamine system induced by intrastriatal 6-hydroxydopamine in the rat. Exp. Neurol. 152, 259–277.

98. **Klawitter, V.,** Morales, P., Johansson, S., Bustamante, D., Goiny, M., Gross, J., Luthman, J., Herrera-Marschitz, M., 2005. Effect of perinatal asphyxia on cell survival, neuronal phenotype and neurite growth evaluated with organotypic triple cultures. Amino Acids. 28,149–155.

99. **Klawitter, V.,** Morales, P., Bustamante, D., Goiny, M., Herrera-Marschitz, M., 2006. Plasticity of the central nervous system (CNS) following perinatal asphyxia: does nicotinamide provide neuroprotection? Amino Acids. 31, 377–384.

100. **Klawitter, V.,** Morales, P., Bustamante, D., Gomez-Urquijo, S., Hökfelt, T., Herrera-Marschitz, M., 2007. Neuronal plasticity of basal ganglia following perinatal asphyxia: neuroprotection by nicotinamide. Exp. Brain Res. 180, 139–152.

101. **Koehler, R.C**., Yang, Z.J., Lee, J.K, Martin, L.J., 2018. Perinatal hypoxic-ischemic brain injury in large animal models: Relevance to human neonatal encephalopathy. J. Cereb. Blood Flow Metab.38(12), 2092-2111.

102. **Kohlhauser, C.,** Mosgöller, W., Höger, H., Lubec, B., 2000. Myelination deficits in brain of rats following perinatal asphyxia. Life Sci. 67(19), 2355-2368.

103. **Kumar, A.,** Ramakrishna, S.V., Basu, S., Rao, G.R., 2008. Oxidative Stress in Perinatal Asphyxia. Pediatr. Neurol. 38(3), 181-185.

104. **Labat-Moleur, F.,** Guillermet, C., Lorimier, P., Robert, C., Lantuejoul, S., Bramilla, E., Negoescu, A., 1998. TUNEL apoptotic cell detection in tissue sections: critical evaluation and improvement. J. Histochem. Cytochem. 46, 327–334.

105. **Labombarda, F.,** González, A., Lima, P., Roig, R., Guennoun, M., Schumacher, A.F., De Nicola, A., 2009. Effects of progesterone on oligodendrocyte progenitors, oligodendrocyte transcription factors, and myelin proteins following spinal cord injury. Glia. 57(8), 884–897.

106. **Latorre, R.,** Carrillo, J., Yamamoto, M., Novoa, J.M., Valdés, A., Insunza, A., Paiva, E., 2006. Gobierno del parto en el Hospital Padre Hurtado: Un modelo

para contener la tasa de cesárea y prevenir la encefalopatía hipóxico-isquémica. Rev. Chil. Obstet. Ginecol. 71(3), 196-200.

107. **Lawn, J.E.,** Cousens, S., Zupan, J., Lancet Neonatal Survival Steering Team., 2005. 4 million neonatal deaths: When? Where? Why? Lancet 365(9462), 891-900.

108. **Lawn, J.E.,** Kerber, K. Enweronu-Laryea, C. Cousens, S., 2010. 3.6 million neonatal deaths-what is progressing and what is not? Semin. Perinatol. 34(6), 371-386.

109. **Leaw, B.,** Nair, S., Lim, R., Thornton, C., Mallard, C., Hagberg, H., 2017. Mitochondria, bioenergetics and excitotoxicity: new therapeutic targets in perinatal brain injury. Front Cell Neurosci. 11,199.

110. **Lespay-Rebolledo, C.,** Perez-Lobos, R., Tapia-Bustos, A., Vio, V., Morales, P., Herrera-Marschitz, M., 2018. Regionally Impaired Redox Homeostasis in the Brain of Rats Subjfected to Global Perinatal Asphyxia: Sustained Effect up to 14 Postnatal Days. Neurotox. Res. 34(3), 660-676.

111. **Lespay-Rebolledo, C.,** Tapia-Bustos, A., Bustamante, D., Morales, P., Herrera-Marschitz, M., 2019. The Long-Term Impairment in Redox Homeostasis Observed in the Hippocampus of Rats Subjected to Global Perinatal Asphyxia (PA) Implies Changes in Glutathione-Dependent Antioxidant Enzymes and TIGAR-Dependent Shift Towards the Pentose Phosphate Pathways: Effect of Nicotinamide. Neurotox Res. 36(3), 472-490.

112. **Li, Y.,** Chen, J., Chen, X.G., Wang, L., Gautam, S.C., Xu, Y.X., Katakowski, M., Zhang, L.J., Lu, M., Janakiraman, N., Chopp, M., 2002. Human marrow stromal cell therapy for stroke in rat: neurotrophins and functional recovery. Neurology. 59(4), 514–523.

113. **Li, Y.,** Chen, J., Zhang, C.L., Wang, L., Lu, D., Katakowski, M., Gao, Q., Shen, L.H., Zhang, J., Lu, M., Chopp, M., 2005. Gliosis and brain remodeling after treatment of stroke in rats with marrow stromal cells. Glia. 49(3), 407–417.

114. **Ligon, K.,** Fancy, S., Franklin, R., Rowitch, D., 2006. Olig gene function in CNS development and disease. Glia. 54,1–10.

115. **Liu, F.,** McCullough, L.D., 2013. Inflammatory responses in hypoxic ischemic encephalopathy. Acta Pharmacol. Sin. 34(9), 1121–1130.

116. **Logica, T.,** Riviere, S., Holubiec, M.I., Castilla, R., Barreto, G.E., Capani, F., 2016. Metabolic Changes Following Perinatal Asphyxia: Role of Astrocytes and Their Interaction with Neurons. Front Aging Neurosci. 8,116.

117. **Lu, Q.R.,** Sun, T., Zhu, Z., Ma, N., Garcia, M., Stiles, C.D., Rowitch, D.H., 2002. Common developmental requirement for Olig function indicates a motor neuron/oligodendrocyte connection. Cell.109, 75–86.

118. **Lubec, B.,** Mark, M., Herrera-Marschitz, M., Labudova, O., Hoeger, H., Gille, L., Nohl, H., Mosgoeller, W., Lubec, G., 1997a. Decrease of heart protein kinase C and cyclin dependent kinase precedes death in perinatal asphyxia of the rat. FASEB J. 11, 482–492.

119. **Lubec, B.,** Dell'Anna, E., Fang-Kircher, S., Mark, M., Herrera-Marschitz, M., Lubec, G., 1997b. Decrease of brain protein kinase C, protein kinase A, and cyclin-dependent kinase correlating with pH precedes neuronal death in neonatal asphyxia of the rat. J. Invest. Med. 45, 284–294.

120. **Lubec, B.,** Chiappe-Gutierrez, M., Hoeger, H., Kitzmueller. E., Lubec, G., 2000. Glucose transporters, hexokinase, and phosphofructokinase in brain of rats with perinatal asphyxia. Pediatr Res. 47(1), 84-8.

121. **Lubec, B.,** Labudova, O., Hoeger, H., Kirchner, L., Lubec, G., 2002. Expression of transcription factors in the brain of rats with perinatal asphyxia. Biol. Neonate 81(4), 266–278.

Lubics, A., Reglödi, D., Tamás, A., Kiss, P., Szalai, M., Szalontay, L., Lengvári, I., 2005. Neurological reflexes and early motor behaviur in rats subjected to neonatal hypoxic–ischemic injury. Behavioural Brain Research 157:157–165.

122. **Mathis, C.,** Collin, L., Borrelli, E., 2003. Oligodendrocyte ablation impairs cerebellum development. Development 130(19), 4709–4718.

123. **Marín-Padilla, M.,** 1997. Developmental neuropathology and impact of perinatal brain damage. II: white matter lesions of the neocortex. J Neuropathol Exp Neurol. 56(3), 219-35.

124. **McKinnon, R.D.,** Waldron, S., Kiel, M.E., 2005. PDGF α-receptor signal strength controls an RTK rheostat that integrates phosphoinositol 3′-kinase and phospholipase Cγ pathways during oligodendrocyte maturation. J. Neurosci. 25, 3499-3508.

125. **Mc Tigue,** D.M., Tripathi, R.B., 2008. The life, death, and replacement of oligodendrocytes in the adult CNS. J. Neurochem. 107(1), 1-19.

126. **Mei, F.,** Wang, H., Liu, S., Niu, J., Wang, L., He, Y., Etxeberria, A., Chan, J.R., Xiao, L., 2013. Stage-specific deletion of Olig2 conveys opposing functions on

differentiation and maturation of oligodendrocytes. J. Neurosci. 8; 33(19), 8454-62.

127. **Meijer, D.H.,** Kane, M.F., Mehta, S., Liu, H., Harrington, E., Taylor, C.M., Stiles, C.D., Rowitch, D.H., 2012. Separated at birth? The functional and molecular divergence of OLIG1 and OLIG2. Nat. Rev. Neurosci. 13, 819–831.

128. **Mercuri, E.,** Barnett, A.L., 2003. Neonatal brain MRI and motor outcome at school age in children with neonatal encephalopathy: a review of personal experience. Neural Plast. 10(1-2), 51-57.

129. **Miller, S.P.,** Ramaswamy, V., Michelsol, D., Barkovich, A.J., Holshouser, B., Wycliffe, N., Glidden, D.V., Deming, D., Partridge, J.C., Wu, Y.W., Ashwal, S., Ferreiro, D.M., 2005. Patterns of brain injury in term neonatal encephalopathy. J. Pediatr. 146(4), 453-460.

130. **Miron, V.E.,** Kuhlmann, T., Antel, J.P., 2011. Cells of the oligodendroglial lineage, myelination, and remyelination. Biochim. Biophys. Acta. 1812(2), 184–193.

131. **Miron, V.E.,** Boyd, A., Zhao, J.-W., Yuen, T.J., Ruckh, J.M., Shadrach, J.L., van Wijngaarden, P., Wagers, A.J., Williams, A., Franklin, R.J., 2013. M2 microglia and macrophages drive oligodendrocyte differentiation during CNS remyelination. Nat. Neurosci. 16, 1211.

132. **Mohammadzadeh, M.,** Halabian, R., Gharehbaghian, A., Amirizadeh, N., Jahanian-Najafabadi, A., Roushandeh, A.M., Roudkenar, M.H., 2012. Nrf-2 overexpression in mesenchymal stem cells reduces oxidative stress-induced apoptosis and cytotoxicity. Cell Stress and Chaperones. 17(5), 553–565.

133. **Molina-Holgado, E.,** Vela, J.M., Arevalo-Martina, A., Guaza, C., 2001. LPS/IFNγ cytotoxicity in oligodendroglial cells: role of nitric oxide and protection by the anti-inflammatory cytokine IL-10. Eur. J. Neurosci. 13, 493-502.

134. **Monin, P.,** Baumann, P.S., Griffa, A., Xin, L., Mekle, R., Fournier, M., Butticaz, C., Klaey, M., Cabungcal, J.H., Steullet, P., Ferrari, C., Cuenod, m., Gruetter, R., Thiran J.P., Hagmann, P., Conus, P., Do, KQ., 2015. Glutathione deficit impairs myelin maturation: relevance for white matter integrity in schizophrenia patients. Mol. Psychiatry. 20(7), 827-838.

135. **Morales, P.,** Reyes, P., Klawitter, V., Huaiquin, P., Bustamante, D., Fiedler, J.L., Herrera-Marschitz, M., 2005. Effects of perinatal asphyxia on cell proliferation and neuronal phenotype evaluated with organotypic hippocampal cultures. Neuroscience. 135(2), 421–431.

136. **Morales, P.,** Huaiquin, P., Bustamante, D., Fiedler, J.L., Herrera-Marschitz, M., 2007. Perinatal asphyxia induces neurogenesis in hippocampus: an organotypic culture study. Neurotox Res. 12, 81–84.

137. **Morales, P.,** Fiedler, J.L., Andrés, S., Berrios, C., Huaiquin, P., Bustamante, D., Cardenas, S., Parra, E., Herrera-Marschitz, M., 2008. Plasticity of hippocampus following perinatal asphyxia: Effects on postnatal apoptosis and neurogenesis. J. Neurosci. Res. 86(12), 2650-2662.

138. **Morales, P.,** Simola, N., Bustamante, D., Lisboa, F., Fiedler, J., Gebicke-Haerter, P., Morelli, M., Tasker, R.A., Herrera-Marschitz, M., 2010. Nicotinamide prevents the effect of perinatal asphyxia on apoptosis, non-spatial working memory and anxiety in rats. Exp. Brain Res. 202, 1–14.

139. **Morales, P.,** Bustamante, D., Espina-Marchant, P., Neira-Peña, T., Gutierrez-Hernandez, M., Allende-Castro, C., Rojas-Mancilla, E., 2011. Pathophysiology of perinatal asphyxia: can we predict and improve individual outcomes? EPMA J. 2(2), 211-230.

140. **Morán, J.,** Stokowska, A., Walker, F.R., Mallard, C., Hagberg, H., Pekna, M., 2017. Intranasal C3a treatment ameliorates cognitive impairment in a mouse model of neonatal hypoxic-ischemic brain injury. Exp. Neurol. 290, 74–84.

141. **Nash, B.,** Ioannidou, K., Barnett, S.C., 2011. Astrocyte phenotypes and their relationship to myelination. J. Anat. 219, 44-52.

142. **Nait-Oumesmar, B.,** Picard-Riéra, N., Kerninon, C., Baron-Van, E., 2008. The role of SVZ-derived neural precursors in demyelinating diseases: from animal models to multiple sclerosis. J. Neurol. Sci. 265(1-2), 26-31.

143. **Neira-Peña, T.,** Rojas-Mancilla, E., Muñoz-Vio, V., Perez, R., Gutierrez-Hernandez, M., Bustamante, D., Morales, P., Hermoso, M.A., Gebicke-Haerter, P., Herrera-Marschitz, M., 2015. Perinatal Asphyxia Leads to PARP-1 Overactivity, p65 Translocation, IL-1β and TNF-α Overexpression, and Apoptotic-Like Cell Death in Mesencephalon of Neonatal Rats: Prevention by Systemic Neonatal Nicotinamide Administration. Neurotox. Res. 27(4), 453–465.

144. **Ness, J.K.,** Romanko, M.J., Rothestein, R.P., Wood, T.L., Levison, S.W., 2001. Perinatal hypoxia-ischemia induces apoptotic and excitotoxic death of periventricular white matter oligodendrocyte progenitors. Dev. Neurosci. 23(3), 203-208.

145. **Nicholas, R.S.,** Wing, M.G., Compston, A. 2001. Nonactivated microglia promote oligodendrocyte precursor survival and maturation through the transcription factor NF-κB. Eur. J. Neurosci. 13, 959-967.

146. **Northington, F.J.,** Ferriero, D.M., Graham, E.M., Traystman, RJ., Martin, L.J., 2001a. Early neurodegeneration after hypoxia-ischemia in neonatal rat is necrosis while delayed neuronal death is apoptosis. Neurobiol. Dis. 8, 207–219.

147. **Northington, F.J.,** Ferriero, D.M., Martin, L.J., 2001b. Neurodegeneration in the thalamus following neonatal hypoxia-ischemia is programmed cell death. Dev. Neurosci. 23(3),186–191.

148. **Novoa, J.M.,** Milad, M., Fabres, J., Fasce, J., Toso, P., Arriaza, M., Gandolfi, C., Samamé, M., Aspillaga, C., 2012. Consenso sobre manejo integral del neonato con encefalopatía hipóxico isquémica. Rev. Chil. Pediatr 83(5), 492-501.

149. **O'Callaghan, J.P.,** Sriram, K. Glial fibrillary acidic protein and related glial proteins as biomarkers of neurotoxicity., 2005. Expert. Opin. Drug Saf., 2005. 4(3), 433–442.

150. **Ohtaki, H.,** Ylostalo, J.H., Foraker, J.E., Robinson, A.P., Reger, R.L., Shioda, S., Prockop, D.J., 2008. Stem/progenitor cells from bone marrow decrease neuronal death in global ischemia by modulation of inflammatory/immune responses. Proc. Natl. Acad. Sci. U.S.A. 105(38), 14638-14643.

151. **Orihuela, R**., McPherson C.A., Harry, G.J., 2016. Microglial M1/M2 polarization and metabolic states. Br. J. Pharmacol. 173(4), 649–665.

152. **Orthmann-Murphy, J.L.,** Freidin, M., Fischer, E., Scherer, S.S., Abrams, C.K., 2007. Two distinct heterotypic channels mediate gap junction coupling between astrocyte and oligodendrocyte connexins. J. Neurosci. 27, 13949-13957.

153. **Ozgen, H.,** Baron, W., Hoekstra, D., Kahya, N., 2016. Oligodendroglial membrane dynamics in relation to myelin biogenesis. Cell Mol. Life Sci. 73(17), 3291-310.

154. **Pang, Y.,** Fan, L.W., Tien, L.T., Dai, X., Zheng, B., Cai, Z., Lin, R.C.S., Bhatt, A., 2013. Differential roles of astrocyte and microglia in supporting oligodendrocyte development and myelination in vitro. Brain Behav. 3, 503-514.

155. **Parpura, V.,** Heneka, M.T., Montana, V., Oliet, S.H., Schousboe, A., Haydon, P.G., Stout, R.F. Spray, D.C., Reichenbach, A., Pannicke, T., Pekny, M., Pekna, M., Zorec, R., Verkhratsky, A., 2012. Glial cells in (patho)physiology. J. Neurochem. 121(1), 4–27.

156. **Perez-Lobos, R.,** Lespay-Rebolledo, C., Tapia-Bustos, A., Palacios, E., Vío, V., Bustamante, D., Morales, P., Herrera-Marschitz, M., 2017. Vulnerability to a

metabolic challenge following perinatal asphyxia evaluated by organotypic cultures: neonatal nicotinamide treatment. Neurotox. Res. 32(3), 426-443.

157. **Polglase, G.,** Ong, T., Hillman, N., 2016. Cardiovascular alterations and multi organ dysfunction after birth asphyxia. Clin. Perinatol. 43(3), 469–483.

158. **Rees, S.,** Inder, T., 2005. Fetal and neonatal origins of altered brain development. Early Hum. Dev. 81(9), 753-761.

159. **Reemst, K.,** Noctor, S.C., Lucassen, P.J, Hol, E.M., 2016. The Indispensable Roles of Microglia and Astrocytes during Brain Development. Front. Hum. Neurosci.10, 566.

160. **Robertson, C.L.,** Scafidi, S., McKenna M.C., Fiskum, G., 2009. Mitochondrial mechanisms of cell death and neuroprotection in pediatric ischemic and traumatic brain injury. Exp. Neurol. 218(2), 371-380.

161. **Rocha-Ferreira, E.,** Hristova, M., 2016. Plasticity in the Neonatal Brain following Hypoxic-Ischaemic Injury. Neural. Plast. 2016,4901014.

162. **Ross, S.E.,** Greenberg, M.E., Stiles, C.D., 2003. Basic helix-loop-helix factors in cortical development. Neuron. 39,13–25.

163. **Saeedi, P.,** Halabian, R., Fooladi, A.A.I., 2019. A revealing review of mesenchymal stem cells therapy, clinical perspectives and Modification strategies. Stem Cell Investig. 6, 34-52.

164. **Sävman, K**., 2008. The Brain and Resuscitation. NeoReviews. 9(11), e513-e519.

165. **Schmidt-Kastner, R.,** van Os, J., W M Steinbusch, H., Schmitz, C., 2006. Gene regulation by hypoxia and the neurodevelopmental origin of schizophrenia. Schizophr. Res. 84(2-3), 253-271.

166. **Seidl, R.,** Stöckler-Ipsiroglu, S., Rolinski, B. Kohlhauser, C., Herkner, K.R., Lubec, B. Lubec, G., 2000. Energy metabolism in graded perinatal asphyxia of the rat. Life Sci. 67(4), 421-435.

167. **Sheikh, A.M.,** Nagai, A., Wakabayashi, K., Narantuya, D., Kobayashi, S., Yamaguchi, S., Kim, S.U., 2011. Mesenchymal stem cell transplantation modulates neuroinflammation in focal cerebral ischemia: contribution of fractalkine and IL-5. Neurobiol. Dis. 41(3), 717-724.

168. **Simola, N.,** Bustamante, D., Pinna, A., Pontis, S., Morales, P., Morelli, M., Herrera-Marschitz, M., 2008. Acute perinatal asphyxia impairs non-spatial

memory and alters motor coordination in adult male rats. Exp Brain Res 185(4), 595-601.

169. **Simons, M.,** Nave, K.M., 2015. Oligodendrocytes: Myelination and Axonal Support. Cold Spring Harb Perspect. Biol. 8(1), a020479.

170. **Singh, S.K.,** Ling, E.A., Kaur, C., 2018. Hypoxia and myelination deficits in the developing brain. Int. J. Dev. Neurosci.70, 3-11.

171. **Skoff, R.P.,** Bessert, D.A., Barks, J.D., Song, D., Cerghet, M., Silverstein, F., 2001. Hypoxic-ischemic injury results in acute disruption of myelin gene expression and death of oligodendroglial precursors in neonatal mice. Int. J. Dev. Neurosci. 19(2), 197-208.

172. **Sochocka, M.,** Satler, B., Leszek, J., 2017. Inflammatory Response in the CNS: Friend or Foe? Mol. Neurobiol. 54(10), 8071–8089.

173. **Soulet, D.,** Rivest, S. 2008. Microglia. Curr. Biol. 18, 506-508.

174. **Streit, W.J.,** Mrak, R.E., Griffin, W.S., 2004. Microglia and neuroinflammation: a pathological perspective. J Neuroinflammation. 1(1),14.

175. **Sullivan, C.,** Porter, R., Evans, C., Ritter, T., Shaw, G., Barry, F., Mary, J., 2014. TNFα and IL-1β influence the differentiation and migration of murine MSCs independently of the NF-κB pathway. Stem Cell Res. Ther. 5(4), 104-117.

176. **Sun, D.,** Jakobs, T.C. 2012. Structural remodeling of astrocytes in the injured CNS. Neuroscientist. 18, 567–588.

177. **Sun, J.,** Wei, Z.Z., Gu, X., Zhang, J.Y., Zhang, Y., Li, J., Wei, L., 2015. Intranasal delivery of hypoxia-preconditioned bone marrow-derived mesenchymal stem cells enhanced regenerative effects after intracerebral hemorrhagic stroke in mice. Exp. Neurol. 272, 78-87.

178. **Swarte, R.,** Lequin, M., Cherian, P., Zecic, A., van Goudoever, J., Govaert, P., 2009. Imaging patterns of brain injury in term-birth asphyxia. Acta Paediatr. 98(3), 586–592.

179. **Szuchet, S.,** Nielsen J. A., Lovas G., Domowicz M. S., de Velasco J. M., Maric D., 2011. The genetic signature of perineuronal oligodendrocytes reveals their unique phenotype. Eur. J. Neurosci. 34, 1906–1922.

180. **Tapia-Bustos, A.,** Perez-Lobos, R., Vío, V., Lespay-Rebolledo, C., Palacios, E., Chiti-Morales, A., Bustamante, D., Herrera-Marschitz, M., Morales, P., 2017.

Modulation of Postnatal Neurogenesis by Perinatal Asphyxia: Effect of D1 and D2 Dopamine Receptor Agonists. Neurotox Res. 31(1):109-121.

181. **Tikoo, R.,** Osterhout, D.J., Casaccia-Bonnefil, P., Seth, P., Koff, A., Chao, M.V., 1998. Ectopic expression of p27Kip1 in oligodendrocyte progenitor cells results in cell-cycle growth arrest. J. Neurobiol. 36(3), 431–440.

182. **Ten, V.S.,** Bradley-Moore, M., Gingrich, J.A., Stark, R.I., Pinsky, D.J., 2003 Brain injury and neurofunctional deficit in neonatal mice with hypoxic–ischemic encephalopathy. Behav Brain Res. 145, 209–219.

183. **Tjalkens, R.B.,** Popichak, K.A., Kirkley, K.A., 2017. Inflammatory Activation of Microglia and Astrocytes in Manganese Neurotoxicity. Adv Neurobiol. 18, 159-181.

184. **Tress, O.,** Maglione, M., May, D., Pivneva, T., Richter, N., Seyfarth, J., Binder, S., Zlomuzica, A., Seifert, G., Theis, M. 2012. Panglial gap junctional communication is essential for maintenance of myelin in the CNS. J. Neurosci. 32, 7499-7518.

185. **Truog, W.E.** Xu, D., Ekekezie, II., Mabry, S., Rezaiekhaligh, M., Svojanovsky, S., Soares, M.J., 2008. Chronic hypoxia and rat lung development: analysis by morphometry and directed microarray. Pediatr. Res. 2008. 64(1), 56–62.

186. **Vaes, J.E.G.,** Vink, M.A, de Theije C.G.M., Hoebeek, F.E., Benders, M.J.N.L., Nijboer, C.H.A., 2019. The Potential of Stem Cell Therapy to Repair White Matter Injury in Preterm Infants: Lessons Learned From Experimental Models. Front Physiol. 10,540-540.

187. **Valerio, A.,** Ferrario, M., Dreano, M., Garotta, G., Spano, P., Pizzi, M., 2002. Soluble interleukin-6 (IL-6) receptor/IL-6 fusion protein enhances in vitro differentiation of purified rat oligodendroglial lineage cells. Mol Cell Neurosci. 21, 602–615.

188. **Vannucci, R.C.,** Connor, J.R., Mauger, D.T., Palmer, C., Smith, M.B., Towfighi, J., Vannucci, S.J., 1999. Rat model of perinatal hypoxic ischemic brain damage. J. Neurosci. Res. 55(2), 158–163.

189. **van Tilborg, E.,** de Theije, C. van Hal, M., Wagenaar, N., de Vries, L., Benders, M., Rowitch, D., Nijboer, C., 2018. Origin and dynamics of oligodendrocytes in the developing brain: Implications for perinatal white matter injury. Glia. 66, 221–238.

190. **van Velthoven, C.T.,** Kavelaars, A., van Bel, F., Heijnen, C.J., 2009. Regeneration of the ischemic brain by engineered stem cells: fuelling endogenous repair processes. Brain Res. Rev. 61(1), 1–13.

191. **van Velthoven, C.T**., Kavelaars, A., van Bel, F., Heijnen, C.J., 2010a. Mesenchymal stem cell treatment after neonatal hypoxic-ischemic brain injury improves behavioral outcome and induces neuronal and oligodendrocyte regeneration. Brain Behav. Immun. 24(3), 387–393.

192. **van Velthoven, C.T.,** Kavelaars, A., van Bel, F., Heijnen, C.J., 2010b. Repeated mesenchymal stem cell treatment after neonatal hypoxia-ischemia has distinct effects on formation and maturation of new neurons and oligodendrocytes leading to restoration of damage, corticospinal motor tract activity, and sensorimotor function. J. Neurosci. 30(28), 9603–9611.

193. **van Velthoven C.T.,** Kavelaars. A., van Bel, F., Heijnen, C.J., 2011. Mesenchymal stem cell transplantation changes the gene expression profile of the neonatal ischemic brain. Brain Behav. Immun. 25(7),1342-138.

194. **Vitalis, T.,** Cases, O., Parnavelas, J.G., 2005. Development of the dopaminergic neurons in the rodent brainstem. Exp. Neurol. 191, 104–112.

195. **Vogel, E**., Britt, R., Trinidad, M.C., Faksh, A., Martin, R. MacFarlane, P., Pabelick, C., Prakash, Y.S., 2015. Perinatal Oxygen in the Developing Lung. Can. J. Physiol. Pharmacol. 93(2),119–127.

196. **Volpe, J.J.,** 1995. Hypoxic-ischemic encephalopathy: neuropathology and pathogenesis. Neurology of the Newborn. London: WB Saunders, 279-313.

197. **Volpe, JJ.** (2001). Perinatal brain injury: from pathogenesis to neuroprotection. Ment Retard Dev Disabil Res Rev 7:56-64.

198. **Volpe, J.J.,** 2008. Neonatal encephalitis and white matter injury: more than just inflammation? Ann. Neurol. 64(3), 232-6.

199. **Volpe, J.J.,** Kinney, H.C., Jensen, F.E., Rosenberg, P.A., 2011. The developing oligodendrocyte: key cellular target in brain injury in the premature infant. Int. J. Dev. Neurosci. 29(4), 423–440.

200. **Voorn, P.,** Kalsbeek, A., Jorritsma-Byham, B., Groenewegen, H.J., 1988. The pre- and postnatal development of the dopaminergic cell groups in the ventral mesencephalon and the dopaminergic innervation of the striatum of the rat. Neuroscience. 25(3), 857–887.

201. **Wang, W.,** Tan, M., Yu, J., Tan, L., 2015. Role of pro-inflammatory cytokines released from microglia in Alzheimer's disease. Ann. Transl. Med. 3(10),136.

202. **Wei, Z.Z.,** Gu, X., Ferdinand, A., Lee, J.H., Ji, X., Ji, X.M., Yu, S.P., Wei, L., 2015. Intranasal delivery of bone marrow mesenchymal stem cells improved neurovascular regeneration and rescued neuropsychiatric deficits after neonatal stroke in rats. Cell Transplant. 24(3), 391–402.

203. **Wei, Z.,** Gu, X., Ferdinand, A., Lee, J., Ji, X., Ji, X., Wei, L., 2015. Intranasal delivery of bone marrow mesenchymal stem cells improved neurovascular regeneration and rescued neuropsychiatric deficits after neonatal stroke in rats. Cell Transplantation. 24, 391–402.

204. **Wilkins, A.,** Majed, H., Layfield, R., Compston, A., Chandran, S., 2003. Oligodendrocytes promote neuronal survival and axonal length by distinct intracellular mechanisms: a novel role for oligodendrocyte- derived glial cell line-derived neurotrophic factor. J. Neurosci. 15(23), 4967-4974.

205. **Young, K.M.,** Psachoulia, K., Tripathi, R.B., Dunn, S.J., Cossell, L., Attwell, D., Tohyama, K., Richardson, W.D., 2013. Oligodendrocyte dynamics in the healthy adult CNS: evidence for myelin remodeling. Neuron. 77(5): 873-885.

206. **Zappia, E.,** Casazza, S., Pedemonte, E., Benvenuto, F., Bonanni I., Gerdoni, E., Giunti, D., Ceravolo, A., Cazzanti, F., Frassoni, F., Mancardi, G., Uccelli, A., 2005. Mesenchymal stem cells ameliorate experimental autoimmune encephalomyelitis inducing T-cell anergy. Blood.106(5), 1755–1761.

207. **Zhang, Z.G.,** Chopp, M., 2009. Neurorestorative therapies for stroke: underlying mechanisms and translation to the clinic. Lancet Neurol. 8(5), 491–500.

208. **Zhang, R.,** Liu, Y., Yan, K., Chen, L., Chen, X.R., Li, P., Chen, F.F., Jiang, X.D., 2013. Anti-inflammatory and immunomodulatory mechanisms of mesenchymal stem cell transplantation in experimental traumatic brain injury. J Neuroinflammation. 10:106-118.

209. **Zhang, Y.,** Sloan, S.A., Clarke, L.E., Caneda, C., Plaza, C.A., Blumenthal, P.D., Vogel, H., Steinberg, G.K., Edwards, M.S., Li, G., 2016. Purification and characterization of progenitor and mature human astrocytes reveals transcriptional and functional differences with mouse. Neuron. 89, 37-53.

210. **Ziemka-Nalecz, M.,** Janowska, J., Strojek, L., Jaworska, J., Zalewska, T., Frontczak-Baniewicz, M., Sypecka, J., 2018. Impact of neonatal hypoxia-ischaemia on oligodendrocyte survival, maturation and myelinating potential. J. Cell. Mol. Med. 22(1), 207-222.

X. SUPPLEMENTARY TABLES

Table 1. Effect of perinatal asphyxia (PA) on myelin basic protein (MBP) at P1, P7 and P14, from control (CS) and asphyxia-exposed (AS) rats.

Experimental groups	**P1**		**P7**		**P14**	
A. Caesarean-delivered (CS); n=5	**DAPI (cells/ mm^3)**	**MBP (pixels/ total pixels)**	**DAPI (cells/ mm^3)**	**MBP (pixels/ total pixels)**	**DAPI (cells/ mm^3)**	**MBP (pixels/ total pixels)**
External capsule	374444 ±45042	nd	355067 ±17917	20.54 ±1.14	367240 ±21229	49.76 ±0.12 **(>2x)a******
Corpus callosum	262787 ±68397	nd	235916 ±24303	4.27 ±1.03	325644 ±41589	49.97 ±0.15 **(>10x)a******
Cingulum	378496 ±105892	nd	300722 ±20739	7.92 ±0.82	388988 ±27324	49.39 ±0.33 **(>6x)a******
Fimbriae of hippocampus	240763 ±67331	nd	264911 ±19963	1.94 ±0.59	449593 ±51446	49.97 ±0.16 **(>25x)a******
B. Asphyxia-exposed (AS); 21 min asphyxia; n=5						
External capsule	521962 ±114815	nd	392315 ±29773	**9.88 ±2.73 (by 50%)b***	398727 ±40493	**49.67 ±0.07 (>5x)a******
Corpus callosum	199665 ±55743	nd	285083 ±19983	**1.51 ±0.47 (by 60%)b***	310779 ±37973	**49.43 ±0.14 (>30x)a******
Cingulum	438835 ±95565	nd	346825 ±22842	**2.29 ±0.62 (by~70%)b*****	411625 ±27658	**49.61 ±0.09 (>20x)a******
Fimbriae of hippocampus	269789 ±45231	nd	286527 ±24323	1.49±0.62	344219 ±31841	**48.65 ±1.19 (>30x)a******

Table 2. Effect of perinatal asphyxia (PA) on myelin basic protein (MBP), Oligodendrocyte transcription factors (Olig-1, Olig-2), and inflammatory cytokines (COX-2, TNF-α, IL-1β, IL-6) mRNA in telencephalon or hippocampus at P1, P7 and P14 in control (CS) and asphyxia-exposed (AS) rats

A. TELENCEPHALON			
Gene transcripts (mRNA) (fold/change)	**P1**	**P7**	**P14**
a. Caesarean delivered (CS); n= 5	**CS**	**CS**	**CS**
MBP	1.000±0.191	**23.23±4.01 (>20x)a******	**1165±258.90 (>1000x)a******
Olig-1	1.000±0.098	1.37±0.05	**2.315±0.13 (>2x)a******
Olig-2	1.000±0.076	1.24±0.03	**1.826±0.181 (> 1.8x)a******
IL-1β	1.000±0.101	1.00±0.13	**2.36±0.18 (>2x)a****
IL-6	1.000±0.201	0.70±0.03	**1.86±0.17 (>1.8x)a*****
TNF-α	1.000±0.208	2.14±0.38	7.02±3.63
Cox-2	1.000±0.255	**5.84±1.50 (>5x)a****	**33.56±8.76 (>30x)a****
b. Asphyxia-exposed (AS); n= 5	**AS**	**AS**	**AS**
MBP	0.91±0.04	**35.63±6.76 (>35x)a******	**768.90±201.30 (>800x)a*****
Olig-1	1.23±0.05	**2.06±0.36 (>1.6x)a* (>1.4X)b***	**2.40±0.25 (>1.9x)a******
Olig-2	1.33±0.15	1.61±0.29	1.81±0.21
IL-1β	1.50± 0.27	1.10±0.08	2.46±0.47
IL-6	0.78± 0.12	**1.16± 0.13 (>1.6x)b****	**1.46±0.20 (>1.8x)a***
TNF-α	2.22± 0.67	8.32±3.63	**40.42±25.11 (>18x)a***
Cox-2	1.16±0.34	**9.80±1.59 (>8x)a******	**23.03±6.00 (>20x)a****

B. HIPPOCAMPUS			
Gene transcripts (mRNA) (fold/change)	**P1**	**P7**	**P14**
a. Caesarean delivered (CS); n= 5	**CS**	**CS**	**CS**
Cox-2	1.000±0.181	6.887±1.730 **(>6x)^{a****}**	28.660±4.452 **(>4x)^{a****}**
TNF-α	1.000±0.253	1.130±0.229	1.676±0.474
IL-1β	1.000±0.192	0.876±0.150	1.196±0.128
IL-6	1.000±0.877	0.642±0.091	0.972±0.105
b. Asphyxia-exposed (AS); n= 5	**AS**	**AS**	**AS**
Cox-2	1.31± 0.195	11.200±1.467 **(>11x)^{a****}**	31.480±4.441 **(>2.5x)^{a****}**
TNF-α	1.526±0.325	0.904± 0.209	1.556±0.359
IL-1β	0.937± 0.06	0.743±0.094	2.021±0.402 **(>2.5x)^{a*}** **(>2x)^{b*}**
IL-6	0.787±0.067	0.822±0.184	0.907±0.318

Table 3. Effect of perinatal asphyxia (PA) on glial cells at P7; control (CS) and asphyxia-exposed (AS) rats**.**

Experimental groups	**P7**			
A. Caesarean delivered (CS); n= 5	**DAPI cells/mm^3**	**MBP-DAPI cells/mm^3**	**GFAP-DAPI cells/mm^3**	**Iba-1-DAPI cells/mm^3**
External capsule	346895±12632	18932±1960	18890±1648	14020±1808
Corpus callosum	214600±14080	10810±1668	19090±3229	8519±561.6
Cingulum	294902±14140	12439±1616	19510±3277	10360±955.6
Fimbriae of hippocampus	275700±15350	8811± 2405	13210±2487	5957±1027
B. Asphyxia-exposed (AS); n= 5				
External capsule	370346±24821	**8603±982.7 (by~50%)b****	21150±3637	15840±1429
Corpus callosum	237200±20170	**3413±637.7 (by~65%)b****	21280±579.6	7380±848.8
Cingulum	334385±18199	**6643±1121 (by~45%)b***	30150±5358	**17800±3047 (>1.5X)b***
Fimbriae of hippocampus	270800±19810	4101±2144	10640±591.70	6014±909.1

XI. SUPPLEMENTARY FIGURES

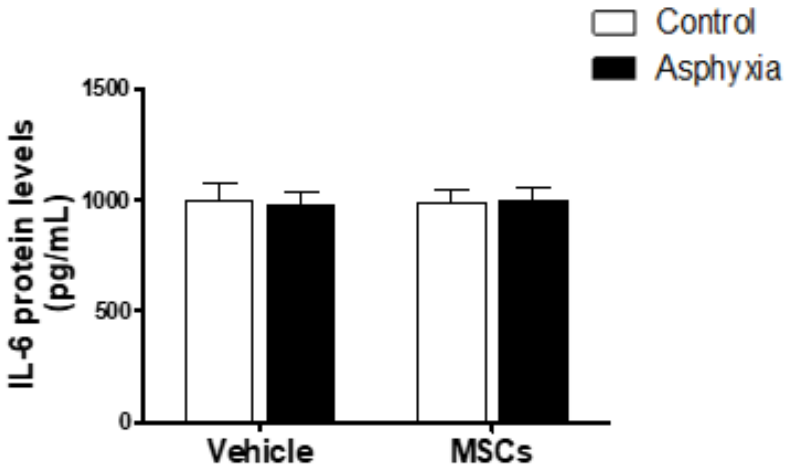

Figure 1. Effect of MSCs treatment on changes of IL-6 protein levels induced by perinatal asphyxia (PA), measured at P7 in telencephalon of CS (a) and AS (b) rat neonates. Effect of PA on IL-6 protein levels (pg/mL) was determined by ELISA analysis. Data are shown as means ± S.E.M., for independent experiments (N=6-8). In telencephalon, unbalanced two-way ANOVA indicated no significant effect of PA on IL-6 protein levels. Benjamini-Hochberg was used as a post hoc test.

XII. ANNEXES

VID INVESTIGACIÓN INNOVACIÓN CREACIÓN ARTÍSTICA
Vicerrectoría de Investigación y Desarrollo
UNIVERSIDAD DE CHILE

CICUA
COMITÉ INSTITUCIONAL DE CUIDADO Y USO DE ANIMALES

Santiago, a 12 de julio de 2017

Certificado n°:**17056-MED-UCH**

CERTIFICADO

El Comité Institucional de Cuidado y Uso de Animales (CICUA) de la Universidad de Chile, certifica que en el protocolo número **CBA0943 FMUCH** del proyecto de investigación titulado **"La asfixia perinatal induce neuroinflamación, daño a largo plazo en los oligodendrocitos y desmielinización en cerebro de ratas: prevención por células madres mesenquimales"** de la **Dra. Andrea Tapia Bustos Ph.D (c)**, Estudiante de Doctorado de Farmacología, Universidad de Chile y cuyo **Investigador Patrocinante-Responsable** es la **Dra. Paola Morales Retamales**, del Laboratorio de Farmacología de Neurocircuitos, Programa Disciplinario de Farmacología Molecular y Clínica, ICBM, Facultad de Medicina, Universidad de Chile, no plantea acciones en sus procedimientos que contravengan las normas de Bioética de manejo y cuidado de animales, así mismo la metodología experimental planteada satisface lo estipulado en el Programa Institucional de Cuidado y Uso de Animales de la Universidad de Chile.

Ambasinvestigadorasse han comprometido a la ejecución de este proyecto de investigación dentro de las especificaciones señaladas en el protocolo revisado y autorizado por el CICUA, a mantener los procedimientos experimentales planteados y a no realizar ninguna modificación sin previa aprobación por parte de este Comité.

Se otorga la presente certificación para el uso de 42ratas *Rattus norvegicus*, (cepa Wistar), provenientes del Bioterio Central, Facultad de Medicina, ICBM, Universidad de Chiledesde marzo de 2017 afebrero de 2019, tiempo estimado de ejecución del proyecto, el cual será financiado con fondos **Fondecyt Regular1120079, Proyecto BNI P09-015-F, Fondecyt 1170712, Conicyt – Chile 21151232. Apoyo económico internacional.**

*El CICUA de la Universidad de Chile, forma parte de la Vicerrectoría de Investigación y Desarrollo, y está constituido por 43 miembros: 5 médicos veterinarios, 39 académicos (12 de ellos médicos veterinarios), y 9 miembros no asociados a la academia o investigación, y que cuentan con experiencia en bioética relacionada a mantención y uso de animales. El certificado que emite el Comité procede de la aprobación del "**Protocolo de Manejo y Cuidado de Animales**" después de un estudio acucioso y de la acogida de los investigadores de las observaciones exigidas por el Comité.*

Dr. Cristián Ugaz Ruiz
Coordinador
CICUA - VID
Universidad de Chile

Dra. Pía Ocampos
Presidente (sub)
CICUA - VID
Universidad de Chile

Comité Institucional de Cuidado y Uso de Animales (CICUA)
Vicerrectoría de Investigación y Desarrollo (VID) – Universidad de Chile
www.uchile/cicua.cl email: coordinador.cicua@uchile.cl